2019-04-01

An Analysis of Decision Boundaries for Left-Turn Treatments

Michael Louis Adamson
Brigham Young University

An Analysis of Decision Boundaries for Left-Turn Treatments

Michael Louis Adamson

A thesis submitted to the faculty of
Brigham Young University
in partial fulfillment of the requirements for the degree of

Master of Science

Grant G. Schultz, Chair
Mitsuru Saito
Gregory Macfarlane

Department of Civil and Environmental Engineering

Brigham Young University

ABSTRACT

An Analysis of Decision Boundaries for Left-Turn Treatments

Michael Louis Adamson
Department of Civil Engineering, BYU
Master of Science

The purpose of this project is to evaluate the safety and operational differences between three left-turn treatments: permitted, protected, and protected-permitted left-turn phasing. Permitted phasing allows vehicles to turn left after yielding to any opposing vehicles; protected phasing provides an exclusive phase for vehicles to turn left that does not allow opposing vehicles; and protected-permitted phasing combines the previous phasing alternatives, allowing vehicles to turn after yielding while also providing some green time for protected left-turns.

As part of evaluating the differences between these left-turn treatments, crashes before and after the change at intersections that had experienced a permanent change from one phase alternative to another were compared. The crashes that took place at these intersections were compared with the number of crashes experienced at a baseline set of intersections. A general increase in total crashes was observed for most intersections, and an increase in left-turn crashes per million entering vehicles was also observed in intersections that had experienced a change from protected to protected-permitted phasing; no other clear trends were observed.

The research team also gathered simulated data using VISSIM traffic modeling software and safety data were extracted from these simulations using the Surrogate Safety Assessment Model (SSAM) created by the Federal Highway Administration to identify decision boundaries between each left-turn treatment. The simulations modeled intersections with 1-, 2-, and 3-opposing-lane configurations with permitted and protected-permitted models (split into green times of 10-, 15-, and 20-seconds) for a total of 12 different simulation models. Each model was divided into 100-225 different volume scenarios, with incremental increases in left-turn vs. opposing volumes. By exporting trajectory files from VISSIM and importing these files into SSAM, crossing conflicts for each volume combination in each model were identified and extracted. These were then entered into MATLAB to create contour maps; the contours of these maps represent the number of crossing conflicts per hour associated with different combinations of left-turn and opposing volume. Basic decision boundaries were observed in the contour maps for each model. To extract an equation to estimate each boundary, JMP Pro statistical analysis software was used to perform a linear regression analysis and develop natural log-based equations estimating the decision boundaries for each configuration and phase alternative. These equations were then charted using Excel and final decision boundaries were developed for the 1-, 2-, and 3-lane configurations between permitted and protected-permitted phasing as well as between protected-permitted and protected phasing.

Keywords: decision boundary, intersection operations, intersection safety, left-turn, safety, signal operations, SSAM, UDOT, VISSIM, warrant

ACKNOWLEDGEMENTS

This research was made possible with funding from the Utah Department of Transportation (UDOT) and Brigham Young University (BYU). I would like to acknowledge those individuals who have supported me in this research, as well as those that have supported me throughout my academic career. First, I would like to thank the members of the UDOT technical advisory committee who provided funding for and guided this research, including: Mark Taylor, Jamie Mackey, Jesse Sweeten, Clancy Black, Carrie Jacobson, Travis Jensen, and Jeff Lewis. Second, I would like to thank the members of my graduate committee who have provided excellent feedback and advice as I have done this research, including: Dr. Schultz, Dr. Saito, and Dr. Macfarlane. I especially thank Dr. Schultz, my graduate committee chair, for his mentorship and guidance in my undergraduate and graduate academic career at BYU. Third I would like to thank Michael Stevens, an undergraduate research assistant hired for this project, for all of his work to make the project a success. Lastly, I would like to thank my family members who have supported me throughout my academic career. My wife, Jennifer, and parents, Jill and Darren, are the reason I strive for excellence in academic and professional pursuits, and I thank them for their continued support. I would also like to thank my in-laws, Brenda and Dean, for their encouragement and support.

TABLE OF CONTENTS

LIST OF TABLES vi
LIST OF FIGURES vii
1 Introduction 1
1.1 Background 1
1.2 Objectives 2
1.3 Organization 5
2 Literature Review 6
2.1 Introduction 6
2.2 Differences in Left-Turn Phasing Alternatives 6
2.3 UDOT Left-Turn Phasing Guidelines 10
2.4 Time of Day Considerations 18
2.5 Comparison of Left-Turn Decision Boundary Alternatives 20
2.6 Chapter Summary 31
3 Analysis Method 33
3.1 Introduction 33
3.2 Analysis of Reported Crash Data 33
3.3 Analysis of Simulated Data 37
3.4 Chapter Summary 49
4 Evaluation of Left-Turn Phasing Changes 51
4.1 Introduction 51
4.2 Results of Crash Data Analysis 51
4.3 Potential Sources of Error in the Crash Analysis 64
4.4 Chapter Summary 65
5 Development of Left-Turn Phasing Decision Boundaries 67
5.1 Introduction 67
5.2 Mapping of Conflict Contours 67
5.3 Development of Decision Boundaries for Selecting Appropriate Left-Turn Phasing ... 76
5.4 Proposed Decision Boundaries for Left-Turn Phasing 80
5.5 Comparison of Decision Boundaries with Actual Intersections Analyzed in the Study 83
5.6 Chapter Summary 89
6 Conclusions and Recommendations 90

6.1 Conclusions 90
6.2 Conclusions from Existing Signalized Intersection Crash Data 90
6.3 Decision Boundaries Derived from Simulation 91
6.4 Recommendations 93
6.5 Future Research Topics 94
6.6 Concluding Remarks 94
References 96
List of Acronyms 100

LIST OF TABLES

Table 2-1: Crash Summary for Change from Protected to Permitted Phasing 8
Table 2-2: Current UDOT Volume Cross Product Thresholds 12
Table 2-3: Proportion of Right-Turning Vehicles to Through Vehicles..... 13
Table 2-4: Potential Increase to UDOT Left-Turn Phasing Thresholds if Right-Turns are Included..... 13
Table 2-5: Dual Left-Turn Signal Warrant 14
Table 2-6: Benefit Value per Crash Provided by FHWA for Each Crash Type..... 17
Table 2-7: Benefit Value per Crash Provided by UDOT for Each Crash Type 17
Table 2-8: Results of State Phasing Practices Survey 18
Table 2-9: Range and Increment of Simulation Input Parameters..... 21
Table 2-10: Base Variables Used to Calibrate DSS Model 28
Table 3-1: Time Gap Analysis Results 44
Table 3-2: Time Gaps Used by Model..... 44
Table 3-3: Crossing Conflict Contours Used to Define Boundary Contours for Each Model 46
Table 3-4: Example of Volume Combinations Obtained from Conflict Contour for Permissive Left-Turn Phasing with 1-Lane Opposing Through Movements..... 47
Table 4-1: Intersections Selected for Baseline..... 52
Table 4-2: Intersections Selected that Changed from Permitted to Protected-Permitted 56
Table 4-3: Intersections Selected that Changed from Protected to Protected-Permitted..... 61
Table 5-1: Signalized Intersections Used for Decision Boundary Comparison 86

LIST OF FIGURES

Figure 2-1: UDOT Left-Turn Phasing Flowchart. 11
Figure 2-2: Analysis of crash risk by time of day, with normalized risk as the y-axis. 19
Figure 2-3: Left-turn decision boundaries. 22
Figure 2-4: Concept validation using existing configurations and traffic counts. 24
Figure 2-5: Threshold for two opposing lanes. 29
Figure 2-6: Threshold for one opposing lane. 29
Figure 3-1: Example of time gap analysis. 43
Figure 3-2: Conflict contour identification using the 1-lane time-gap analysis. 46
Figure 3-3: Linear regression output example for the permitted 1-lane case. 48
Figure 4-1: Total crashes (Baseline). 53
Figure 4-2: Injury related crashes as a ratio of total crashes (Baseline). 53
Figure 4-3: Left-turn related crashes per MEV (Baseline). 54
Figure 4-4: Total crashes per MEV by time of day (Baseline). 55
Figure 4-5: Left-turn related crashes per MEV by time of day (Baseline). 55
Figure 4-6: Total crashes (Permitted to Protected-Permitted). 57
Figure 4-7: Injury-related crashes as a ratio of total crashes (Permitted to Protected-Permitted). 58
Figure 4-8: Left-turn related crashes per MEV (Permitted to Protected-Permitted). 58
Figure 4-9: Total crashes per MEV by time of day (Permitted to Protected-Permitted). 59
Figure 4-10: Left-turn crashes per MEV by time of day (Permitted to Protected-Permitted). 60
Figure 4-11: Change in total crashes (Protected to Protected-Permitted) 61
Figure 4-12: Left-turn related crashes as a ratio of total crashes (Protected to Protected-Permitted) 62
Figure 4-13: Left-turn related crashes per MEV (Protected to Protected-Permitted). 62
Figure 4-14: Total crashes per MEV by time of day (Protected to Protected-Permitted). 63
Figure 4-15: Left-turn crashes per MEV by time of day (Protected to Protected-Permitted). 64
Figure 5-1: Contour map for permitted left-turn phasing with an opposing 1-lane configuration. 68
Figure 5-2: Contour map for permitted left-turn phasing with an opposing 2-lane configuration. 69

Figure 5-3: Contour map for permitted left-turn phasing with an opposing 3-lane configuration. 69
Figure 5-4: Contour map for protected-permitted left-turn phasing with a 10-second protected green time and opposing 1-lane configuration. 70
Figure 5-5: Contour map for protected-permitted left-turn phasing with a 15-second protected green time and opposing 1-lane configuration. 71
Figure 5-6: Contour map for protected-permitted left-turn phasing with a 20-second protected green time and opposing 1-lane configuration. 71
Figure 5-7: Contour map for protected-permitted left-turn phasing with a 10-second protected green time and opposing 2-lane configuration. 72
Figure 5-8: Contour map for protected-permitted left-turn phasing with a 15-second protected green time and opposing 2-lane configuration. 73
Figure 5-9: Contour map for protected-permitted left-turn phasing with a 20-second protected green time and opposing 2-lane configuration. 73
Figure 5-10: Contour map for protected-permitted left-turn phasing with a 10-second protected green time and opposing 3-lane configuration. 74
Figure 5-11: Contour map for protected-permitted left-turn phasing with a 15-second protected green time and opposing 3-lane configuration. 75
Figure 5-12: Contour map for protected-permitted left-turn phasing with a 20-second protected green time and opposing 3-lane configuration. 75
Figure 5-13: Decision boundaries for 1-lane opposing approach configuration. 77
Figure 5-14: Decision boundaries for 2-lane opposing approach configuration. 79
Figure 5-15: Decision boundaries for 3-lane opposing approach configuration. 80
Figure 5-16: Final decision boundaries for 1-lane opposing approach configuration. 82
Figure 5-17: Final decision boundaries for 2- and 3-lane opposing approach configurations. 82
Figure 5-18: Existing 1-lane intersections within the proposed decision boundaries for 1-lane opposing approach configuration. 84
Figure 5-19: Existing 2-lane intersections within the proposed decision boundaries for 2- and 3-lane opposing approach configurations. 84
Figure 5-20: Existing 3-lane intersections within the proposed decision boundaries for 2- and 3-lane opposing approach configurations. 85
Figure 5-21: Existing 2-lane intersections outside of the proposed decision boundaries for 2- and 3-lane opposing approach configurations. 85
Figure 5-22: Existing 3-lane intersections outside of the proposed decision boundaries for 2- and 3-lane opposing approach configurations. 86

Figure 6-1: Left-turn phasing decision boundary for the 1-lane opposing approach configuration. 92
Figure 6-2: Left-turn phasing decision boundary for the 2- and 3-lane opposing approach configuration. 93

1 INTRODUCTION

1.1 Background

The Utah Department of Transportation (UDOT) continues to place safety and mobility of state roadways at the forefront of their priorities. However, improving safety and optimizing mobility may at times conflict with each other, especially when related to left-turn phasing. Although it is desirable to provide protected left-turn phasing whenever possible in an effort to improve the safety of left-turn movements, the time allocated to the protected movement may have a negative impact on through traffic movements (i.e., mobility).

The topic of left-turn phasing is not new to UDOT and a variety of research projects have been conducted recently (or are ongoing) to evaluate safety of left-turns as well as to evaluate the warranting of left-turn signal phasing. More particularly, UDOT is currently performing studies to determine possible methods for dynamic left-turn phasing assignment based on time-of-day variance in traffic volume. Even with the previously performed research, there is a need to better understand the safety and operational effects of left-turn signal phasing and to identify boundaries for left-turn treatments at signalized intersections based on actual data from across the state.

The purpose of this research is to evaluate the mixture of left-turn and opposing through traffic volumes for permitted vs. protected left-turn phasing at intersections and to identify cut-off points that would help to identify when to switch from permitted to protected phasing at

signalized intersections. To meet the purpose of the research, the research team completed a literature review to gain insight and understanding on existing decision boundaries for left-turn treatments at signalized intersection and to identify how best to utilize the data that are available in Utah to address the needs outlined. The safety differences between the left-turn phasing alternatives were evaluated using crash data from existing intersections. However, because of the randomness of crash data and limits to the data that were available, the field measured data was supplemented with simulation data using VISSIM (PTV 2015) and the Surrogate Safety Assessment Model (SSAM) developed by the Federal Highway Administration (FHWA) (FHWA 2008) to develop decision boundaries between different left-turn treatments. This allowed the research team to control the left-turn volume and opposing traffic volume levels to aid in determining meaningful boundaries for the different left-turn treatments. From this simulated analysis, practical guidelines were established to evaluate permitted single left-turn lanes and protected-permitted single left-turn lanes in order to determine decision boundaries between permitted and protected-permitted left-turn phasing as well as between protected-permitted and protected left-turn phasing.

1.2 Objectives

The primary objective of this research is to evaluate the mixture of left-turn and opposing through traffic volumes for permitted vs. protected left-turn phasing at intersections and to identify cut-off points as a result of the data that would help to identify when to switch from permitted to protected phasing at intersections. This was accomplished by:

1. Evaluating left-turn phasing as a function of safety and mobility using crash data from existing intersections.

2. Evaluating the mixture of left-turn and opposing through traffic volumes for permitted vs. protected left-turn phasing at intersections using simulation data.

3. Identifying cut-off points as a result of the simulated data that would help to identify when to switch from permitted to protected-permitted left-turn phasing or protected-permitted to protected left-turn phasing at intersections.

This section will address each of these objectives, starting first with a discussion of the data collection and evaluation of crashes at existing intersections that experienced a left-turn phase change, followed by a discussion on how simulated data will be analyzed using SSAM and a discussion on the derivation of the left-turn phase decision boundaries.

1.2.1 Data Collection and Evaluation of Left-Turn Phasing

The primary purpose of this task was to utilize existing data to develop specific graphical decision boundaries for Utah, using existing data in the state. This required close coordination with the UDOT Traffic Management Division (TMD) to collect the mobility data for the signalized intersections across the state as well as coordination with the UDOT Traffic and Safety Division for the safety analysis. The data included signal timing, left-turn volume, opposing volume, and intersection-related crashes. In addition, other variables such as number of lanes and speed limit were considered when discussing crashes at existing intersections.

1.2.2 Perform Sensitivity Analysis Using SSAM

The FHWA provides and supports a wide range of data and safety analysis tools designed primarily to assist state and local practitioners in understanding safety problems on their roadways. One tool is the SSAM, which helps traffic engineers perform comparative safety

analysis of highway design alternatives using traffic simulation models. The software is free of charge and combines traffic microsimulation and automated conflict analysis. It is designed to be compatible with a variety of simulation models, including VISSIM, Parametrics, AIMSUN, and TEXAS. SSAM uses the best possible surrogate measures that are observable in simulation models and supports flexible analysis to provide different aggregations of statistics and different visualization types (FHWA 2008).

This project utilized SSAM to perform a sensitivity analysis between left-turn and opposing traffic volumes at signalized intersections to evaluate simulated near-misses, or conflicts. The VISSIM model was used as the base for the analysis. Generic signalized intersections were modeled in VISSIM and evaluated using the SSAM model to export data on the number of crossing conflicts (simulated left-turn movements that conflicted with opposing through or right-turn movements) to comma separated values (.csv) files. These data were then assessed using MATLAB and JMP Pro to develop left-turn decision boundaries.

1.2.3 Data Analysis and Development of Left-Turn Phase Boundary Models

Data were reviewed and statistical analyses were conducted to develop left-turn phase boundary models. These models helped the research team to identify guidelines for cut-off points for different left-turn phasing that could be used for both signal design and dynamic left-turn phasing assignment. The research team summarized the results of the data collected and identified limited recommendations on decision boundaries for left-turn treatment at signalized intersections.

1.3 Organization

The body of the report is organized into the following chapters:

- Chapter 1 includes an introduction of the research, project objectives, and the organization of the report.
- Chapter 2 includes a literature review of studies assessing differences in safety between left-turn treatments, left-turn signal phasing practices, differences in time-of-day left-turn treatments, and left-turn signalized phasing boundaries.
- Chapter 3 includes general discussion on the methods used to assess left-turn crash data from existing intersections throughout Utah, as well as to derive left-turn decision boundaries using simulation.
- Chapter 4 includes a discussion on the assessment of left-turn crash data from existing intersections throughout Utah, including the findings of this assessment.
- Chapter 5 includes a discussion on the development of simulation models, extraction of safety-related crossing conflict data, and derivation of decision boundaries for 1-, 2-, and 3-lane opposing approach configurations, including the final decision boundaries selected.
- Chapter 6 includes the conclusions for this research, recommendations for future research, and concluding remarks.
- References and a List of Acronyms follow the main chapters.

2 LITERATURE REVIEW

2.1 Introduction

This section provides a review of literature pertinent to the research presented in this report. This research includes both an evaluation of decision boundaries between left-turn phase alternatives and a discussion of possible improvements to time-of-day changes in left-turn phasing. Thus, the literature review focuses on literature on the current state of practice for signal phasing and then discusses research projects that have developed both decision boundaries between left-turn phasing alternatives and boundaries for time-of-day phasing changes.

The literature review consists of the following sections: differences in left-turn phasing alternatives, current UDOT left-turn phasing guidelines, time-of-day considerations, a comparison of left-turn decision boundary alternatives, and a chapter summary.

2.2 Differences in Left-Turn Phasing Alternatives

One of the most important considerations when evaluating safety at signalized intersections is the phasing alternatives for through and left-turn traffic. Improper phasing and timing of signals at signalized intersections can lead to congestion, delay, and crashes. Thus, it is important to understand the relationships between traffic volumes, signal timings, and lane configurations that could potentially affect the overall operations and safety of a signalized intersection. This section is divided into two subsections: the first outlines the different levels of

phasing operations, while the second provides a safety comparison of different left-turn phasing alternatives.

2.2.1 Left-Turn Phasing Operations

To prevent conflicts at intersections where left-turn movements occur, different left-turn phasing alternatives are applied. Three major left-turn phasing alternatives used for left-turn movements are permitted, protected, and protected-permitted. As explained by the *Manual on Uniform Traffic Control Devices* (MUTCD) the permitted phasing provides no exclusive phase for left-turn movements. Instead, it requires yielding to both opposing traffic and pedestrians. By contrast, the protected left-turn phasing provides an exclusive phase in which left-turn movements can occur uninterrupted. The protected-permitted left-turn phasing is a combination of the two phasing alternatives, allowing both a protected and a permitted phase for left-turn movements. The protected and permitted phases in this left-turn treatment are balanced with each other based on operational demands for the intersection (FHWA 2009).

Generally, left-turn movements are performed from single left-turn lanes and most research studies on safety and mobility assume this lane configuration. However, dual left-turn lanes are also used frequently to improve throughputs of left-turn phases. In the case of dual left-turn lanes, the UDOT left-turn phasing guidelines recommend that left-turn movements be exclusively protected to ensure the safety and operational efficiency of both the left-turn and opposing movements. Because of this, dual left-turn lanes are generally not considered in the discussion of left-turn decision boundaries.

2.2.2 Difference in Safety Between Left-Turn Phase Alternatives

Each left-turn phasing alternatives has different safety and mobility benefits. The more protection a left-turn treatment has, the more safely left-turning vehicles can complete a movement at a given intersection. However, as protection increases, mobility tends to decrease. A study performed by the University of Utah concluded that whereas permitted left-turn phasing tends to be better from a mobility standpoint, it tends to be less safe than protected-permitted or protected phasing (Shea et al. 2016). A before-after crash analysis performed by Agent (1979) supports this conclusion. Agent's study was carried out over a one-year period at three signalized intersections that had experienced a permanent change from protected to permitted left-turn phasing. The results of this analysis can be seen in Table 2-1.

Table 2-1: Crash Summary for Change from Protected to Permitted Phasing (Agent 1979)

Location	Crashes			
	Year Before Total	Year After		
		Total	Related*	Other
Tates Creek Road (KY 1974) at Gainesway Drive	14	17	7	10
Tates Creek Road (KY 1974) at New Circle Road (KY 4)	19	35	11	24
Harrodsburg Road (US 68) at New Circle Road (KY 4)	11	26	17	9

*Related to the permitted left-turn phasing

The Agent (1979) analysis showed that, whereas there were only 44 crashes in the year prior to making the phase change, 78 crashes occurred in the year after the phase change. In the case of these signalized intersections, the increase in crashes illustrates that the left-turn volume

vs. opposing volume cross product was too high for permitted phasing, demonstrating the need for a defined safety threshold to determine which phase type would be best for the site.

Research performed by Asante et al. (1996) evaluated different phasing alternatives and provided a rudimentary form of decision boundaries for these alternatives. In this study, the operational performance of left-turn phasing was examined under a controlled environment using microsimulation. Microsimulation provided a uniform and flexible environment, allowing control of the differences in local signalization policies among various jurisdictions. The study showed that protected-only left-turn phasing resulted in the highest delay. Protected-permitted left-turn phasing, on the other hand, yielded acceptable delays for left-turns, shared through/right-turns, and the total approach traffic. Thus, protected-permitted left-turn phasing may be preferable when it comes to mobility. Higher levels of protection are advisable as the left-turn vs. opposing volume cross product increases. Based on the Asante et al. (1996) study, permitted only phasing gives the lowest through movement and approach delays for all turning movements. However, fully permitted left-turn phasing without protected intervals should only be implemented when left-turn volume is under 100 vehicles per hour (vph) and opposing volumes are less than 300 vph and 600 vph for one and two opposing lanes, respectively. Above these volumes, protected or protected-permitted left-turn phasing is recommendable. Asante et al. (1996) indicated that this base boundary would also be flexible. For example, for safety reasons, full left-turn protection may be necessary for approaches with greater than 15 percent trucks in the total left-turning traffic. Shea et al. (2016), Agent (1979), and Asante et al. (1996)

reiterate that permitted left-turn phasing provides high mobility but lower safety, and fully protected left-turn phasing increases safety while lowering mobility.

However, a study performed by Chen et al. (2015) cautioned that any left-turn phasing should be carefully selected and implemented by considering trade-offs between safety and mobility. This may include factors such as crash experience, traffic flow, heavy vehicle percentage, and intersection geometry.

2.3 UDOT Left-Turn Phasing Guidelines

UDOT published their most recent guidelines for left-turn phasing at signalized intersections on November 13, 2014. These guidelines are presented in Figure 2-1 (UDOT 2014). According to these guidelines, the analyst must first choose between three options based on the left-turn volume on each approach of the intersection: below 100 vph, between 100 and 250 vph, or over 250 vph. Each of these options leads to the next criterion in the flowchart. As the left-turn phasing guidelines flowchart is followed, the 'yes or no' questions need to be answered. Once all the criteria on the flowchart have been answered, the flowchart yields the recommended left-turn phasing for each approach of the intersection (UDOT 2014).

The flowchart can be broken down into four main parts: volume-based warrants, dual left-turn signal warrants, history of severe left-turn crashes, and cycle failure/queuing issues. The following subsections present a brief discussion of each part.

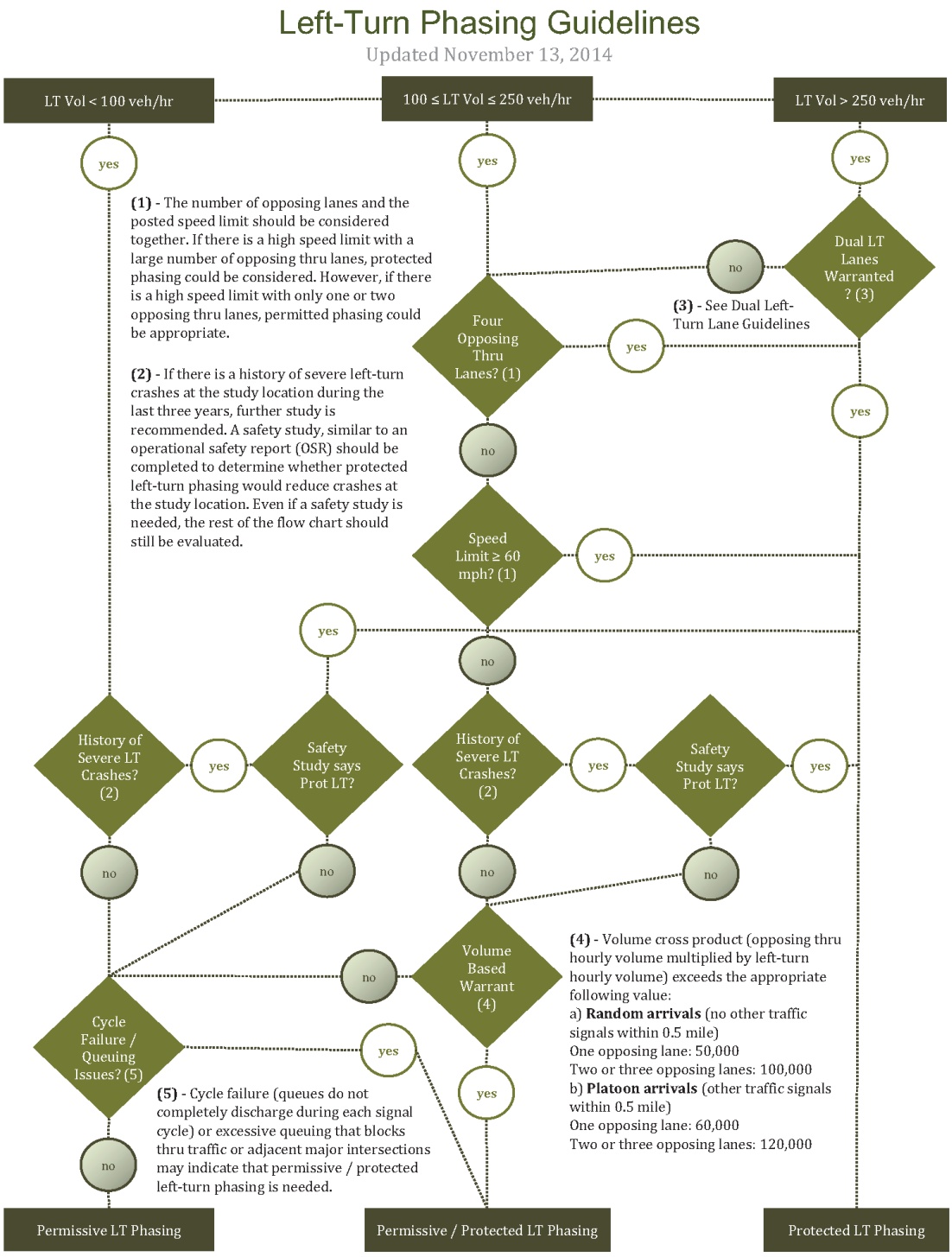

Figure 2-1: UDOT Left-Turn Phasing Flowchart (UDOT 2014).

2.3.1 Volume Based Warrants

Volume-based warrants include volume cross product thresholds, where the cross product is defined as the left-turn volume multiplied by the opposing through volume. These thresholds are shown in Table 2-2 (UDOT 2014). The volume threshold is based on the number of opposing through lanes and the type of arrival. It should be noted that UDOT does not currently include right-turn volumes in its opposing through volume counts. With respect to the volume-based warrant section of the UDOT left-turn signal warrants, a hybrid of the cross product threshold guidelines given by the FHWA (FHWA 2013) and in the Highway Capacity Manual (HCM) 2010 Edition (TRB 2010) has been adopted. However, the actual volumes used in the cross product for the random arrival have been adopted from the HCM 2010 (UDOT 2014). The threshold consists of two different warrants depending on the type of arrival: random arrivals and platoon (or group) arrivals. Should the cross product for a given approach be above this threshold, some form of protection would be recommended.

Table 2-2: Current UDOT Volume Cross Product Thresholds (UDOT 2014)

Number of Opposing Lanes	Volume Cross Product	
	Random Arrivals	Platoon Arrivals
1	50,000	60,000
2 or 3	100,000	120,000
Adopted November 13, 2014		

Consideration has been taken to include the left-turn lane, opposing right-turn lane, and pedestrian volumes in the volume cross product. A study performed by Hales Engineering, in which they compared the volume cross products of several departments of transportation (DOTs), determined the proportion of right-turning vehicles to through vehicles based on the number of through lanes on each approach. This proportion did not include left-turning vehicles.

The results of the peak hour turning movement counts can be seen in Table 2-3 (Hales Engineering 2016).

Table 2-3: Proportion of Right-Turning Vehicles to Through Vehicles (Hales Engineering 2016)

Number of Through Lanes	Percent of Right Turns
1	42%
2	11%
3	14%

One alternative for including opposing right-turn vehicle volume in the volume cross-product calculations would be to increase the thresholds of the cross product proportionally to the percent of right turns. The potential volume cross product thresholds are shown in Table 2-4, assuming a proportional increase (Hales Engineering 2016). It has been recommended that more analysis be done on the volumes before selecting the exact percentages, as the Hales Engineering study represents only one such approach. The percentages outlined here are to be considered an example of a methodology that could be used to include right-turn volumes and other factors in volume cross product thresholds (Schultz et al. 2017)

Table 2-4: Potential Increase to UDOT Left-Turn Phasing Thresholds if Right-Turns are Included (Hales Engineering 2016)

Potential Increase to UDOT Left-Turn Phasing Thresholds			
Number of Opposing Lanes	Volume Cross Product		
	Random Arrivals	Platoon Arrivals	% Increase
1	70,000	84,000	40%
2 or 3	112,000	135,000	12%

If the change to the volume cross product to include the percentage of right-turning vehicles were implemented, the accuracy of the left-turn warrant procedure currently utilized by

UDOT could potentially be increased to match the field conditions of the intersection under study. However, the number of lanes in the downstream direction of the crossing approach would need to be considered, to account for the distance pedestrians have to cross and their impact to right-turning vehicles. Ultimately, the effects of including right-turn volume counts would need to be analyzed further to determine if these changes would overall positively or negatively impact the operations or safety of the intersection in question (Schultz et al. 2017).

2.3.2 Dual Left-Turn Signal Warrants

The UDOT guidelines for dual left-turn signal warrants are shown in Table 2-5. Although it has already been stated that dual left-turn situations will not be addressed in this research, it is still important to address decision boundaries associated with them to better understand possible alternatives for protected phasing decision boundaries. It should be noted that the table is to be used only in assisting to make the decision for dual left-turns and that the volume to capacity (v/c) ratio is calculated using HCM 2010 methods (UDOT 2014, TRB 2010).

Table 2-5: Dual Left-Turn Signal Warrant (UDOT 2014)

Left-Turn Volume (vph)	v/c Ratio of Opposing Through ≥ v/c	Recommend
250-269	0.95	Dual Left-Turn Lanes
270-279	0.75	Dual Left-Turn Lanes
280-319	0.65	Dual Left-Turn Lanes
320-359	0.60	Dual Left-Turn Lanes
360-389	0.55	Dual Left-Turn Lanes
390-420	0.50	Dual Left-Turn Lanes
≥420		Dual Left-Turn Lanes

Table 2-5 shows that there is an inverse relationship between the left-turn volume and the minimum recommended opposing through v/c ratios. In addition to the dual left-turn lane capacity analysis guidelines in Table 2-5, six other guidelines for deciding whether or not to implement dual-left-turns are provided in the UDOT guidelines (UDOT 2014):

1. The number of hours where left-turn volume meets the guidelines of Table 2-5. A comparison with the vehicle delays should be made during the other nonpeak hours in the day as well.
2. The lane usage and distribution should also be considered. For example, if the intersection is close to a freeway on-ramp, there may not be balanced lane utilization since vehicles will favor the lane providing the best access to the ramp. As such, unconventional configurations and usages will have different guidelines.
3. Consideration should be given for the need to minimize the left-turn green time on one approach so that added green time is available for other phases to reduce delays.
4. Compatibility of the dual left-turn lane protected phasing operations with the signal coordination should be evaluated.
5. The Region Traffic Operations Engineer and the Division of Traffic and Safety should be consulted before adding dual left-turn lanes when the peak hour left-turn volume is less than 420 vph.
6. If there is no opposing through movement, such as at a three-way “T” intersection, then no additional signal phase is needed. Consideration should then be given to opposing pedestrian phases, available right-of-way needed for the additional lane, and existing left-turn queue lengths at the intersection

2.3.3 History of Severe Left-Turn Crashes

The *Highway Safety Manual* (HSM) defines a crash as "a set of events that result in injury or property damage due to the collision of at least one motorized vehicle and may involve collision with another motorized vehicle, bicyclist, pedestrian, or object. Crash frequency is defined as the number of crashes occurring at a particular site, facility, or network in a one-year period" (AASHTO 2010). Crash severity is often measured using the KABCO scale, which is split into five categories of severity (AASHTO 2010). These categories are shown as follows, with their corresponding UDOT crash severity levels also shown (NHTSA 2017).

- K (UDOT level 5) - Fatal injury
- A (UDOT level 4) - Incapacitating injury
- B (UDOT level 3) - Non-incapacitating injury
- C (UDOT level 2) - Possible injury
- O (UDOT level 1) - No injury/Property Damage Only (PDO)

Each severity type corresponds to a monetary value for use in benefit-cost analysis. The primary source for the monetary values is FHWA (2018). UDOT has its own set values associated with determining the value of each crash severity type. However, it should be noted that the UDOT monetary values are based on previous values provided by FHWA. The major difference between the FHWA values and the UDOT values is that UDOT uses the same monetary value for the fatal (K) and disabling injuries (A). This has been done to balance the benefit of reducing fatal and serious injury crashes since the circumstances of each are often very similar. Disabling injuries may cost more over time than fatal crashes because of lingering medical costs and the potential of the persons involved in these incapacitating injuries being

prevented from ever working again (Saito et al. 2016). The FHWA and UDOT monetary values are presented in Table 2-6 and Table 2-7, respectively.

Table 2-6: Benefit Value per Crash Provided by FHWA for Each Crash Type (FHWA 2018)

Severity Description	KABCO Severity	UDOT Severity No.	Value
PDO	O	1	$11,900
Possible Injury	C	2	$125,600
Evident Injury	B	3	$198,500
Disabling Injury	A	4	$655,000
Fatal	K	5	$11,295,400

Table 2-7: Benefit Value per Crash Provided by UDOT for Each Crash Type (Wall 2016)

Severity Description	KABCO Severity	UDOT Severity No.	Value
PDO	O	1	$3,200
Possible Injury	C	2	$62,500
Evident Injury	B	3	$122,400
Disabling Injury	A	4	$1,961,100
Fatal	K	5	$1,961,100

2.3.4 Cycle Failure and Queuing Issues

Cycle failure was defined previously in Figure 2-1 as "queues that do not completely discharge during each signal cycle" (UDOT 2014). The cycle failure/queuing issues guideline of the flowchart can be seen in the bottom left hand corner of Figure 2-1. This part of the UDOT guideline is completed by quantifying the number or percent of cycles during which a queue did not completely clear the intersection during the allocated green interval. If there is a low number of times that queuing or split failure occurs for left-turn movements, permitted left-turn phasing

may be assigned. If there is a high number, protected-permitted left-turn phasing will be installed to reduce queuing and cycle failure (Searle 2017).

2.4 Time of Day Considerations

While knowing the left-turn phasing guidelines for UDOT is essential for this research, it is also important to consider the phasing practices of other states. Schultz et al. (2017) performed a survey of 44 states in the US; of these, 32 responded to questions of whether or not they use Flashing Yellow Arrow (FYA) signals for permitted left-turn phasing, as well as whether or not they use time of day signal phasing plans. The findings of this survey are shown in Table 2-8.

Table 2-8: Results of State Phasing Practices Survey (Schultz et al. 2017)

States that Utilize Time of Day Signal Phasing (16 States)	States that Have Warrants / Guidelines for Time of Day Signal Phasing (5 States)
Alaska Arkansas Delaware Florida Indiana Kentucky Minnesota Mississippi Nebraska New York North Carolina Texas Vermont Virginia Washington Wisconsin	Indiana Minnesota Mississippi Vermont Washington

Of the 32 respondents, only 16 utilize time of day signal phasing plans, or variable signal phasing. Of the 16, only 5 states utilize warrants or guidelines to enforce time of day phasing

practices like Utah does. The state entities analyzed the different times of day to find if a certain signal phasing can be warranted during those hours. Often, these states prefer to use protected-permitted left-turn phasing during off-peak hours of the day and protected-only left-turn phasing during the peak hours of the day (Schultz et al. 2017).

A study performed by Davis et al. (2015) attempted to identify the exact times of day at which permitted phasing should be changed to protected only phasing. The study included an analysis of the normalized risk of crashes at different times of day compared to a standard eight-hour turning movement count for a four-leg intersection with two opposing approach. The results of this analysis are shown in Figure 2-2. It is important to note that the dotted line represents the threshold at which the relative risk (the y-axis) goes above 1.00, representing a higher risk for crash occurrence than the standard intersection. Although this analysis is only applicable to the system studied by Davis et al. (2015), similar analyses could be performed for other systems, including those in Utah.

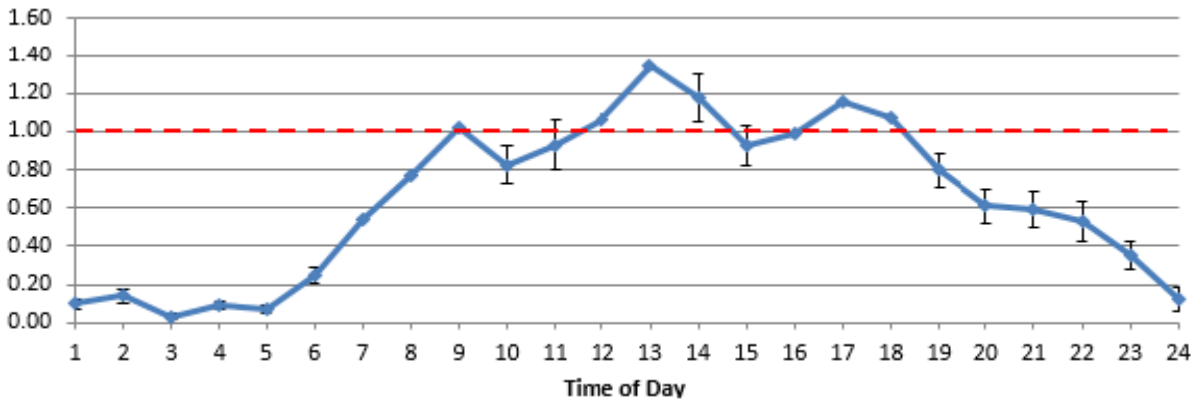

Figure 2-2: Analysis of crash risk by time of day (Davis et al. 2015), with normalized risk as the y-axis.

2.5 Comparison of Left-Turn Decision Boundary Alternatives

UDOT, as well as several other state DOTs, are looking for ways to improve left-turn phasing decision boundaries and guidelines. Several studies have been performed to better define decision boundaries between permitted, protected, and protected-permitted left-turn phasing. Each study has taken a different approach, but in many cases the studies have discovered similar boundaries between left-turn treatments that could be used. This section discusses several of these approaches and the resulting decision boundaries reported by the literature for permitted, protected, and protected-permitted left-turn phasing.

2.5.1 Permitted Left-Turn Phasing

Having a clear decision boundary for permitted phasing is important to ensure safety for left-turn and through movements. This being the case, most of the decision boundaries found in the literature between permitted and protected or permitted and protected-permitted left-turn phasing were fairly firm, offering little flexibility.

In a study performed by Stramatiadis et al. (2016), microsimulation in VISSIM and safety analysis with SSAM were used to develop left-turn decision boundaries between permitted and protected phasing for 1-, 2-, and 3-lanes opposing the left-turns. To analyze data for a broad range of circumstances, this study also varied the following parameters: opposing volumes, cycle length, percentage green time, and percentage of left-turn capacity used. The range of values for each of these parameters is shown in Table 2-9.

Table 2-9: Range and Increment of Simulation Input Parameters (Stramatiadis et al. 2016)

	Variables			
	Opposing Volumes (vph)	**Cycle Length (sec)**	**Green Time Percentage**	**Left-Turn Capacity Percentage**
Range	500-3000	90-210	30-70	20-100
Increments	500	30	10	20

Once data were collected for each of these parameters, a linear regression analysis was performed and an equation was derived to estimate the crossing conflicts, or $X_{Crossing}$, that might occur as shown in Equation 2-1.

$$X_{Crossing} = \frac{(LTDown^2 * OppVolOut * OpposingLanes^3)}{(\%Green^{\frac{1}{3}})} \quad (2\text{-}1)$$

Where:

$X_{Crossing}$ = Crossing conflicts

LTDown = Approaching left-turn volume

OppVolOut = Approaching opposing volume

OpposingLanes = Number of opposing lanes

%Green = Percentage of green time

Using the $X_{Crossing}$ value, the left-turn crossing conflicts can be estimated using Equation 2-2.

$$Left\ Turn\ Crossing\ Conflicts = 4.45 * 10^{-9} * X_{Crossing} + 0.144 \quad (2\text{-}2)$$

Using Equations 2-1 and 2-2, it was possible to estimate the crossing conflicts caused by left-turn movements, developing decision boundaries for instances of 1-, 2-, and 3-lane total opposing volumes. These decision boundaries define the point at which permitted phasing should be changed to protected phasing, and vice versa, as shown in Figure 2-3 (Stramatiadis et al.

2016). It should be noted that the x-axis represents left-turn volume while the y-axis represents opposing approach volume. This figure shows that the higher the number of opposing lanes, the lower boundary between permitted and protected left-turn phasing (assuming that the opposing volume is given in vehicles per hour per lane, or vphpl). Permitted left-turn phasing is recommended when combined left-turn and opposing volumes of an intersection fall below the threshold for permitted left-turn phasing of a given number of opposing lanes in Figure 2-3. Otherwise, protected or protected-permitted left-turn phasing is recommended, based on engineering judgment.

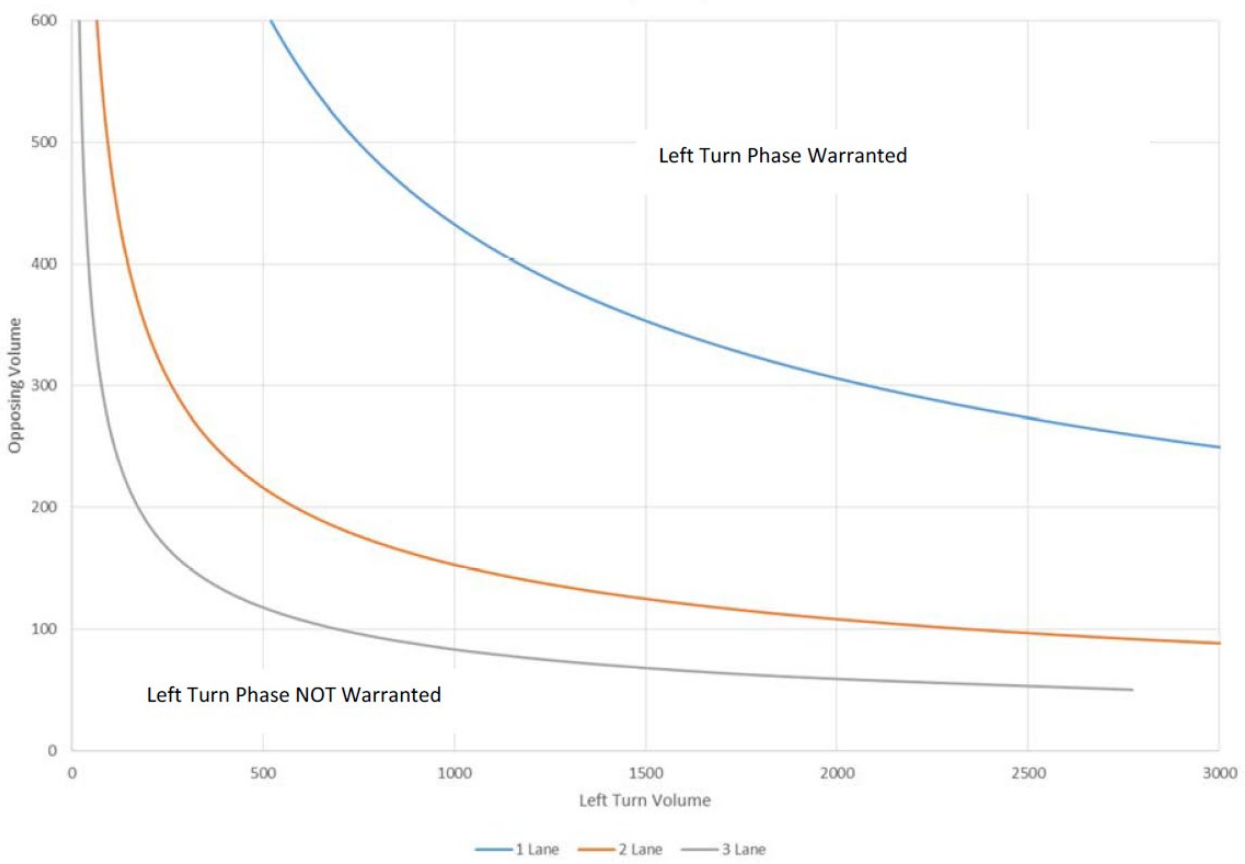

Figure 2-3: Left-turn decision boundaries (Stramatiadis et al. 2016).

The 1- and 2-lane boundaries for left-turn phasing type selection shown in Figure 2-3 match up very closely to similar boundaries for permitted left-turn phasing developed by Raessler and Yang (2017). Their research focused on evaluating the left-turn delay conditions at the boundary between different left-turn phasing configurations to establish practical guidelines and tools to facilitate the creation of left-turn decision boundaries. They used delay points derived from a Synchro non-linear analysis of scenarios comparing a permitted single left-turn lane and a protected permitted single left-turn lane. Only a 2-lane opposing approach configuration was tested in this study. Figure 2-4 shows the derived decision boundaries with the x-axis representing opposing volume and the y-axis representing left-turn volume, which is opposite of the decision boundaries derived by Stramatiadis et al. (2016), but more common in the literature. The boundary between the permitted and protected-permitted left-turn phasing alternatives, shown as the solid red line, is very similar to those derived for the 2-lane approach by Stramatiadis et al. (2016). The boundary between protected-permitted and protected left-turn phasing is denoted by the transition zone between the dotted green and the dotted grey lines, with the grey area between the lines symbolizing that either protected or protected-permitted phasing could be acceptable.

The left-turn delay (seconds/vehicle) for the permitted single left-turn lane option was obtained using Equation 2-3 (Raessler and Yang 2017).

$$D_I = 0.14 * V_{LT}^{.28} * V_{OPP}^{.56} \quad (2\text{-}3)$$

Where:

D_I = Average delay in seconds per vehicle (sec/veh)

V_{LT} = Left-turn volume in vph

V_{OPP} = Opposing volume in vph

The average delay for the protected-permitted phasing for the single left-turn lane case is obtained using Equation 2-4 (Raessler and Yang 2017).

$$D_2 = 0.66 * {V_{LT}}^{0.09} * {V_{OPP}}^{0.46} \quad (2\text{-}4)$$

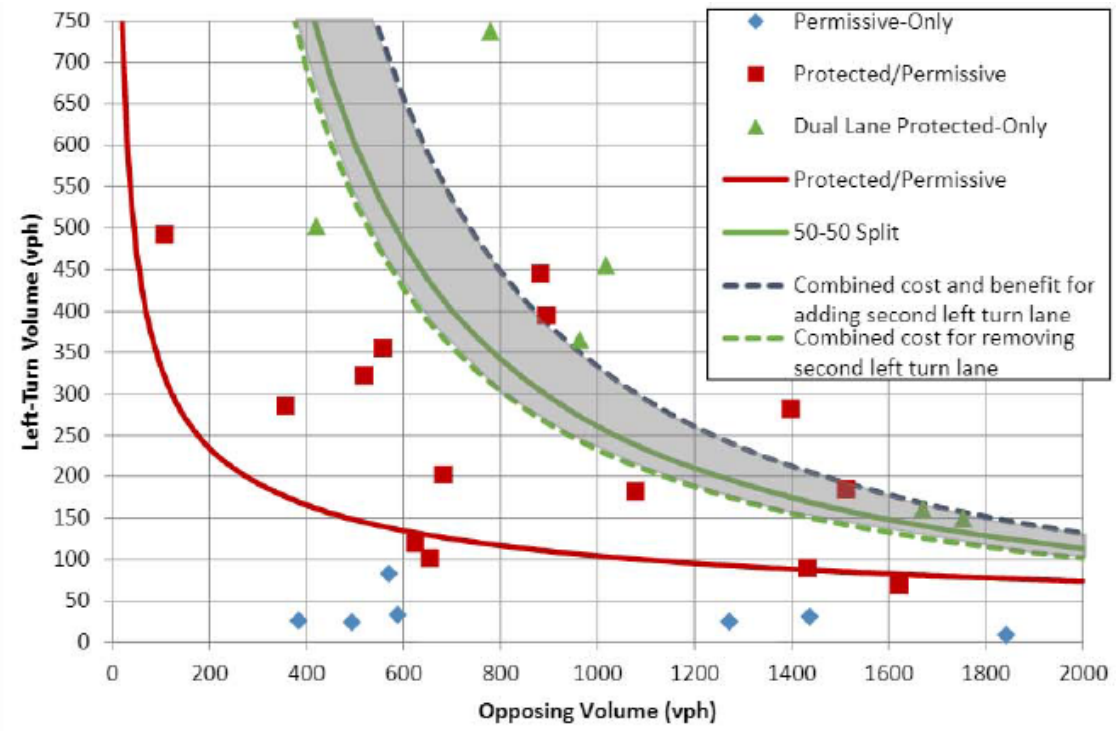

Figure 2-4: Concept validation using existing configurations and traffic counts (Raessler and Yang 2017).

Setting D_1 in Equation 2-3 equal to D_2 in Equation 2-4 and raising both sides of the equation to the power of 7.42, Equation 2-5 is obtained. Raising both sides to the power of 7.42 is used to set the cross product constant to 100,000 for consistency with the base product analysis equation (Equation 2-6), which consistently has 100,000 as the cross product constant (Raessler and Yang 2017).

$$100{,}000 = {V_{LT}}^{1.41} * {V_{OPP}}^{0.74} \quad (2\text{-}5)$$

$$100{,}000 = {V_{LT}}^1 * {V_{OPP}}^1 \quad (2\text{-}6)$$

Equation 2-5 is referred to as the "Simulated Analysis," and was compared to the traditional cross product analysis equation, Equation 2-6, also known as the "Product Analysis." Equation 2-5 was used as the boundary between permitted and protected-permitted left-turn phasing, labelled as "protected/permissive" in Figure 2-4. The similarities in the boundaries between permitted and protected-permitted left-turn phasing derived by Stramatiadis et al. (2016) and Raessler and Yang (2017) confirm that a consistent boundary can be derived for this decision boundary. However, the boundaries that have been derived between protected-permitted and protected left-turn phasing are not as consistent.

2.5.2 Protected Left-Turn Phasing

The protected left-turn phasing boundary is essential, but can be difficult to derive because it requires balancing not only safety and efficiency of left-turn movements, but also the additional financial costs required to implement protected left-turn phasing. This is particularly the case when considering dual left-turn lanes, which require extensive changes to intersection geometry.

Stramatiadis et al. (2016) and Raessler and Yang (2017) both developed boundaries for protected left-turn phasing. In the case of Stramatiadis et al. (2016), the same boundary used for permitted left-turn phasing for 1-, 2-, and 3- lanes can be used for protected left-turn phasing. As shown previously in Figure 2-3, at any intersection with left-turn and opposing volumes that fall above the corresponding boundary, protected left-turn phasing would be recommended. However, Raessler and Yang (2017) derived a more flexible decision boundary between protected-permitted and protected left-turn phasing, specifically for protected dual left-turn lanes.

The protected left-turn phasing boundary, shown previously in Figure 2-4 as "50-50 Split," (so named because it was assumed that the dual left-turn lanes would have a 50-50 split of left-turn volume) was derived in a similar fashion to Equation 2-6. The derived equation for protected left-turn phasing is shown in Equation 2-7. Note that, like with the permitted boundary shown in Equation 2-5, the "130,000" is a cross product constant, but for protected left-turn phasing rather than permitted.

$$130{,}000 = {V_{LT}}^{0.89} * {V_{OPP}}^{1.04} \quad (2\text{-}7)$$

The protected phasing decision boundary derived by Raessler and Yang (2017) also took into account construction and maintenance costs and the safety impact. To do so, the outputs of Equation 2-7 were shifted downward 1 percent to create a range of tolerance to change from protected dual left-turn lanes to protected-permitted left-turn phasing and upward 6 percent to create a range of tolerance to change from protected-permitted left-turn phasing to protected dual left-turn lanes. The exact percentages for these shifts were found by doing an analysis of financial costs for adding or removing protected phasing, and are shown as the green and blue dashed lines in Figure 2-4. These tolerance ranges were intended to show the areas in which engineering judgment can be made for intersections with unusual conditions.

Although the two studies described here are similar for the boundary between protected-permitted and protected left-turn phasing, one major difference is the range of tolerance between protected-permitted and dual protected left-turn phasing provided by Raessler and Yang (2017), which is useful for providing flexibility to engineers and planners. Applying principles from the Raessler and Yang study, it would be possible to create a range of tolerance not only between protected-permitted and dual-lane protected left-turn phasing, but between protected-permitted and single-lane left-turn phasing as well.

2.5.3 Protected-Permitted Left-Turn Phasing

Protected-permitted left-turn phasing has perhaps the most flexible decision boundaries, due to the fact that the split of a given left-turn movement could be adjusted to include either a long or short protected left-turn phase. Although the Raessler and Yang (2017) approach did consider protected-permitted left-turn phasing and provided flexibility for when to switch from protected-permitted to protected left-turn phasing, there are other approaches that also looked at this particular phasing alternative.

One such study was completed by Radwan et al. (2013). This study was completed in two phases. Both phases addressed the implementation of variable left-turn phases and presented the framework for a decision support system (DSS) for the dynamic evaluation of left-turn phasing in Central Florida. The purpose of the DSS framework was to allow "an interactive evaluation of left-turn phasing and ultimately recommend phasing by time of day and Traffic Management Center (TMC) data to be fed into the DSS so that intersections requiring attention/modification of left-turn [phasing] can be flagged" (Radwan et al. 2013). The variables tested as part of calibrating this system are shown in Table 2-10. Such a system would provide high flexibility, particularly in cases of protected-permitted left-turn phasing.

Using the system developed by Radwan et al. (2013), the phasing of a given intersection could be determined dynamically, allowing different levels of protection based on the time-of-day demand. Another study performed by Chalise et al. (2017) worked toward a similar goal of more dynamic decision boundaries for left-turn phase alternatives. The authors used VISSIM to simulate a base scenario and alternative scenario of the protected left-turn phase. Several parameters were taken into account in the research and VISSIM modeling, such as time of day, hour, land use, area type, crossing lanes, permitted green times, permitted left-turn volume, total

left-turn volume, left-turn truck percentage, and left-turn delay. A statistical analysis was then conducted to validate the model using JMP software (SAS 2018). The results of these analyses are summarized in Figure 2-5 and Figure 2-6. It should be noted that the percent reduction in delay refers to left-turn delay.

Table 2-10: Base Variables Used to Calibrate DSS Model (Radwan et al. 2013)

Traffic Data	Crash Data	Signal Data	Geometry Data	Land Use
Left-turn traffic volume	Historical crash data (1-3 years)	Signal timing plans	3-leg/4-leg/5-leg	Residential (urban/rural)
Opposing through traffic volume	Number of left turn-related crashes	Mode	Number of conflicts or sight obstructions (bike/ped crossings)	Commercial (urban/rural)
Heavy vehicles percentage	Driver behavior (aggressive or nonaggressive)	Sequence	Left turn storage length	Downtown (mixed use)
Left-turn delay	Bike and pedestrian count	Cycle length	Number of lanes	Tourist area
Through delay		Platoon progression (coordinated or isolated)	Posted speed limits	School zone (school/ped crossings)
Volume to capacity ratio on both approaches		Number of failed cycles	Criteria (wide/skewed/median/ramp terminal/single lane)	
Headway (critical gap)		Splits	Crossing lanes (opposing plus exclusive lanes)	
Queueing conditions		Signal display		

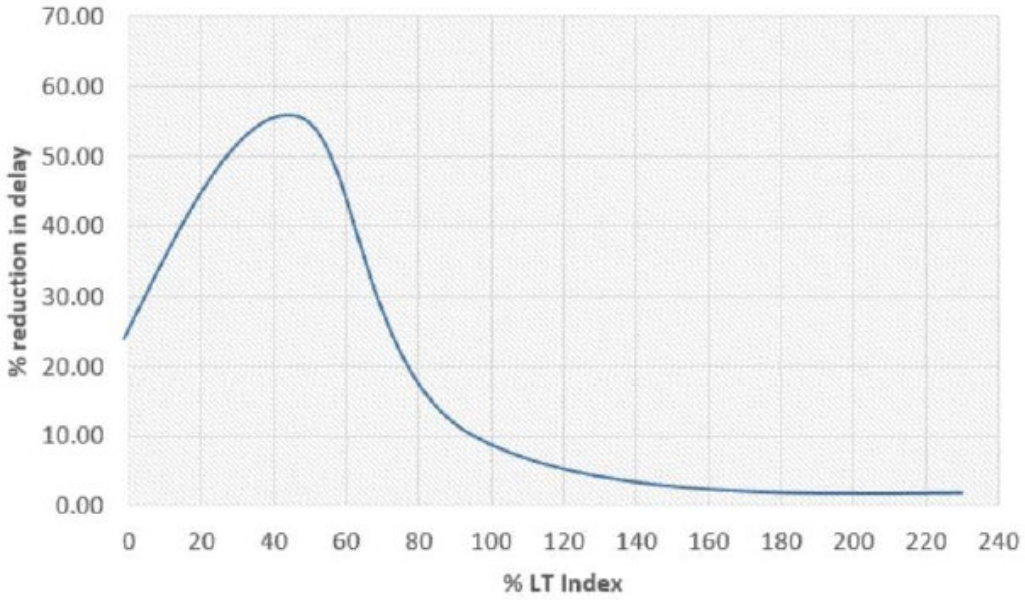

Figure 2-5: Threshold for two opposing lanes (Chalise et al. 2017).

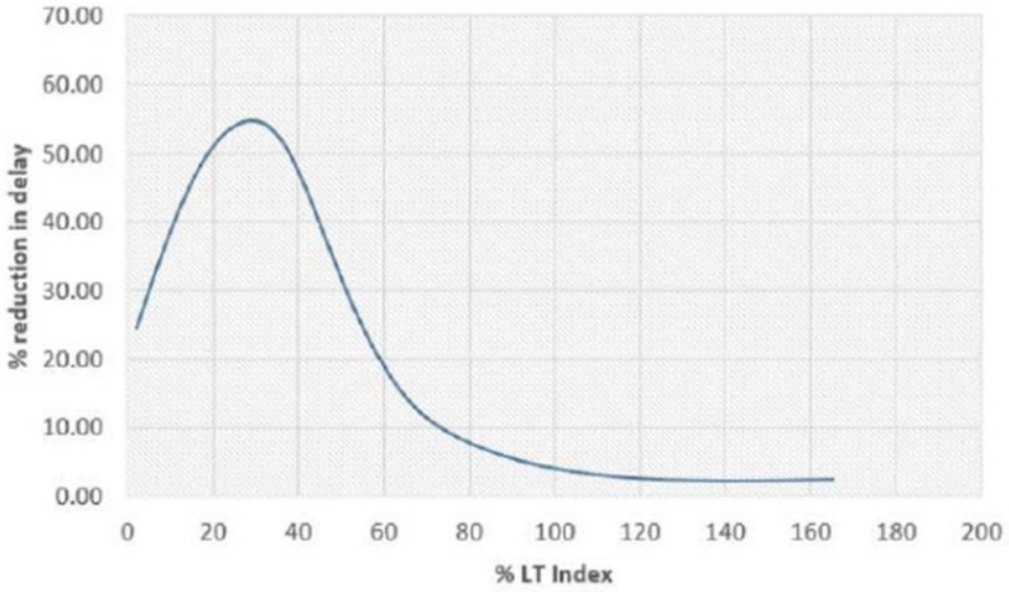

Figure 2-6: Threshold for one opposing lane (Chalise et al. 2017).

The Percentage Left-Turn Index (*% LT Index*) in Figure 2-5 and Figure 2-6 is calculated by multiplying the percentage of left-turn volume during the permitted left-turn phase by the percentage of opposing volume during the same permitted left-turn phase, the outcome being

divided by the percentage of permitted green time in an hour as illustrated in Equation 2-8. Upon completion of the second phase of their research project, it was found that the variables used by the DSS to calculate the %LT Index were yielding a high correlation between the selected independent and dependent variables, with a coefficient of correlation reaching $R^2 = 0.9$ (Radwan et al. 2016).

$$\%\ LT\ Index = \frac{\left(\frac{PT\ V_{LT}}{Tot\ V_{LT}} * 100\right) * \left(\frac{PT\ V_{OPP}}{Tot\ V_{OPP}} * 100\right)}{\left(\frac{PT\ Green\ Time}{3600} * 1000\right)} \quad (2\text{-}8)$$

Where:

Percent V_{LT} = Left-Turn Volume during the Permitted Time

Percent V_{OPP} = Opposing Volume during the Permitted Time

Tot V_{LT} = Total Left-Turn Volume in vph

Tot V_{OPP} = Total Opposing Volume in vph

Percent Green Time = Permitted Green Time in seconds

The thresholds shown previously in Figure 2-5 and Figure 2-6 use the left-turn and opposing through volume during the permitted left-turn phase with the total volumes and permitted phase duration to create a safety index for different levels of protection under protected-permitted left-turn phasing. The left side of the peak %LT Index in both figures expresses areas with low left-turn flow or completely protected left-turn phasing, whereas the right side express areas of either high left-turn flow or completely permitted left-turn phasing (Chalise et al. 2017). This model is very dynamic, providing a flexible protected-permitted left-turn decision boundary with similar functionality to Raessler and Yang (2017) and Stramatiadis et al. (2016) without having to create a DSS to evaluate left-turn phasing in real-time, as with Radwan et al. (2017). Whatever decision boundary is chosen for protected-permitted phasing, it is important to note that it must be flexible, taking into account both left-turn and opposing

volumes as well as the percentage of time that the left-turn movements are permitted. Whereas the permitted to protected-permitted left-turn phasing boundary can be more static, a more flexible boundary should exist between protected-permitted and protected left-turn phasing.

2.6 Chapter Summary

The purpose of this chapter was to provide a review of literature pertinent to both left-turn phase decision boundaries and possible improvements to time-of-day changes in left-turn phasing. The review discussed literature on the current state of signal phasing followed by research projects that have developed both decision boundaries between left-turn phasing alternatives and boundaries for effectuating time-of-day phase shifts.

There are three typical left-turn phasing alternatives to accommodate left-turning vehicles. The first is permitted phasing, which requires left-turning vehicles to yield to all opposing traffic. The second is protected phasing, which gives an exclusive phase to left-turning vehicles that is uninterrupted by opposing traffic. The third is protected-permitted phasing, which is a combination of the two other phase alternatives that provides both exclusive phasing to left-turn movements and time where left-turning vehicles yield to opposing traffic. UDOT uses these three left-turn phasing alternatives, applying them to one-lane left-turn approaches. Additionally, UDOT uses dual left-turn lanes, exclusively applying protected phasing to this lane configuration. Dual left-turn lane configurations will not be considered in this research, because in Utah they always have fully protected phasing and thus can be addressed under the single-lane protected left-turn phasing boundary.

The literature review on decision boundaries for left-turn phasing alternatives indicated that the boundaries between permitted and protected-permitted or protected phasing tended to be

well defined. While the approaches used to create these boundaries were different among the references reviewed, their boundaries tended to be comparable. Approaches taken to create decision boundaries between protected-permitted and protected left-turn phasing tended to yield boundaries with more flexibility. This was attributed to the fact that the amount of time dedicated to a protected portion of the protected-permitted left-turn phasing can vary based on different factors found at intersections. Thus, when developing a decision boundary for protected-permitted left-turn phasing, more factors must be taken into account, and flexibility needs to be considered in setting a range for the boundary.

This literature review found that there is a need to further study left-turn operations and safety for multiple opposing approach lane configurations and develop decision boundaries for each configuration. Using the approaches learned in this literature review, the Brigham Young University (BYU) research team developed a method for creating and/or updating decision boundaries for UDOT. The next chapter of the report presents the method by which these boundaries were developed and analyzed.

3 ANALYSIS METHOD

3.1 Introduction

This chapter presents the method used to evaluate the safety and operational differences between left-turn treatments, including a before-after analysis of existing intersections and development of decision boundaries for left-turn phasing using microsimulation. This chapter consists of a discussion on the analysis of reported crash data, followed by a similar discussion on the analysis of simulated data, and a chapter summary.

3.2 Analysis of Reported Crash Data

The first step in the analysis method was to evaluate existing intersection data to determine safety impacts of various left-turn phasing alternatives. A list of UDOT-controlled signalized intersections that had received changes to the left-turn phasing of at least one approach was provided by UDOT, with information regarding the location, date of the change, approach(es) changed, and type of change in left-turn phasing. This list was supplemented by intersection data from a study performed by the University of Utah (Medina et al. 2019). The signalized intersections provided in this list were then assessed to determine which of them would be suitable for subsequent analysis. Members of the UDOT Technical Advisory Committee (TAC) specified that changes made in left-turn phasing needed to be recent enough to obtain reliable data but old enough that at least two years of crash data could be obtained. Intersections where only one approach experienced a change were not considered for the

analysis. Additionally, some intersections found in the list did not have traffic volume data available; since volume data was used to determine crashes per million entering vehicles (MEV), these intersections without volume data were not used.

The number of intersections in the final list was reduced to 26 intersections that met the data requirements for analysis. Intersections in the list were then grouped and compared by the type of left-turn signal phasing change that took place: permitted to protected-permitted phasing, permitted or protected-permitted to protected phasing, and protected to protected-permitted phasing. Additionally, 10 intersections that had not experienced any change in left-turn phasing were analyzed as a baseline.

Crash data for each intersection were obtained from the UDOT crash database that records information about vehicle crashes in Utah (UDOT 2019b). This information includes the date of the crash, the intersection it occurred at, the approaches involved, and the type of crash that occurred. For each intersection, the crash data within three years of the change (for all signalized intersections in the UDOT-provided list with available data for three years) were selected. The "Intersection-related" filter was applied to ensure only crashes either caused by interaction with or within the intersection were included. If only two approaches had a change in left-turn phasing, an additional filter was applied that limited results to crashes that involved at least one vehicle on the approaches of interest.

Once the data were obtained for each intersection, two analyses were performed. The first analysis looked at the total crashes at the intersection, whereas the second analysis looked at only the left-turn-related crashes. In both analyses, the crashes within the date range corresponding to each intersection were exported to .csv files, and crashes that fell outside of the required range of three years before the change in left-turn signal phasing and three years after were eliminated.

Crashes within a one-month buffer before and after the change were also eliminated to account for drivers that were unaccustomed to the change. The crashes before and after the change were then sorted first by the crash type then by injury severity. Various figures were created to compare these statistics and to show how the crashes changed from before the change to after the change. The crashes were also sorted by time of day and day of the week to determine if a trend could be identified. The numbers from both analyses were then summarized for each left-turn signal phasing change.

In addition to crashes, traffic volumes for each location were determined. Hourly volumes were determined from UDOT's Automated Traffic Signal Performance Measures (ATSPM) website (UDOT 2019a). The website displays, among other measures, the 15-minute volumes for each approach at UDOT-managed signalized intersections across the state. As this system is relatively new, some intersections did not have accurate volume data available, further limiting the total number of intersections that could be analyzed. Volume data near the date of the change in left-turn signal phasing was mostly unavailable, so weekday dates were chosen at random (avoiding holidays, other irregular volume days, and Fridays). From this data, peak hour volumes were determined and included in the respective summary file for each intersection. Annual average daily traffic (AADT) was also determined from UDOT's "Traffic Maps" page (UDOT 2018). The AADT values from one year before the change in left-turn signal phasing took place and one year after the change were also included in the summary reports.

Additionally, various ratios of crashes were found to further supplement the analysis, determined from the AADT values. Ratios were calculated by dividing the number of crash types by the total number of crashes with the approaches that experienced a change in left-turn signal phasing. The total number of crashes per MEV for each intersection was calculated by dividing

the number of crashes by AADT, the number of days per year, and the number of years of analysis, as shown in Equation 3-1 (AASHTO 2010).

$$RMEV = \frac{1{,}000{,}000 * C}{365 * N * AADT} \quad (3\text{-}1)$$

Where:

$RMEV$ = Crash rate per MEV

C = Number of crashes

N = Number of years

$AADT$ = Annual Average Daily Traffic Volumes

A third analysis was performed with a set of 10 additional intersections. This third dataset included UDOT-controlled intersections that experienced no change in left-turn signal phasing during the study period, determined using Google Maps Street View imagery. Intersections selected were spaced out across the Salt Lake Valley rather than all in the same municipality. These intersections operated with protected-permitted left turn phasing. An identical analysis to the previous two analyses was performed for this collection of intersections. This dataset is meant to act as a baseline, from which the two previously described analyses can be compared against.

In summary, for each analysis, graphs were created from the compiled data previously discussed to compare the changes in crash occurrence from before the change in left-turn signal phasing to after for each intersection analyzed. An additional analysis involving the timeline of all crashes from all intersections that experienced a change in left-turn signal phasing was also included. Each crash was graphed according to the date of the event, and categorized as a "Before" or "After" event, indicating that the crash occurred either before or after the change in

left-turn phasing. To confirm trends observed, a preliminary statistical analysis was also performed. These figures and a discussion on them will be provided in Chapter 4.

3.3 Analysis of Simulated Data

The second task of this project was to simulate intersections using VISSIM and analyzing conflicts, or near-misses, by SSAM to determine the number of potential crossing conflicts for different left-turn vs. opposing through and right-turn volume combinations. Using these potential crossing conflicts and volume combinations, it was possible to derive guidelines for decision boundaries that can be used by UDOT using MATLAB (MathWorks 2017) and JMP Pro (SAS 2018). This section will first outline analyses used in previous studies, followed by descriptions on the model building and analysis process including the model configurations, evaluation of gap-time in VISSIM, and determining conflict contours. The final sub-section will discuss the process of defining the final decision boundaries using the simulated data obtained.

3.3.1 Analyses Used by Previous Studies

To prepare for the analysis, a review of the literature was performed to determine which traffic simulation programs would be most useful to meet the objective of the study, as outlined in Chapter 2. During the literature review, it was determined that the VISSIM traffic modeling software can be used to create intersection and network models for use in the research (PTV 2015). Additionally, it was found that SSAM could be used to provide effective simulated safety analysis of signalized intersections whose results could be compared to the results of the analysis of actual crash data (FHWA 2008). SSAM is a program funded by the FHWA to help with safety analysis of intersections using conflict analysis. This program allows users to retrieve conflict

data for intersections by importing vehicle trajectory files from VISSIM or another traffic simulation software such as Aimsun or Paramics.

A study performed by Saito et al. (2017) analyzed the efficiency of using SSAM to analyze the safety of intersection and network models built using VISSIM. The authors divided a section of University Parkway between the I-15 interchange in Orem, UT and University Avenue in Provo, UT into seven sections. Each section was then analyzed by exporting trajectory files from VISSIM to SSAM, then extracting the conflicts generated in the section using SSAM. The focus of the analysis was to find the general relationship between the occurrence of conflicts in the simulation and the actual crash occurrences along the stretch of University Parkway.

A statistical analysis of the results of this study found that a comparison between the simulated conflicts and actual crashes along the section studied resulted in none of the relation indices being outside of the 95 percent confidence interval. These relation indices were calculated as a ratio between the number of crashes of a given crash type and the number of conflicts estimated. The study concluded that SSAM could be used effectively to evaluate safety impacts of access management alternatives (Saito et al. 2017).

Upon establishing the usefulness of SSAM as a safety assessment software, it was important to also identify a possible method that could be used to model both theoretical and actual intersections or networks to analyze using SSAM. One such methodology was presented in a study performed by Saleem (2012). As with the study performed by Saito et al. (2017), this study used SSAM to analyze conflicts contained within trajectory files exported from VISSIM. However, this study began with building its models in Synchro, because of the ease of use of the program. Once the models were created, they were exported into .csv files and then imported into VISSIM. This transfer from Synchro to VISSIM allowed for the creation of complicated

intersections easily using Synchro making them compatible with SSAM using the trajectory file export function in VISSIM.

The study in this report will use a similar methodology to both Saito et al. (2017) and Saleem (2012), building models in VISSIM for performing conflict analyses using SSAM, and using Synchro as a reference point for defining signal timing.

3.3.2 Simulation Model Configurations

A total of 12 models were built to develop decision boundaries for left-turn phasing. There were three different opposing lane configurations used: 1-, 2-, and 3-lane. For each lane configuration, four models were built to represent different left-turn treatments: a permitted-only model and three protected-permitted models with 10-, 15-, and 20-second green time for the protected portion of the phase, respectively. Additionally, a variety of scenarios were built for these base models using different left-turn and opposing through volume increments. Note that the total opposing through and right-turn volume for the 2- and 3-lane configurations were decided based on a lane capacity of 900 vph. As such, the 2-lane configuration tested up to 1,800 vph of opposing (through and right-turn) volume, and the 3-lane only tested up to 2,700 vph. Three simulations were run per scenario. The increments of approach volumes are different according to the number of opposing lanes, and they are presented as follows:

- 1-Lane Configuration:
    - 45 vehicles per increment for left-turns (60 vehicles for protected-permitted):
        - 450 vehicle maximum left-turn volume (600 vehicle maximum for protected-permitted)
    - 100 vehicles per increment for opposing volume:

        - 1,000-vehicle maximum opposing volume
    - 10 increments each for left-turn and opposing volume, for a total of 100 scenarios
- 2-Lane Configuration:
    - 30 vehicles per increment for left-turns (40 vehicles for protected-permitted):
        - 450-vehicle maximum left-turn volume (600-vehicle maximum for protected-permitted)
    - 120 vehicles per increment for opposing volume:
        - 1,800-vehicle maximum opposing volume
    - 15 increments each for left-turn and opposing volume, for a total of 225 scenarios
- 3-Lane Configuration:
    - 30 vehicles per increment for left-turns (40 vehicles for protected-permitted):
        - 450-vehicle maximum left-turn volume (600-vehicle maximum for protected-permitted)
    - 180 vehicles per increment for opposing volume:
        - 2,700-vehicle maximum opposing volume
    - 15 increments each for left-turn and opposing volume, for a total of 225 scenarios

The different left-turn and opposing volumes selected for each increment were chosen to match the maximum left-turn and opposing volumes selected by UDOT. Because 1,000/1,800/2,700 vph and 450/600 vph were selected for opposing and left-turn volume respectively (contingent on the lane configuration and type of left-turn treatment), these

maximum volumes were divided into 10 increments of volume each when the maximum volume was lower, and 15 increments of volume each when the maximum volume was higher to give more data points.

It should be noted that the model was built so that only the northbound and southbound approaches have traffic volume. Timing was optimized prior to building the model by building the same model in Synchro 10 (Trafficware 2018). All models were built using the following assumptions:

- Cycle length of 120 seconds
- Left-turn bay unrestricted in length
- Approach speed of 35 mph

In choosing the approach speed, UDOT recommended that models be built to determine whether the safety of the simulated intersections varied by change in speed. However, it was found that increasing the approach speed to 45 mph had no significant effect on safety for the simulated intersections. As such, 35 mph was selected as the approach speed for all models.

3.3.3 Evaluation of Gap-Time for VISSIM

In the beginning of the model building process, it had been proposed that the Conflict Area function in VISSIM would be used to define where vehicles would conflict. This was done to narrow the number of conflicts that would be recorded to trajectory files when simulations were run. However, during the process of exporting trajectory files, it was discovered that the Conflict Area function used an acceptable gap time that would make no left-turning vehicle conflicting with opposing vehicles in the conflict area. This prevented crossing conflicts from being generated in the trajectory files.

To make the simulation more realistic, the Priority Rule function was used instead of the Conflict Area function. The Priority Rule function of VISSIM is very similar to the Conflict Area function but the Priority Rule function distributes the gaps drivers will accept around a base accepted gap time that can be edited, allowing some vehicles in the simulation to accept gaps larger or smaller than the gap input. However, it was important to derive the accepted gap time to use for simulation that would adjust gap acceptance within VISSIM to better approximate actual driving conditions.

The default value for the gap time, entitled "Min. Gap Time," is set to 3.0 seconds for the Priority Rule function of VISSIM. However, this default value is for a merge movement case, and does not represent driver behavior for crossing (left-turn) movements. Based on the American Association of State Highway and Transportation Officials (AASHTO) *A Policy of Geometric Design of Highways and Streets* (AASHTO Green Book), the design value for gap time in the Case B3 – Crossing Maneuver is 5.5 seconds (AASHTO 2011). However, when testing this value, it was found that the 5.5-second gap prevented any crossing conflicts from occurring. This is most likely due to the fact that the maximum accepted gap time threshold defined by SSAM for a conflict to occur is approximately 3.0 seconds.

To find a time gap that would accurately represent a distribution of driver behaviors, time gaps were tested in 0.5-second increments from 1.5 seconds (assumed to be a case in which 100 percent of drivers would accept a gap below the safe level of 3.0 seconds defined by SSAM) to 5.5 seconds (assumed to be a case in which 0 percent of drivers would accept a time gap below safe levels). Ten simulations were run for each gap time increment. Once the crossing conflicts for each of these accepted gap time intervals were found, they were graphed and a tangential analysis was performed to determine when the time gap vs. crossing conflicts curve has an

inflection point. Tangent lines were drawn manually along the observed curve. An example of this analysis, performed for a specific volume combination within the permitted 1-lane case, is shown in Figure 3-1. This inflection point represented the point at which the time gap would allow for a plausible number of conflicts, based on VISSIM's pre-programmed driver behaviors, and the safe gap was found to be around 3.3 seconds within the bounds of these driver behaviors.

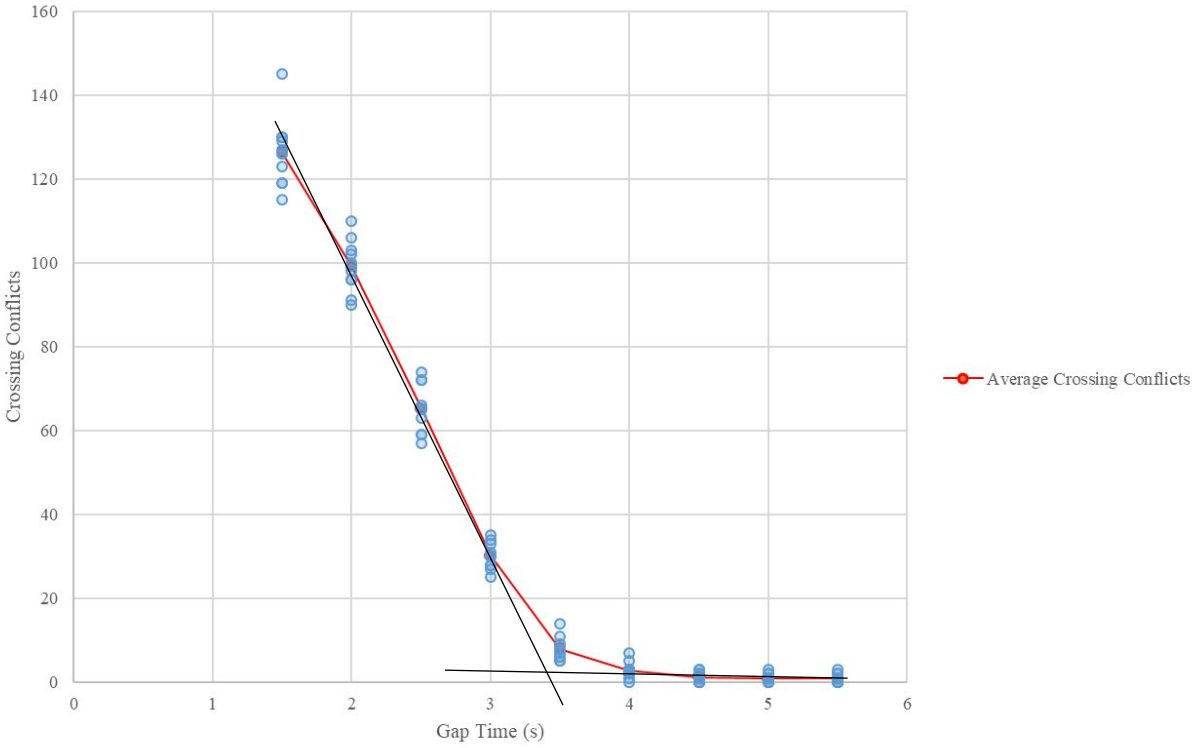

Figure 3-1: Example of time gap analysis.

To make sure that the 3.3 second gap time was representative of all volume combinations within the permitted 1-lane model, the following volume combinations were tested: 300 opposing vehicles to 270 left-turning vehicles, 400 opposing vehicles to 180 left-turning vehicles, 500 opposing vehicles to 225 left-turning vehicles, 600 opposing vehicles to 270 left-

turning vehicles, and 800 opposing vehicles to 180 left-turning vehicles. The observed time gaps and the resulting average calculated are shown in Table 3-1.

Table 3-1: Time Gap Analysis Results

Scenario	Observed Time-Gap (sec)
300 Opp 270 LT	3.3
400 Opp 180 LT	3.3
500 Opp 225 LT	3.4
600 Opp 270 LT	3.4
800 Opp 180 LT	3.3
Average	3.3

It was found that several of the opposing approach lane configurations and phase alternatives required slightly different gap times. As such, the previously stated method was repeated for all pertinent models. The final minimum gap times for all pertinent models are shown in Table 3-2.

Table 3-2: Time Gaps Used by Model

Configuration		Time-Gap (sec)
1-Lane	Permissive	3.3
	Protected-Permissive	3.5
2-Lane	Permissive	3.6
	Protected-Permissive	3.5
3-Lane	Permissive	3.7
	Protected-Permissive	3.7

3.3.4 Developing Conflict Contours for Contour Maps

Once all volume combination scenarios were run three times for each lane configuration and phase alternative, the trajectory files for these scenarios were analyzed using SSAM. The

SSAM conflict results were then saved as .csv files, and crossing conflicts were averaged and counted for each scenario. The counted conflicts were entered into MATLAB (MathWorks 2017) and various contour maps to derive decision boundaries. These contour maps demonstrate the change in conflicts as the left-turn and opposing volume increase for each lane configuration and phase alternative.

Using the contour maps created in MATLAB, basic decision boundaries could be identified by defining the point at which the conflicts begin to spike. It has been noted in previous discussions that this boundary will likely be established by finding an exact crossing conflict contour on each conflict contour map that represents an inflection point where a certain left-turn phase alternative would no longer be acceptable. To determine the conflict contour boundary for each model, the conflicts corresponding to the appropriate time-gaps were identified for each phase-alternative and lane configuration. An example of how to identify this from the previously performed time-gap analyses is shown in Figure 3-2, using the time-gap analysis chart from Figure 3-1. Using the chart, the exact conflict contour could be identified by drawing a line from the derived time-gap on the curve to the crossing conflict axis. As with the time-gap analysis, crossing conflicts used to create the conflict contour were gained for five different volume combinations and averaged for each pertinent model. Table 3-3 shows the resulting crossing conflicts to use for the contour maps, and the corresponding gap times for each model.

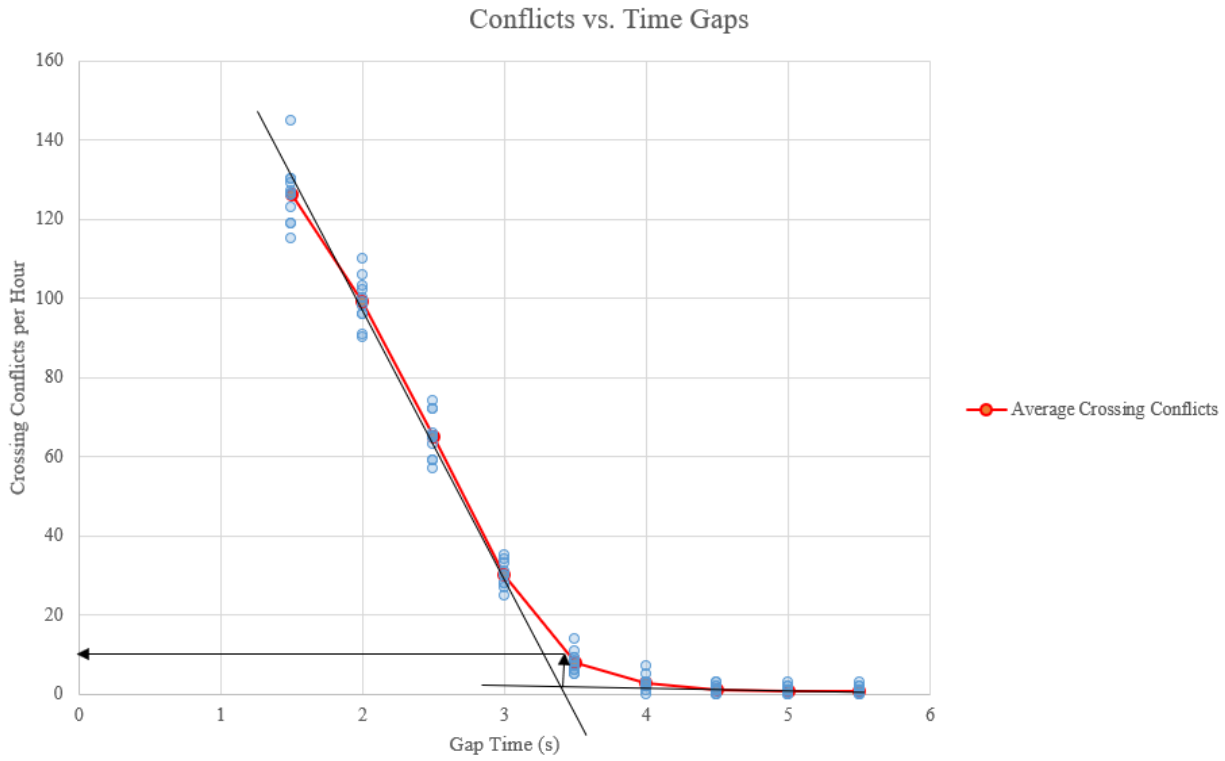

Figure 3-2: Conflict contour identification using the 1-lane time-gap analysis.

Table 3-3: Crossing Conflict Contours Used to Define Boundary Contours for Each Model

Configuration		Time-Gap (sec)	Crossing Conflicts per Hour
1-Lane	Permitted	3.3	10
	Protected-Permitted	3.5	25
2-Lane	Permitted	3.6	20
	Protected-Permitted	3.5	40
3-Lane	Permitted	3.7	30
	Protected-Permitted	3.7	95

Using these boundary values to create conflict contours, the maximum conflicts for the contour maps were defined for each model. The contour maps are described and analyzed in Chapter 5.

3.3.5 Defining Final Decision Boundaries

Once the conflict contour maps were defined for all 12 models (four for each lane configuration), final decision boundary equations were derived. To do this, left-turn vs. opposing volume combinations were extracted along the conflict contours depicted in each contour map. An example of the volume combinations, extracted along the contour of permitted 1-lane contour map, is shown in Table 3-4.

Table 3-4: Example of Volume Combinations Obtained from Conflict Contour for Permissive Left-Turn Phasing with 1-Lane Opposing Through Movements

Left-Turn Volume	Opposing Volume
450	100
405	100
360	100
315	100
270	200
225	200
135	300
135	400
90	500
90	600
90	700
90	800
90	900
90	1000

To develop an equation from these volume combinations, JMP Pro 14 statistical analysis software (SAS 2018) was used. A linear regression analysis was performed for each set of volume combinations to determine a predicted equation for each model. However, it can be noted from the contour maps in Section 5.1 that the observable decision boundaries are not linear. As such, a log transformation was done on both the left-turn and opposing volumes before

the linear regression analysis was performed. An example of the linear regression results as shown in JMP Pro for the permitted 1-lane case is shown in Figure 3-3. As shown in the analysis of variance table in Figure 3-3, the probability (p-value) is less than 0.001, which is less than the significance level $\alpha = 0.05$, indicating that the projected model is statistically significant when compared to the volume combination data points. The "Parameter Estimates" show the predicted model coefficients are also statistically significant. As such, the parameter estimates can be used to develop equations to model the volume combinations observed along the conflict contour in the contour map.

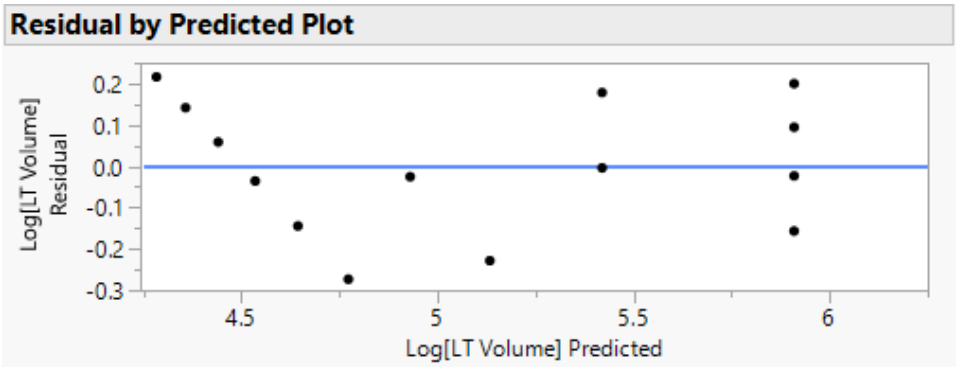

Summary of Fit

RSquare	0.940368
RSquare Adj	0.935398
Root Mean Square Error	0.164762
Mean of Response	5.112553
Observations (or Sum Wgts)	14

Analysis of Variance

Source	DF	Sum of Squares	Mean Square	F Ratio
Model	1	5.1369907	5.13699	189.2329
Error	12	0.3257567	0.02715	Prob > F
C. Total	13	5.4627474		<.0001*

Parameter Estimates

Term	Estimate	Std Error	t Ratio	Prob>|t|	Lower 95%	Upper 95%
Intercept	9.160735	0.297557	30.79	<.0001*	8.5124141	9.8090558
Log[Opp Volume]	-0.706049	0.051326	-13.76	<.0001*	-0.817879	-0.59422

Figure 3-3: Linear regression output example for the permitted 1-lane case.

Using the parameter estimates for each model, basic linear equations were derived. An example equation for the permitted 1-lane case is shown in Equation 3-2 using the parameter estimates given in Figure 3-3. The derived equations, however, model a linear version of the decision boundary. As such, the equations had to be transformed back from linear to non-linear form. An example of the format for this equation is shown in Equation 3-3.

$$Ln(V_{LT}) = 9.161 - 0.706 * Ln(V_{Opp}) \quad (3\text{-}2)$$

$$C = n * {V_{LT}}^{1} * {V_{Opp}}^{k} \quad (3\text{-}3)$$

Where:

C = Statistical intercept, transformed back from log form

n = Number of opposing lanes

V_{LT} = Left-turn volume (vehicles)

V_{Opp} = Left-turn volume (total vehicles)

k = Opposing volume statistical parameter estimate

An example of the final equation for the permitted 1-lane case given in Equation 3-4. All of the final decision boundary equations are reported in Section 5.3.

$$9519 = V_{LT} * {V_{Opp}}^{0.706} \quad (3\text{-}4)$$

3.4 Chapter Summary

The purpose of this chapter was to outline the methods used to evaluate both existing intersections and simulated data to delineate the difference between left-turn treatments and derive decision boundaries between these treatments.

In evaluating existing intersection crash data to identify differences between different types of phasing, a total of 36 intersections were evaluated. With the exception of the 10 baseline intersections, all intersections studied experienced some permanent change to their left-turn phasing. The crashes three years before and after were assessed for those intersections that had experienced no change or a change from protected to protected-permitted left-turn phasing. For those intersections that had experienced a change from permitted to protected-permitted left-turn phasing, two years of crash data were used to increase the sample size. Crash rates per MEV were derived as well as crashes by time of day.

To derive the decision boundaries, 12 models were built in VISSIM to simulate 1-, 2-, and 3-opposing-lane configurations as well as all permitted and protected-permitted left-turn treatments. Trajectory files were then exported from VISSIM for several volume combinations within each model and analyzed in SSAM to find the number of crossing conflicts for each volume combination. From these, contour maps were created in MATLAB and analyzed using JMP Pro to derive equations that estimate the decision boundaries for each model. From these base decision boundaries, final decision boundaries were developed for each lane configuration and confirmed with UDOT. The detailed results for these analyses are provided in Chapter 4 and Chapter 5.

4 EVALUATION OF LEFT-TURN PHASING CHANGES

4.1 Introduction

Existing Utah intersections were analyzed in several different ways to discover general trends in crash data after left-turn phasing was changed. The method for this chapter was outlined in Section 3.2. This chapter discusses the results of the crash data analysis, followed by a discussion of the possible sources of error, and a chapter summary.

4.2 Results of Crash Data Analysis

To assess the safety differences between left-turn treatments, crash data from existing intersections in Utah were analyzed in several different ways to discover trends. It is important to remember while observing these trends that, while clear outliers were removed, these are only general trends and are not meant to be used to make decisions for individual intersections because of the small sample size available to perform the analysis. Additionally, no disproportionate number of crashes, caused by driver adjustment to the changes in phasing were observed before or after the dates of each change in phasing. This section will first discuss the trends observed in the baseline analysis, followed by the trends from intersections that experienced a change from permitted to protected-permitted left-turn phasing and trends from intersections that experienced a left-turn phase change from protected to protected-permitted.

4.2.1 Baseline Trends

To create a baseline for comparison, 10 intersections that experienced no change in left-turn phasing were analyzed. The selected intersections are listed in Table 4-1. An arbitrary control date of January 1, 2015 (the approximate middle of the study period for the datasets that involved left-turn phase changes) was chosen and three years of crash data before and after this date were collected and analyzed.

Based on the results of the baseline intersection analysis, there did not seem to be a clear trend indicating an increase or a decrease in the number of total crashes, as shown in Figure 4-1. Individual intersections may have exhibited either a clear increase or decrease, but taking all baseline intersections into account at once yields no specific trend. Figure 4-2 displays the change in the ratio of injury-related crashes (crashes where UDOT severity levels 2-5 occurred) as a ratio of total crashes, and likewise exhibits no clear trend of an increase or a decrease from before the control date to after the date. Additionally, Figure 4-3 shows left-turn related crash rate in crashes per MEV, which also does not show any clear trend.

Table 4-1: Intersections Selected for Baseline

Location	Configuration
2300 E and SR-266 (4500 S), Holladay	1-Lane
SR-68 (Redwood Rd) and 12800 S, Riverton	1-Lane
SR-71 (700 E) and 10600 S, Sandy	2-Lane
SR-48 (7800 S) and 2700 W, West Jordan	2-Lane
4800 W and SR-171 (3500 S), West Valley City	2-Lane
SR-68 (Redwood Rd) and Shields Ln (9800 S), South Jordan	2-Lane
S Temple and SR-186 (N State), Salt Lake City	2-Lane
SR-71 (12600 S) and 2700 W, Riverton	2-Lane
SR-68 (Redwood Rd) and 1700 S, Salt Lake City	3-Lane
SR-268 (600 N) and US-89 (300 W), Salt Lake City	3-Lane

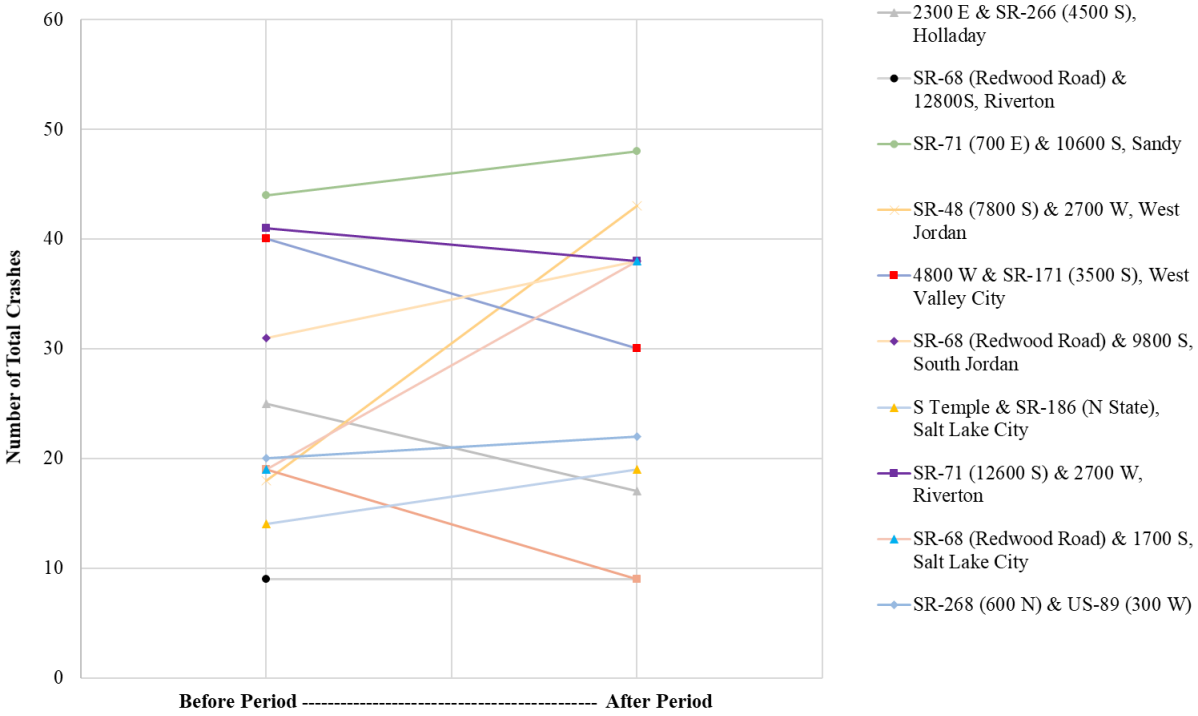

Figure 4-1: Total crashes (Baseline).

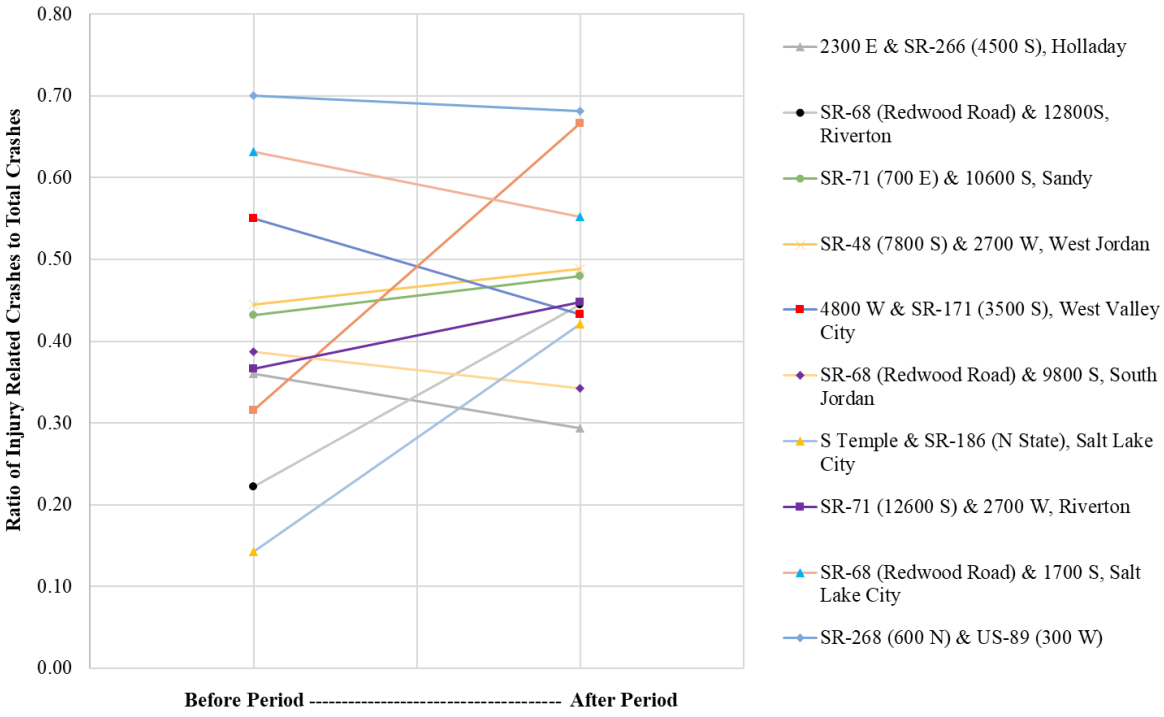

Figure 4-2: Injury related crashes as a ratio of total crashes (Baseline).

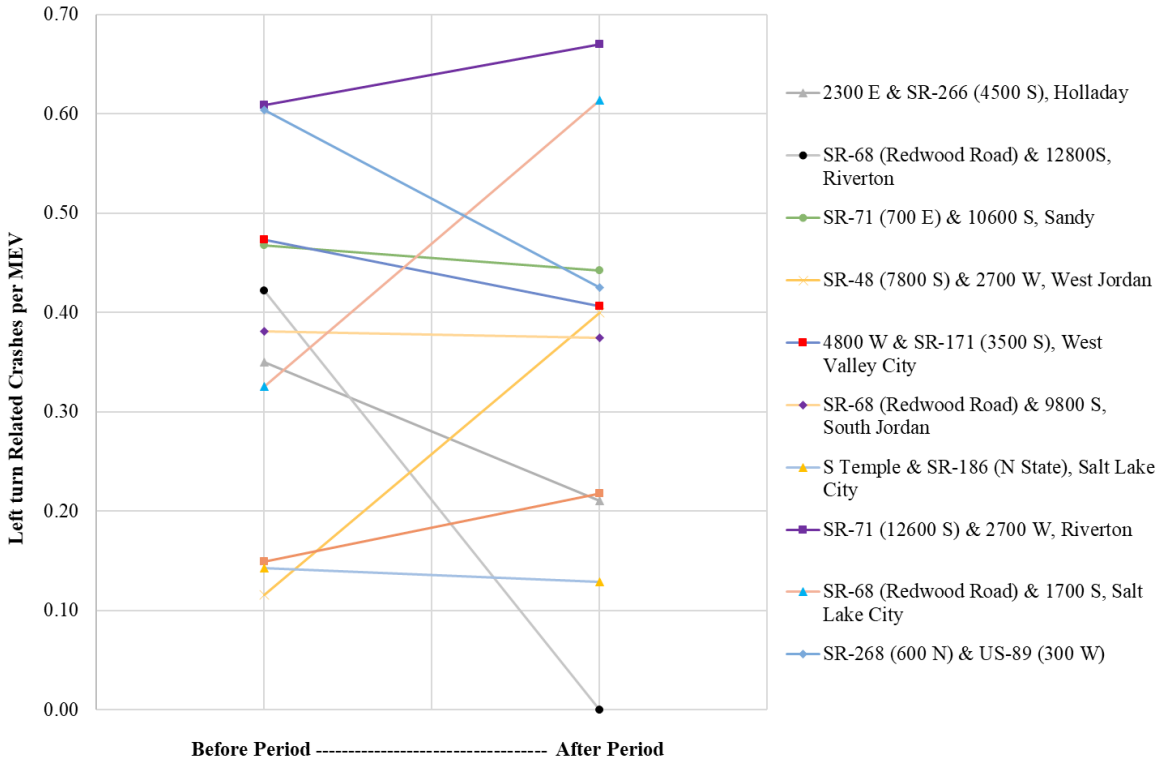

Figure 4-3: Left-turn related crashes per MEV (Baseline).

The total crashes and left-turn related crashes normalized by MEV at the 10 intersections where before-after analyses were performed are shown in Figure 4-4 and Figure 4-5, respectively. Figure 4-4 appears to display a slightly higher peak in crash rates during the typical afternoon peak traffic time (3:00-6:00 PM) after the control date compared to before. It appears to show a lower morning peak crash rate after the control date compared to before. The left turn crash rates displayed in Figure 4-5 appear to spike during the 12:00 PM and 3:00 PM hours, as well as during the night-time hours (11:00 PM – 5:00 AM) after the control date. These observed peaks will be used as a baseline when analyzing time of day graphs for the intersections that experienced changes in left-turn phasing.

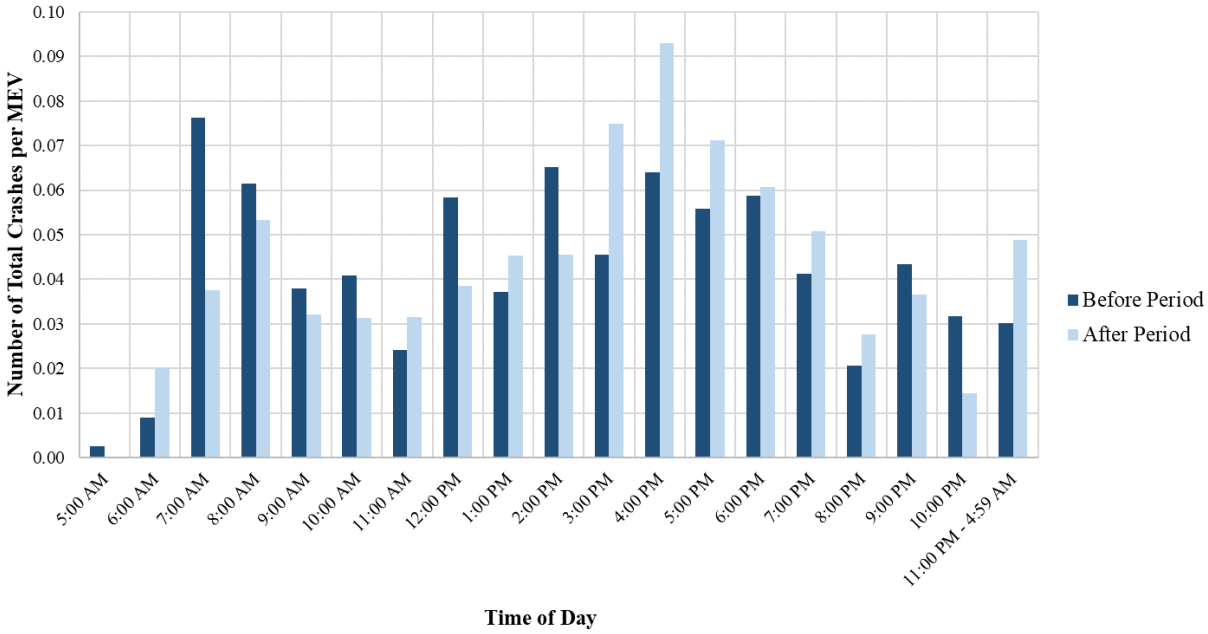

Figure 4-4: Total crashes per MEV by time of day (Baseline).

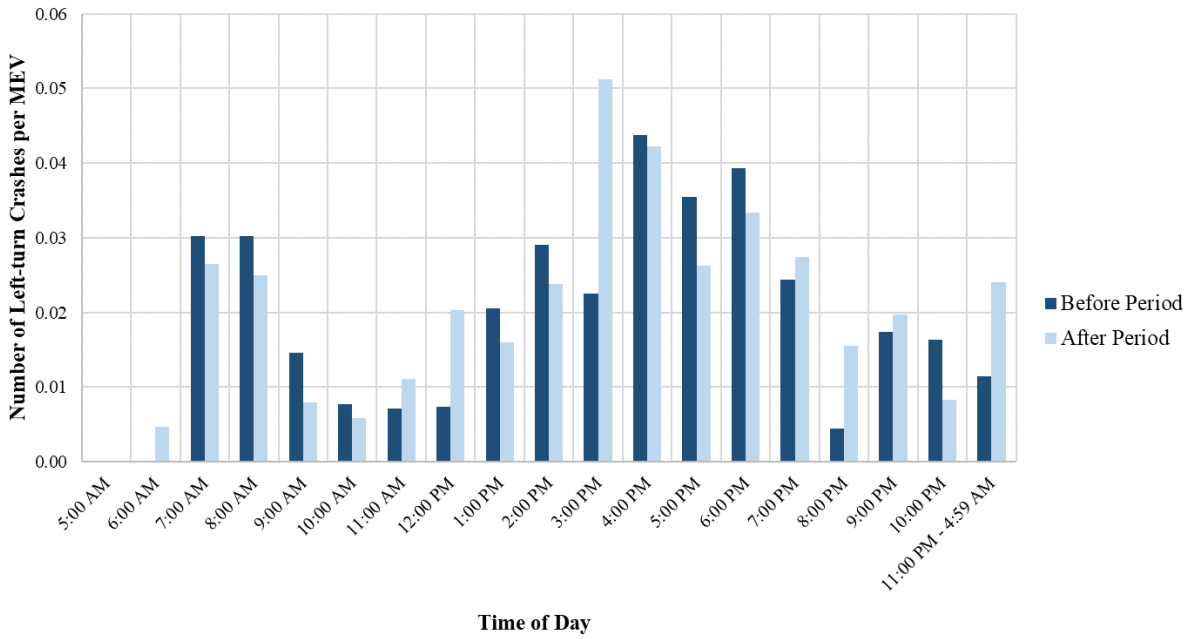

Figure 4-5: Left-turn related crashes per MEV by time of day (Baseline).

4.2.2 Permitted to Protected-Permitted Left-Turn Phasing Trends

Two years of crash data were analyzed before and after the phasing change for a total of 17 intersections that had experienced a change from permitted to protected-permitted left-turn phasing. The selected intersections are listed in Table 4-2. Figure 4-6 includes the results of the analysis, and shows a clear increase in total crashes. Figure 4-1, which represented the total crashes from the baseline analysis, doesn't show a clear trend with the increase in crashes, strengthening the theory that the increase in total crashes observed in Figure 4-6 may be connected to the change in left-turn phasing. However, this increase in crashes may still be caused by an increase in AADT or changes in intersection geometry.

Table 4-2: Intersections Selected that Changed from Permitted to Protected-Permitted

Location	Configuration
SR-235 (Washington Blvd) and North St, Ogden	1-Lane
SR-30 (200 N) and SR-252 (1000 W), Logan	1-Lane
SR-203 (Harrison Blvd) and SR-79 (30th St), Ogden	1-Lane
US-91 and 1700 S, Logan	1-Lane
SR-68 (Redwood Rd) and 14400 S, Bluffdale	2-Lane
SR-156 (Main St) and 800 N, Spanish Fork	2-Lane
SR-266 (4700 S) and 2200 W, Taylorsville	2-Lane
SR-151 (South Jordan Pkwy) and 3200 W, South Jordan	2-Lane
SR-171 (3300 S) & 2000 E, Millcreek	2-Lane
SR-193 and H St, Clearfield	2-Lane
SR-71 (12600 S) and 1830 W, Riverton	2-Lane
SR-36 and Erda Way, Erda	2-Lane
SR-36 and 2400 N, Erda	2-Lane
SR-173 (5400 S) and 1900 W, Taylorsville	2-Lane
SR-111 (8400 W) & 3100 S, Magna	2-Lane
US-89 (State St) and 1700 S, Salt Lake City	3-Lane
SR-68 (Redwood Rd) and 600 N (Foxboro Dr), North Salt Lake	3-Lane

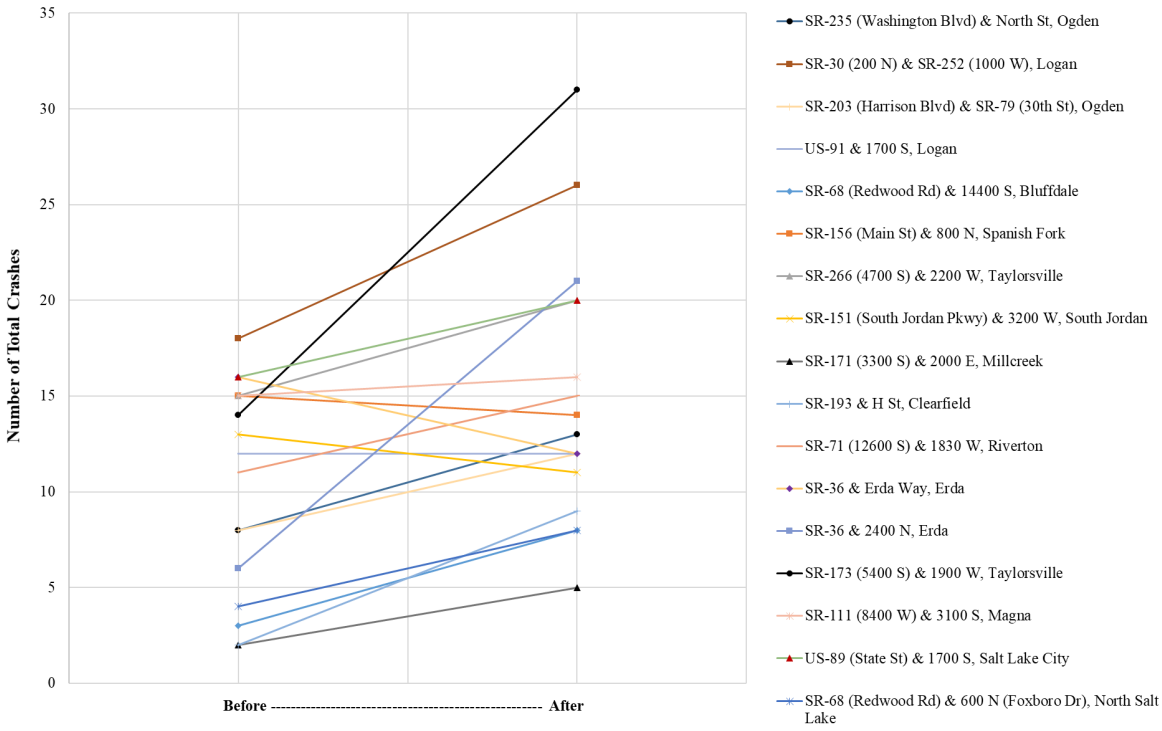

Figure 4-6: Total crashes (Permitted to Protected-Permitted).

Since total crash trends may not be sufficient to understand changes in left-turn related crash occurrences at the study intersections, a ratio of left-turn crashes against total crashes was determined. The ratio of injury-related crashes (crashes with UDOT severity levels from 2-5) to total crashes yielded mixed results, increasing at some intersections and decreasing at other intersections, as shown in Figure 4-7. No clear trend can be determined from the data.

Figure 4-8 shows the left-turn crashes per MEV for before and after the change from permitted to protected-permitted. Once again, no clear conclusion could be drawn from the crash data analysis for this change. This may be because the number of intersections analyzed and the two years of crash data before and after the change were not sufficient to confidently draw conclusions.

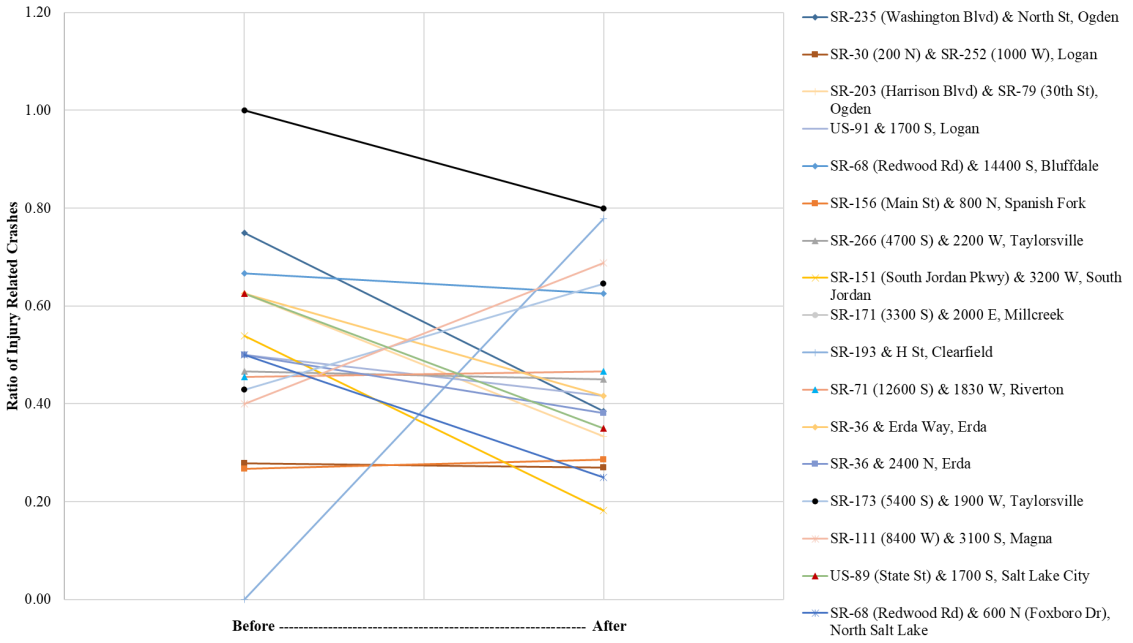

Figure 4-7: Injury-related crashes as a ratio of total crashes (Permitted to Protected-Permitted).

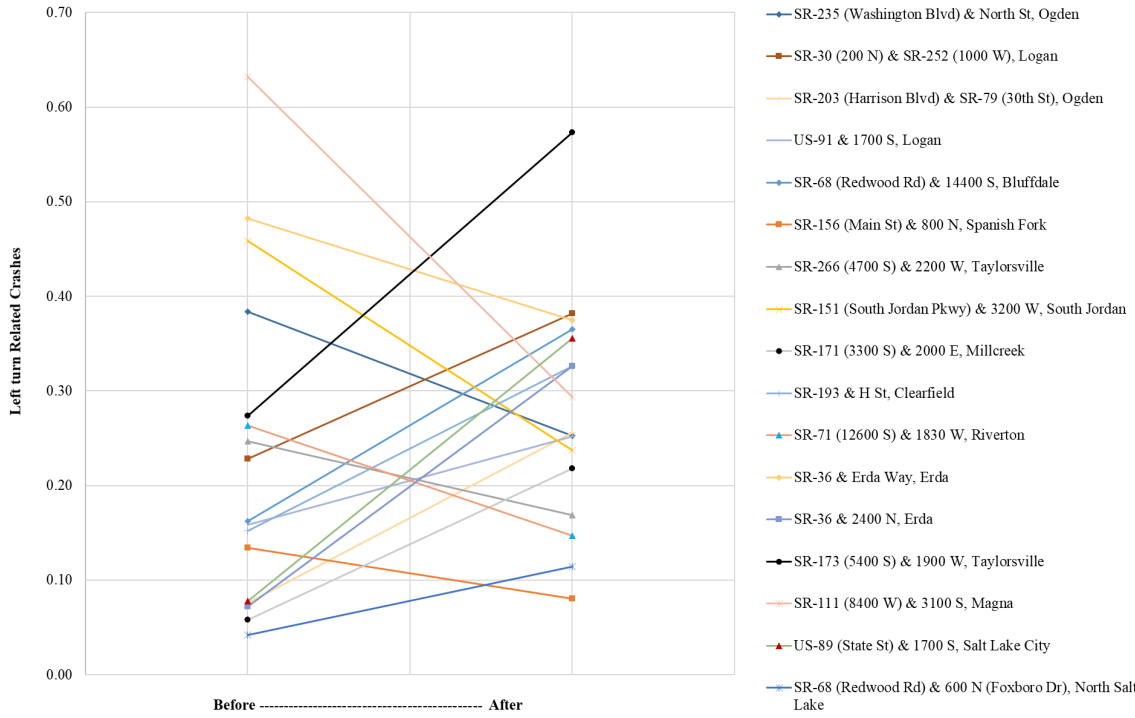

Figure 4-8: Left-turn related crashes per MEV (Permitted to Protected-Permitted).

To better understand how crashes vary throughout the day, a time of day analysis was conducted as well. Figure 4-9 shows the total crashes per MEV by time of day. Figure 4-10 shows the left-turn crashes per MEV. There appears to be a spike in the number of total and left-turn-related crashes during the peak hours after the change in left-turn treatment was made. This trend matches that of the baseline intersections, meaning that it may not be attributable to the change in left-turn phasing.

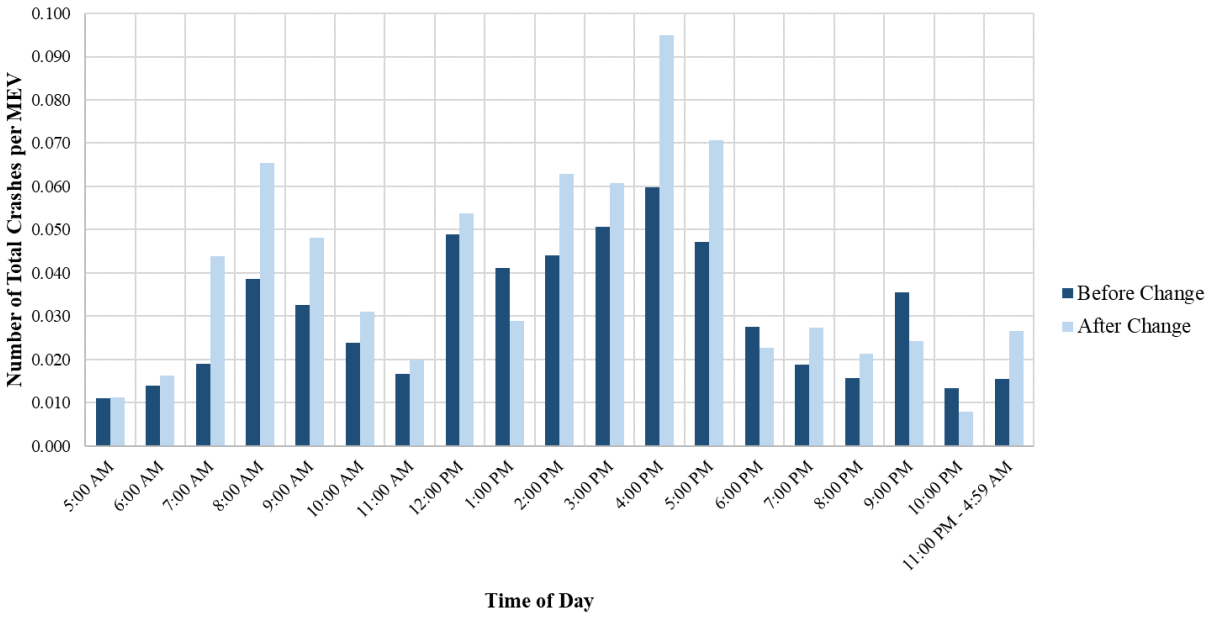

Figure 4-9: Total crashes per MEV by time of day (Permitted to Protected-Permitted).

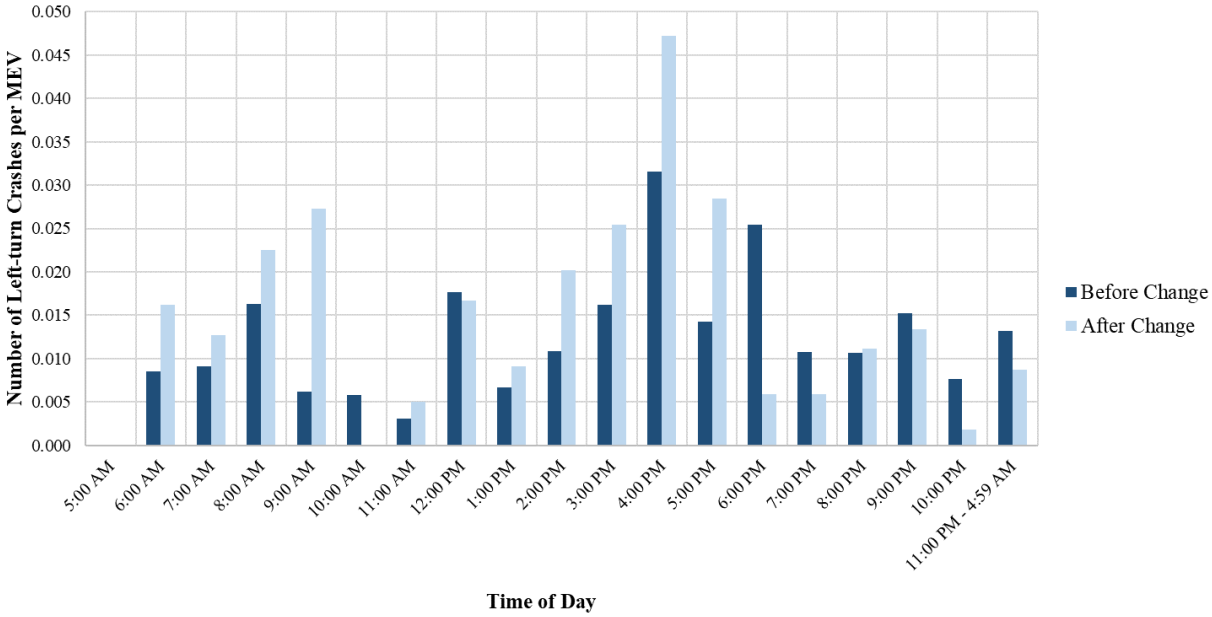

Figure 4-10: Left-turn crashes per MEV by time of day (Permitted to Protected-Permitted).

4.2.3 Protected to Protected-Permitted Trends

Nine intersections that experienced the change in left-turn treatment from protected only phasing to protected-permitted phasing were available for analysis. Crash data for three years before and after the left-turn phasing change were analyzed. Only one additional intersection would have been added had the before-after time threshold been reduced to two years. As such, a three-year analysis was used to assess the intersections listed in Table 4-3.

Unlike the baseline intersections and intersections that changed from permitted to protected-permitted left-turn phasing, the results from this analysis show a consistent trend. Almost all measures indicate a decrease in safety, with consistent increases in total crashes after the change compared to before the change as shown in Figure 4-11. Although this could be due to increases in AADT over the period studied, one important measure in determining if the change in left-turn phasing had an effect on crashes is the change in left-turn crashes as a ratio of

total crashes. Every intersection had an increase in the frequency of left-turn crashes as a ratio of total crashes, as shown in Figure 4-12. Figure 4-13 shows the left-turn crash rate in crashes per MEV for before and after the change, thus normalizing the crashes using AADT. This figure shows a similar trend to Figure 4-12.

Table 4-3: Intersections Selected that Changed from Protected to Protected-Permitted

Location	Configuration
SR-266 (4500 S) and 260 W, Murray	2-Lane
SR-173 (5400 S) and 1300 W, Taylorsville	2-Lane
SR-152 (Van Winkle) and 5600 S, Murray	2-Lane
SR-71 (900 E) and 6600 S, Murray	2-Lane
SR-71 (700 E) and 1300 S, Salt Lake City	3-Lane
SR-71 (700 E) and 1700 S, Salt Lake City	3-Lane
US-89 (State St)and 1300 S, Salt Lake City	3-Lane
US-89 (State St) and Vine St, Murray	3-Lane
US-89 (State St) and 4800 S, Murray	3-Lane

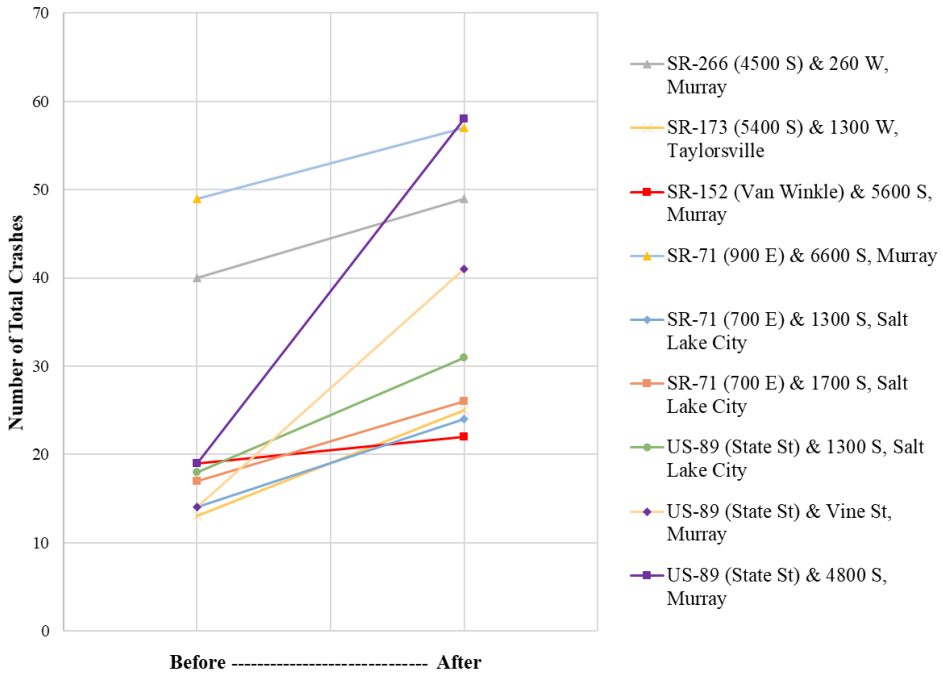

Figure 4-11: Change in total crashes (Protected to Protected-Permitted).

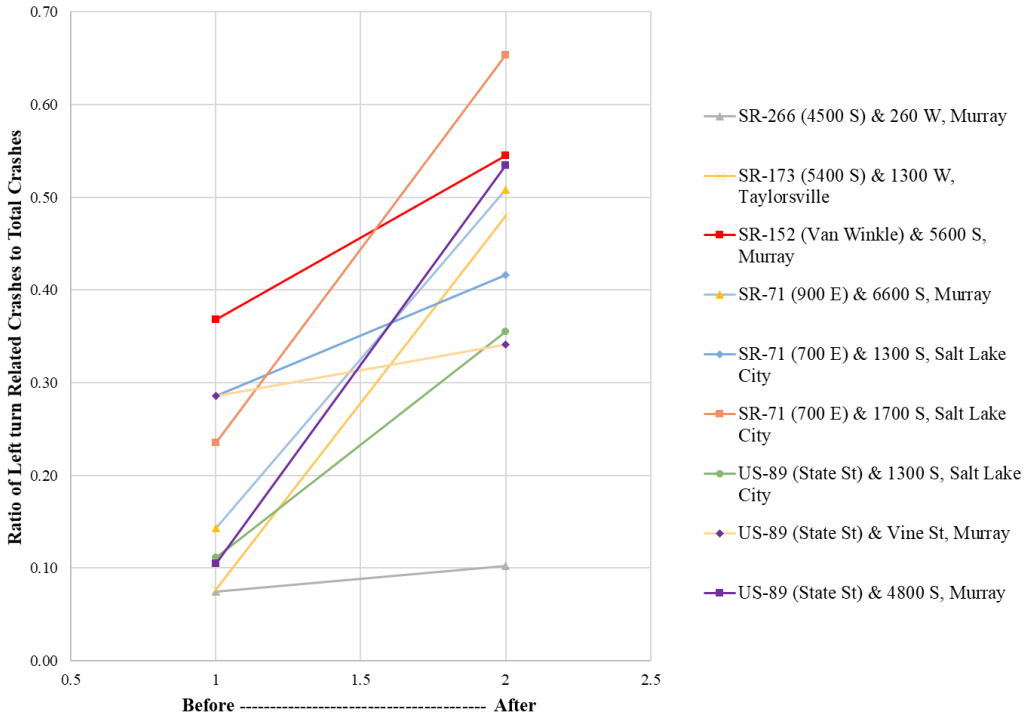

Figure 4-12: Left-turn related crashes as a ratio of total crashes (Protected to Protected-Permitted).

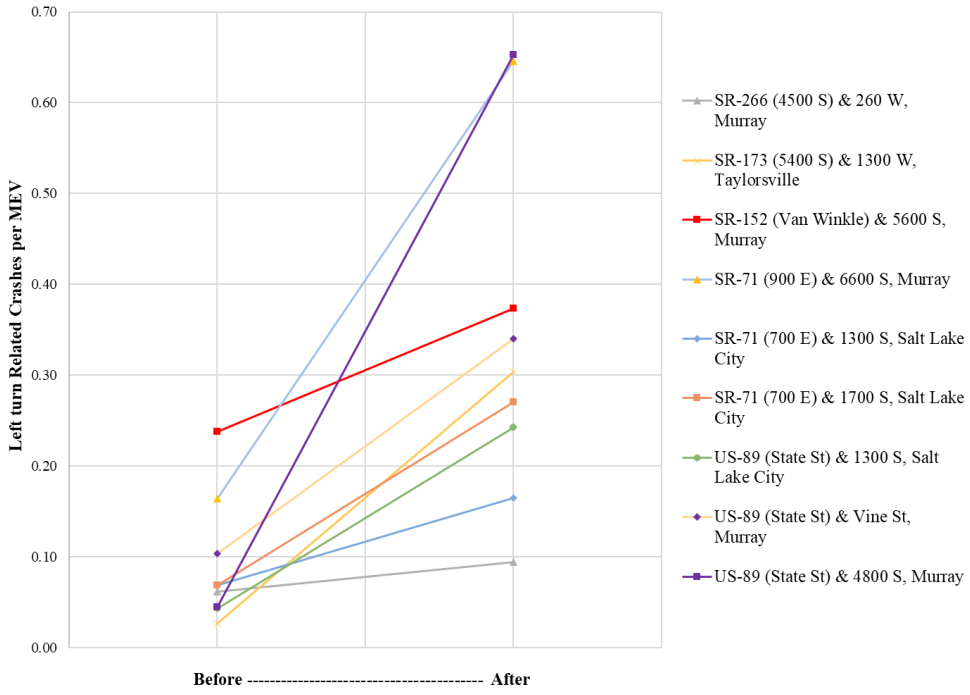

Figure 4-13: Left-turn related crashes per MEV (Protected to Protected-Permitted).

The time of day analysis for the left-turn signal phasing change provided further confirmation for the same type of analysis performed in Section 4.2.2. Both total crashes and left-turn crashes before the phasing change appear to peak during the early afternoon (1:00-4:00 PM). However, crashes after the phasing change appear to peak during the afternoon and evening peak hours (3:00-8:00 PM). These trends are presented in Figure 4-14 and Figure 4-15. These intersections may need to have the protected only left-turn phasing during the peak hours to increase safety. Figure 4-15 shows that left-turn related crashes per MEV increased when the left-turn phasing changed from protected to protected-permitted. The difference between the before and after crash rates by time of day is higher in these figures than in the figures shown in the baseline analysis denoting a possible decrease in safety as a result of changing to protected-permitted from protected left-turn phasing.

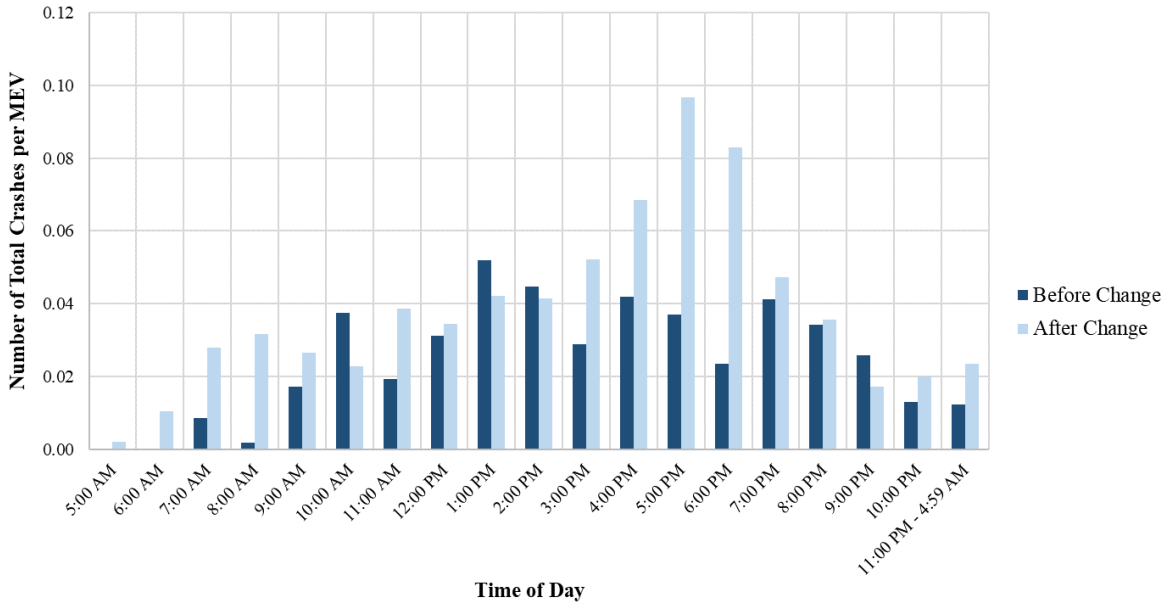

Figure 4-14: Total crashes per MEV by time of day (Protected to Protected-Permitted).

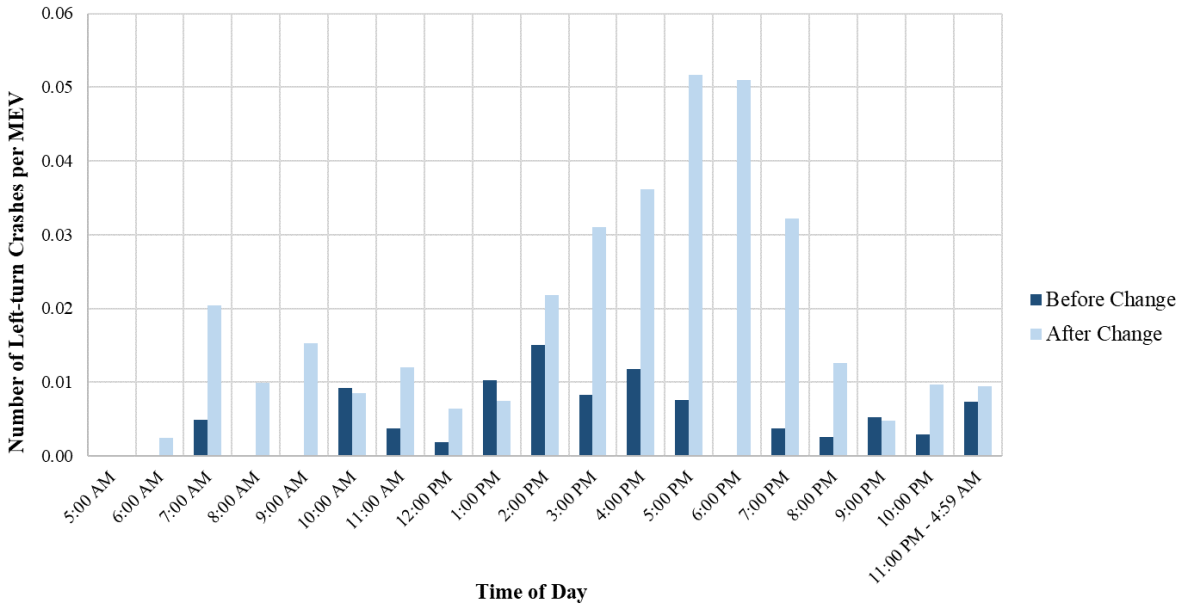

Figure 4-15: Left-turn crashes per MEV by time of day (Protected to Protected-Permitted).

4.3 Potential Sources of Error in the Crash Analysis

Much of what has been analyzed and concluded depends on the accuracy of the data sources. The UDOT crash database is a complete database of all the crashes that have been collected from police crash reports across the state. However, the accuracy in this data depends on consistency in crash data reporting between officers, a complete collection of all crash reports that have been filed, and accurate representation of crashes in the crash reports. Although it is not anticipated that the crash data are incorrect, there is the possibility of error.

Another potential source of error is the lack of complete data that can be used for the analysis. While significant effort has been expended in identifying intersections that meet the criteria established, nine to 17 intersections available per type of left-turn phasing change may not be a large enough sample size to make reliable inferences on the trend in crash occurrence. It is a rule of thumb that statistical analysis of transportation systems have a minimum of 30

samples (Fricker and Whitford 2016). Additionally, the use of two years of before and after crash data is not ideal for determining trends in crash occurrence; the availability of three years would be preferred.

4.4 Chapter Summary

This chapter focused on an analysis of the safety differences between left-turn treatments by assessing the crashes that occurred during time periods before and after existing intersections experienced changes from one type of left-turn treatment to another. A total of 36 intersections were assessed, including intersections that had experienced a change in left-turn phasing from permitted to protected-permitted or protected to protected-permitted. As part of these 36 intersections, 10 intersections that experienced no change were evaluated as a baseline.

A general trend found in all three analyses, from permitted to protected-permitted and from protected to protected-permitted as well as the baseline analysis, is an increase in the number of total crashes. It may be that traffic growth over the last several years in Utah might have contributed to the increase in the number of total crashes. Another trend found by the analysis appears to be an increase in left-turn crashes at intersections where left-turn treatment changed from protected to protected-permitted phasing. This increase is also expected, as protected left-turn phasing has been reported in the literature as safer than protected-permitted left-turn phasing, leading to less potential for conflicts. Similar trends were observed in a preliminary statistical analysis that was performed by the research team.

Another trend that is consistent across both sets of left-turn signal phasing changes is the notable increase in the number of crashes during the peak hours. In all six time-of-day crash analysis figures, an increase in the number of crashes takes place during the peak hours, while

during off-peak hours of the day crash occurrence appears to remain relatively unchanged before and after the changes in left-turn signal phasing. This finding may indicate further investigation into crashes by time of day is needed.

This study performed three separate analyses for a total of 36 intersections with either a change in left-turn phasing or no change, and with either two or three years of crash data for both before and after the change in phasing. This may not be a large enough sample size to draw statistically significant conclusions; it is a rule of thumb with transportation statistical analyses to have a minimum of 30 samples per treatment. Additionally, the use of two years of crash data is not generally adequate for determining trends in crash occurrence, but was done as part of this analysis in an attempt to increase the sample size. Additional investigation is recommended after more data has been collected and additional intersections have been added.

5 DEVELOPMENT OF LEFT-TURN PHASING DECISION BOUNDARIES

5.1 Introduction

This chapter presents the results of the procedures to derive decision boundaries for permitted, protected-permitted, and protected left-turn phasing. The methods and procedures for determining these boundaries were discussed in Section 3.3. First, the mapping of conflict contours is discussed, followed by the development of decision boundaries for selecting appropriate left-turn phasing. This is followed by the proposed decision boundaries for left-turn phasing and a comparison of these decision boundaries with actual intersections used in the study, as well as a chapter summary.

5.2 Mapping of Conflict Contours

This section details the development of contour maps for crossing conflicts obtained for each left-turn phasing alternative and opposing lane configuration. The methods for this chapter were discussed in Section 3.3. The contour maps for permitted left-turn phasing are presented first, followed by the results for protected-permitted phasing for 1-, 2-, and 3-lane opposing approach configurations.

5.2.1 Permitted Left-Turn Phasing

All volume scenarios described in Section 3.3 were simulated in VISSIM three times for each lane configuration and the trajectory files for these scenarios were read using SSAM. The

SSAM conflict identification results were exported as .csv files and crossing conflicts were extracted, averaged, and counted for each scenario. The crossing conflicts identified by SSAM were then analyzed using MATLAB and various contour maps were created to determine decision boundaries. The crossing conflict scales on the contour maps were determined using the conflict contour values identified using the method in Section 3.3.4. These contour maps are shown in Figure 5-1, Figure 5-2, and Figure 5-3, and show how the conflicts increase as left-turn and total opposing volume (in vph) increases. Note that each contour map includes a red line representing the base decision boundary curve determined for that configuration. These base decision boundary curves will be discussed further in Section 5.3.

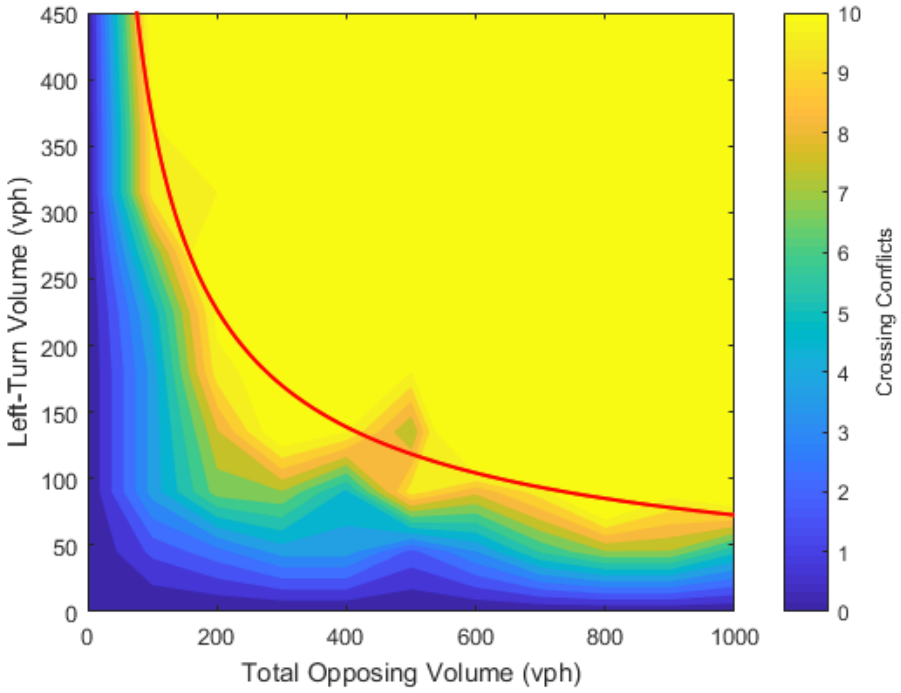

Figure 5-1: Contour map for permitted left-turn phasing with an opposing 1-lane configuration.

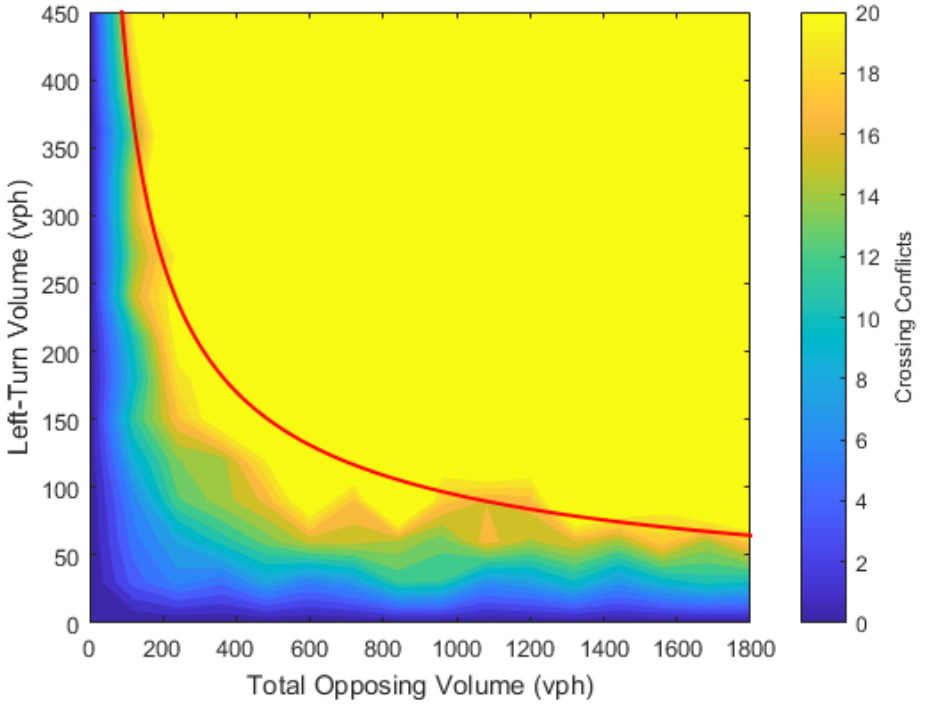

Figure 5-2: Contour map for permitted left-turn phasing with an opposing 2-lane configuration.

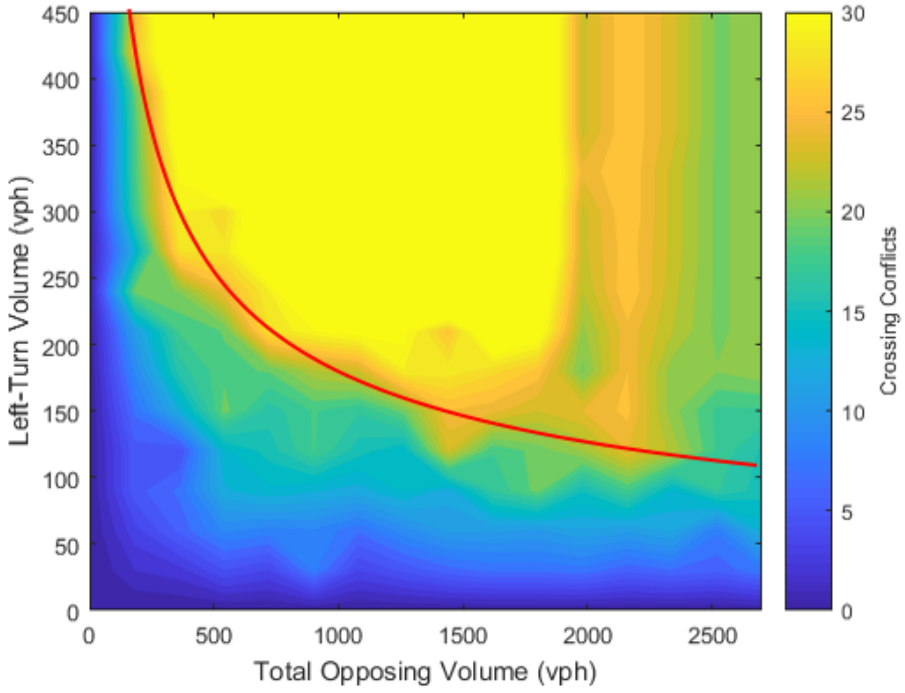

Figure 5-3: Contour map for permitted left-turn phasing with an opposing 3-lane configuration.

5.2.2 Protect-Permitted Left-Turn Phasing for Opposing 1-Lane Configuration

Using the same process as the contour maps in Section 5.2.1, contour maps were derived for protected-permitted left-turn phasing in an opposing 1-lane configuration case. Three alternatives were analyzed for the protected green time at the intersection. These included a protected green time of 10-, 15-, and 20-seconds. The results of these analyses are shown in Figure 5-4, Figure 5-5, and Figure 5-6, respectively.

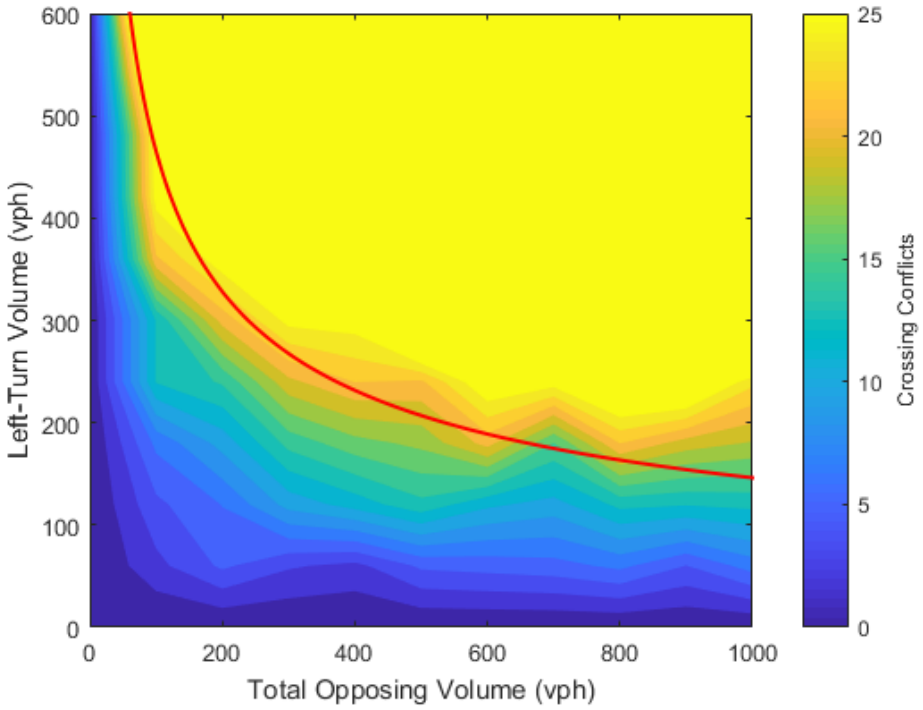

Figure 5-4: Contour map for protected-permitted left-turn phasing with a 10-second protected green time and opposing 1-lane configuration.

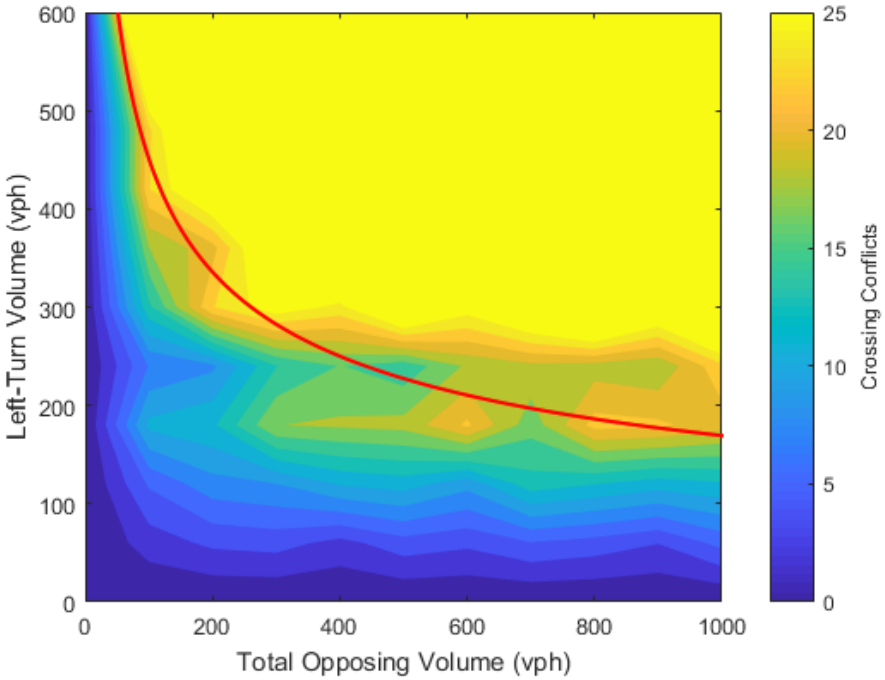

Figure 5-5: Contour map for protected-permitted left-turn phasing with a 15-second protected green time and opposing 1-lane configuration.

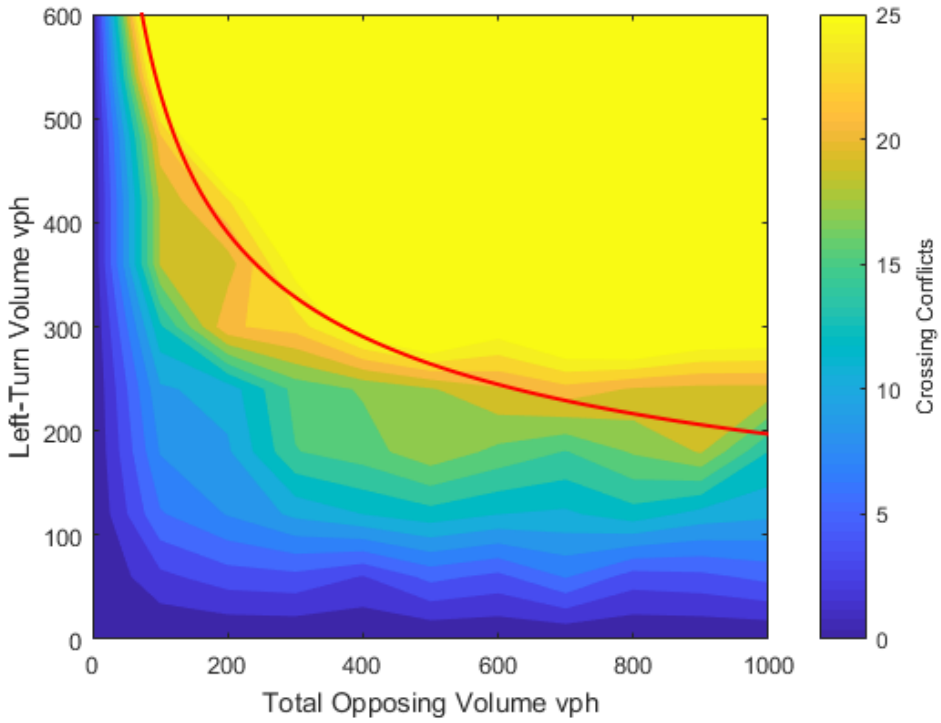

Figure 5-6: Contour map for protected-permitted left-turn phasing with a 20-second protected green time and opposing 1-lane configuration.

5.2.3 Protect-Permitted Left-Turn Phasing for Opposing 2-Lane Configuration

Contour maps were also derived for protected-permitted left-turn phasing in an opposing 2-lane configuration case. Alternatives were again analyzed for protected green times of 10-, 15-, and 20-seconds. The results of these analyses are shown in Figure 5-7, Figure 5-8, and Figure 5-9, respectively.

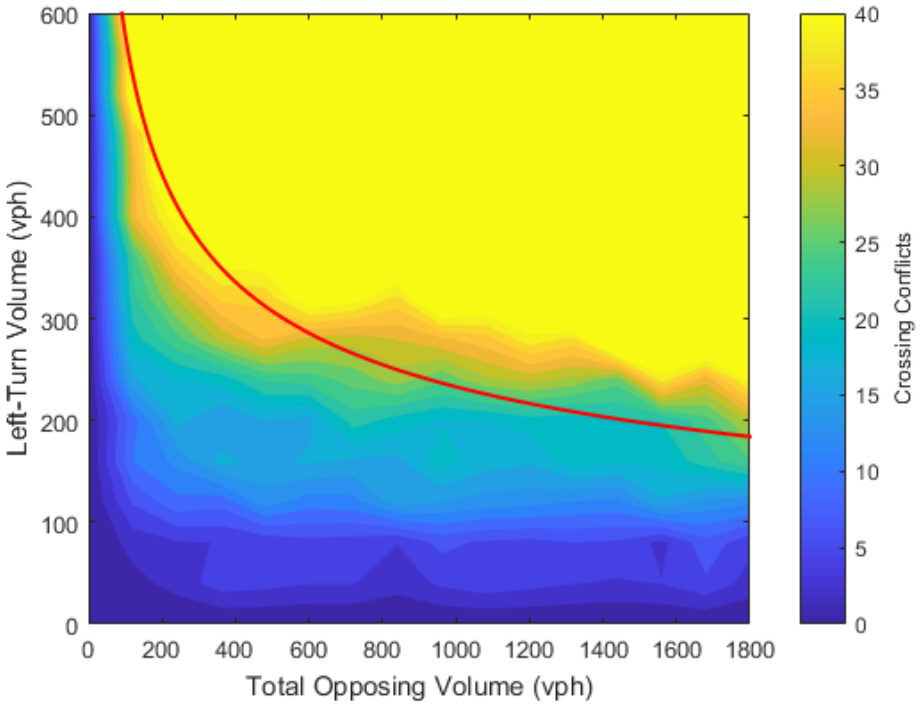

Figure 5-7: Contour map for protected-permitted left-turn phasing with a 10-second protected green time and opposing 2-lane configuration.

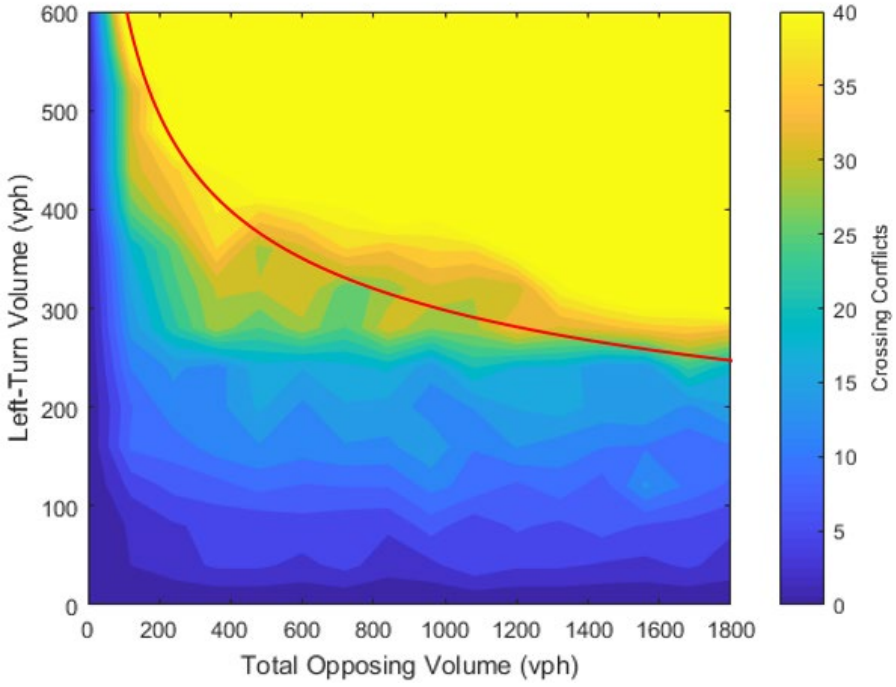

Figure 5-8: Contour map for protected-permitted left-turn phasing with a 15-second protected green time and opposing 2-lane configuration.

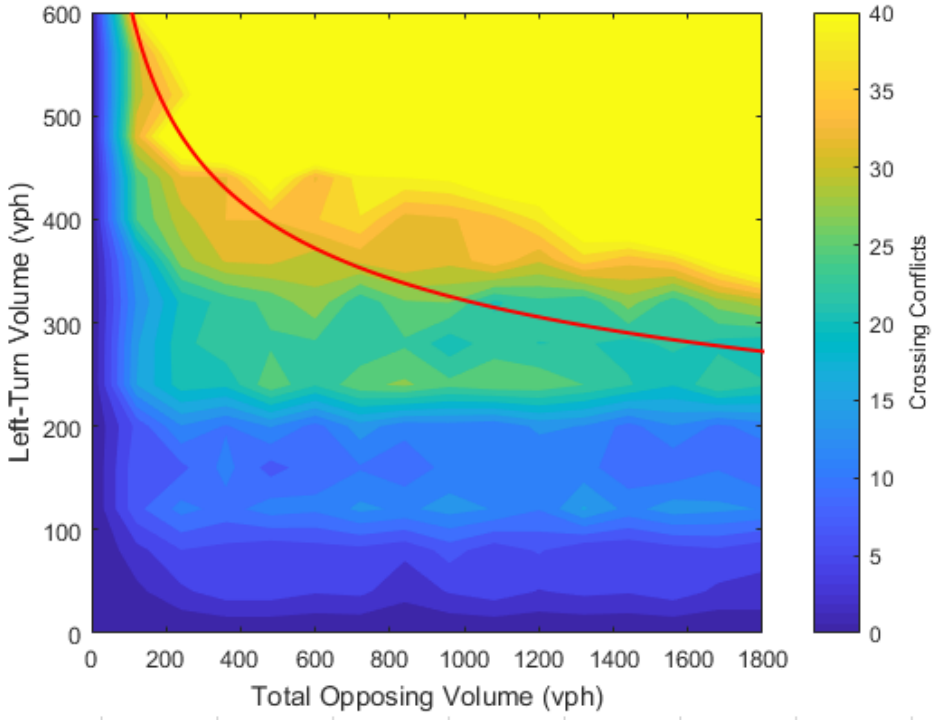

Figure 5-9: Contour map for protected-permitted left-turn phasing with a 20-second protected green time and opposing 2-lane configuration.

5.2.4 Protect-Permitted Left-Turn Phasing for Opposing 3-Lane Configuration

Contour maps were also derived for protected-permitted left-turn phasing in an opposing 3-lane configuration case. Alternatives were again analyzed for protected green times of 10-, 15-, and 20-seconds. The results of these analyses are shown in Figure 5-10, Figure 5-11, and Figure 5-12 respectively.

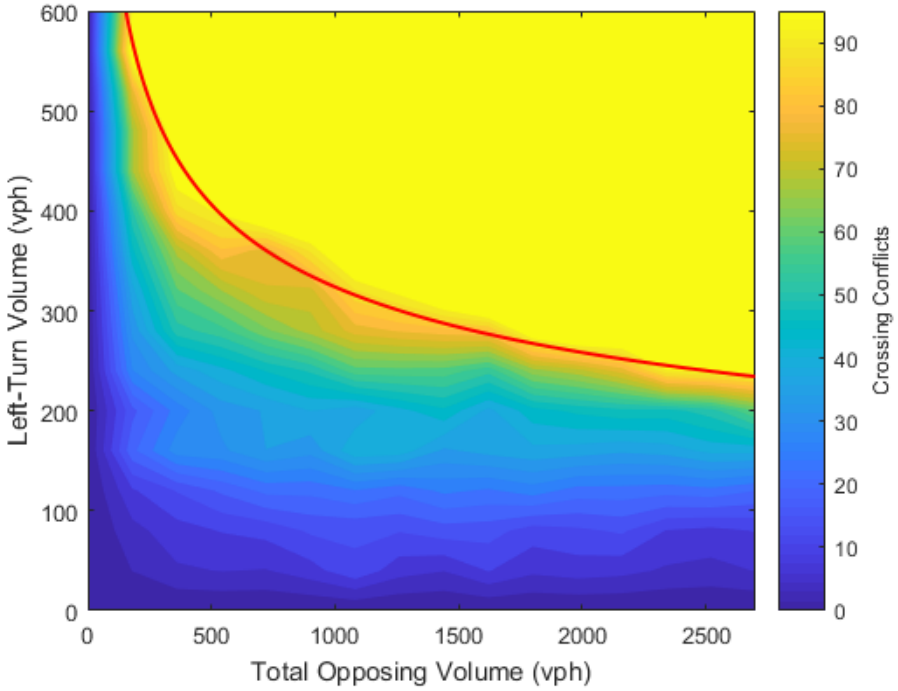

Figure 5-10: Contour map for protected-permitted left-turn phasing with a 10-second protected green time and opposing 3-lane configuration.

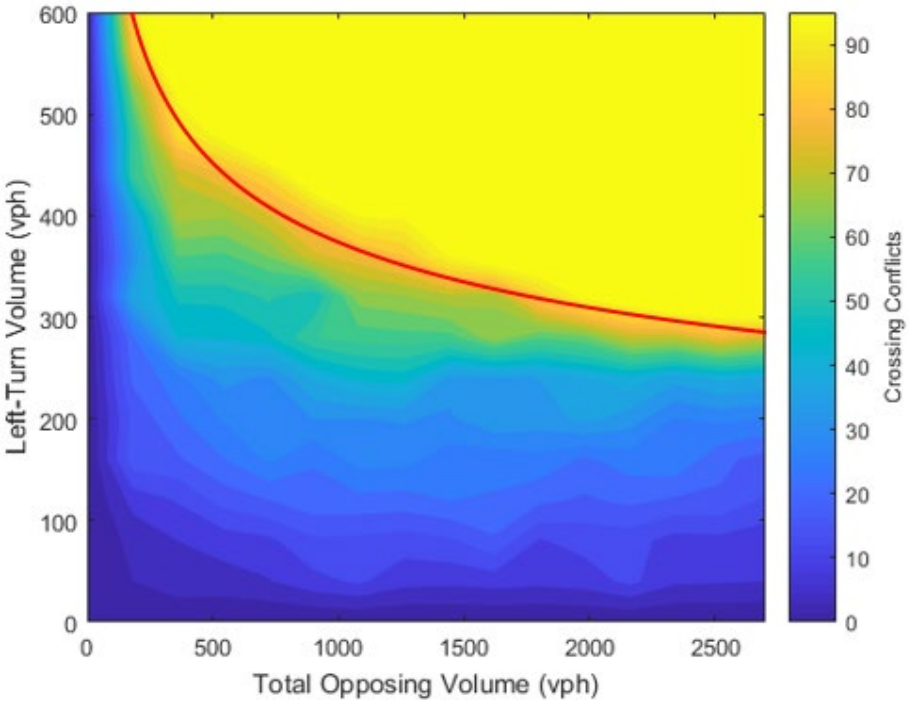

Figure 5-11: Contour map for protected-permitted left-turn phasing with a 15-second protected green time and opposing 3-lane configuration.

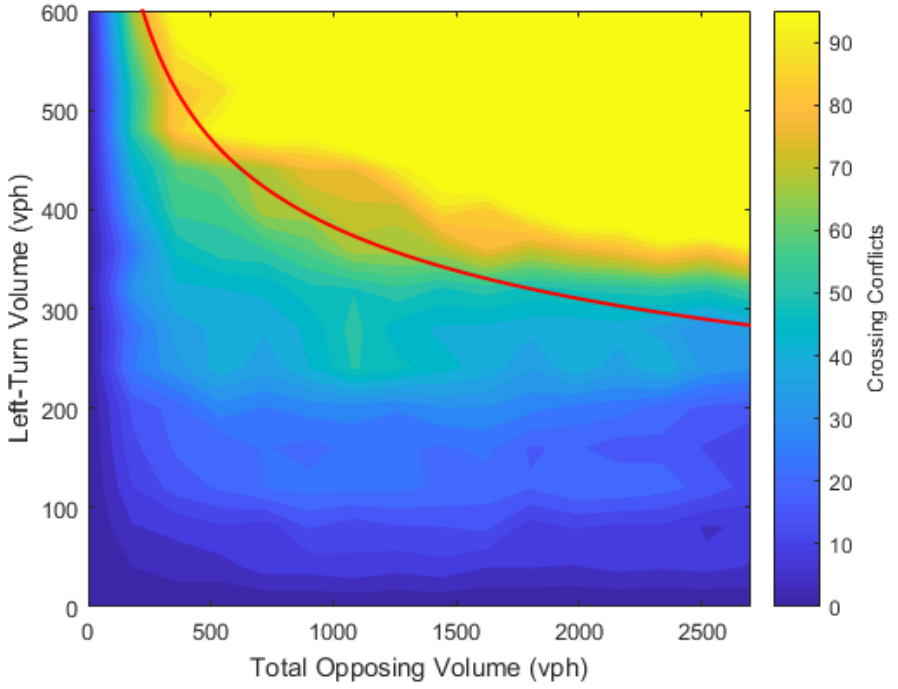

Figure 5-12: Contour map for protected-permitted left-turn phasing with a 20-second protected green time and opposing 3-lane configuration.

5.3 Development of Decision Boundaries for Selecting Appropriate Left-Turn Phasing

Using the contour maps shown in Section 5.2, and applying the method outlined in Section 3.3.5, decision boundary equations were derived for both the boundary between permitted and protected-permitted left-turn phasing and the boundary between protected-permitted and protected left-turn phasing. The protected-permitted to protected left-turn signal phasing boundary was formatted as a transition boundary, with upper and lower limits determined based on the boundaries found for the protected-permitted left-turn phasing with 10-, 15-, and 20-second protected green time. To present the decision boundaries and their respective equations, this section is divided into sub-sections detailing the development of left-turn phasing decision boundaries for the opposing 1-, 2-, and 3-lane configurations.

5.3.1 Decision Boundaries for Opposing 1-Lane Configuration

By performing linear regression analyses for each 1-lane opposing approach configuration model, phasing type boundary equations were generated for permitted and protected-permitted 10-, 15-, and 20-second protected green times as shown in Equations 5-1, 5-2, 5-3, and 5-4, respectively.

$$9519 = V_{LT} * {V_{Opp}}^{0.706} \quad (5\text{-}1)$$

$$4638 = V_{LT} * {V_{Opp}}^{0.500} \quad (5\text{-}2)$$

$$3134 = V_{LT} * {V_{Opp}}^{0.421} \quad (5\text{-}3)$$

$$3696 = V_{LT} * {V_{Opp}}^{0.425} \quad (5\text{-}4)$$

It should be noted that these equations are adjusted so that the opposing volume (x-axis) is in units of vphpl. Using these left-turn phasing boundary equations, a chart with all of the

decision boundaries was compiled, similar to that used by Raessler and Yang (2017), as shown in Figure 5-13.

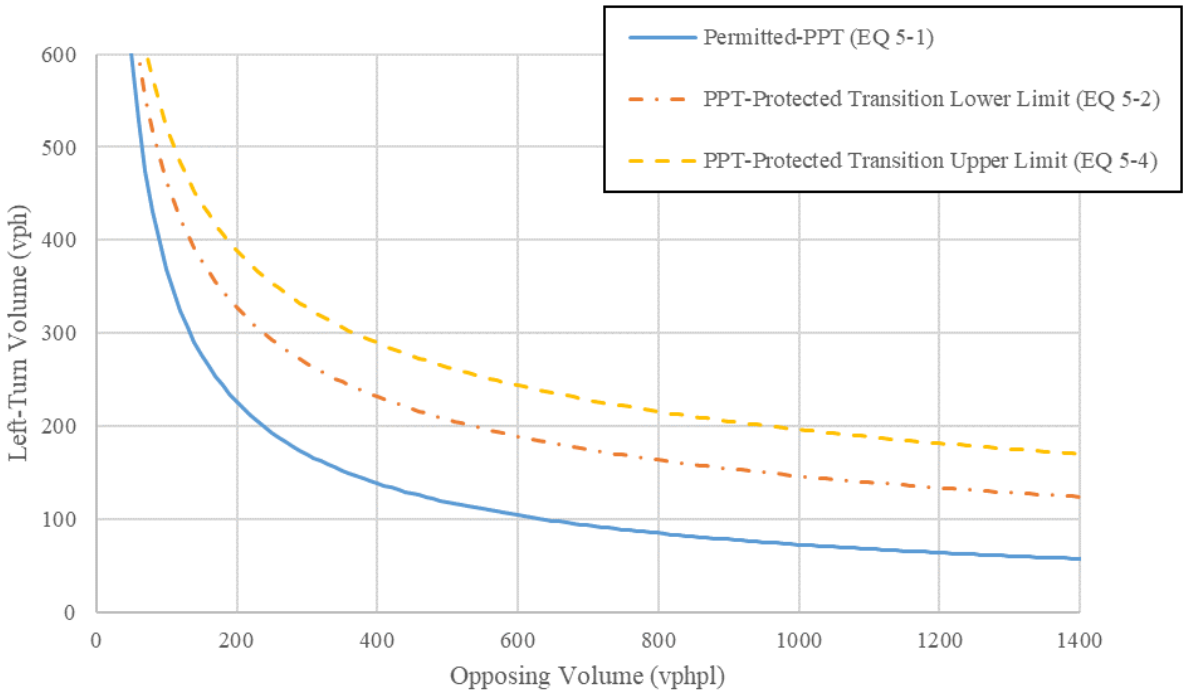

Figure 5-13: Decision boundaries for 1-lane opposing approach configuration.

The 10-second protected green boundary was selected to represent the lower limit of the boundary between the protected-permitted and protected phasing, while the 20-second boundary was selected as the upper limit. These boundaries were given in Equation 5-2 and Equation 5-4, respectively. The protected-permitted 15-second protected green boundary, shown in Equation 5-3, was not used in the decision boundary graph, as it was found to lie between the 10- and 20-second protected green boundaries. Protected-permitted is denoted as "PPT" in the legend of

Figure 5-13 (as well as Figure 5-14 and Figure 5-15). This is the same for the 2- and 3-lane opposing approach configuration decision boundaries.

In interpreting the decision boundaries, permitted left-turn phasing is recommended below the blue line and protected-permitted phasing is recommended between the blue line and the orange dashed line. Either protected-permitted or protected phasing would be acceptable between the orange and yellow dashed lines, and protected phasing is recommended above the yellow dashed line.

5.3.2 Decision Boundaries for Opposing 2-Lane Configuration

Phasing type boundary equations were also generated for each 2-lane approach model for permitted and protected-permitted 10-, 15-, and 20-second protected green times as shown in Equations 5-5, 5-6, 5-7, and 5-8, respectively.

$$7974 = 2 * V_{LT} * {V_{Opp}}^{0.642} \quad (5\text{-}5)$$

$$3782 = 2 * V_{LT} * {V_{Opp}}^{0.404} \quad (5\text{-}6)$$

$$2687 = 2 * V_{LT} * {V_{Opp}}^{0.318} \quad (5\text{-}7)$$

$$2312 = 2 * V_{LT} * {V_{Opp}}^{0.285} \quad (5\text{-}8)$$

A chart with all of the decision boundaries was compiled, as in Section 5.3.1. This chart is shown in Figure 5-14. The 10- and 20-second protected green times were again selected to represent the lower and upper limits, respectively.

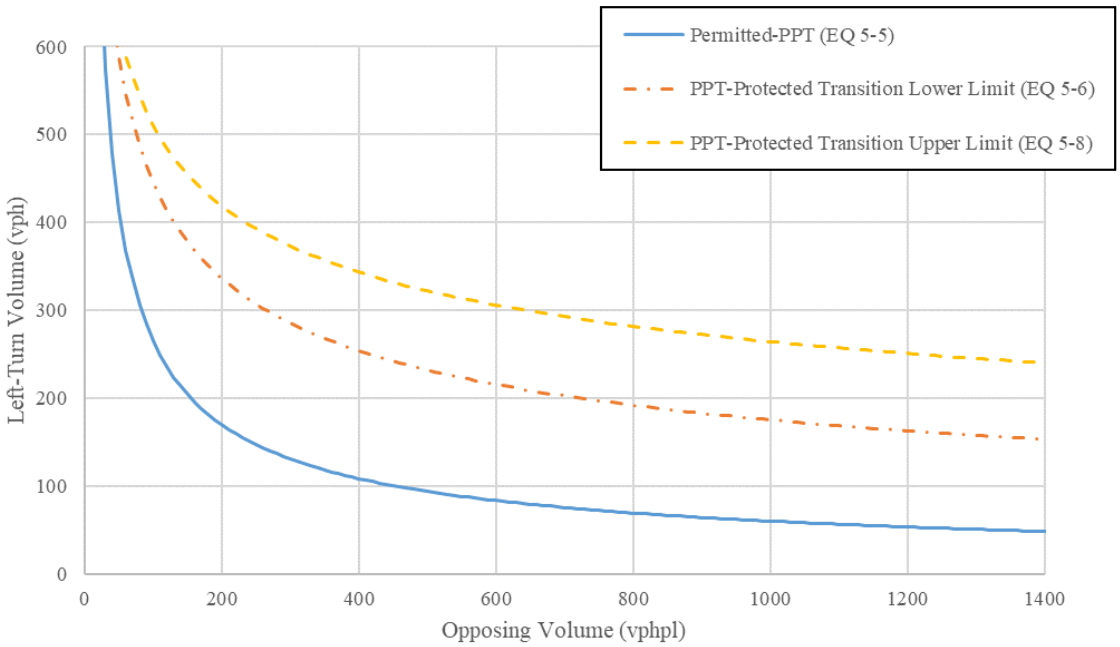

Figure 5-14: Decision boundaries for 2-lane opposing approach configuration.

5.3.3 Decision Boundaries for Opposing 3-Lane Configuration

Phasing type boundary equations were also generated for each 3-lane approach model for permitted and protected-permitted 10-, 15-, and 20-second protected green times as shown in Equations 5-9, 5-10, 5-11, and 5-12, respectively.

$$5861 = 3 * V_{LT} * {V_{Opp}}^{0.504} \quad (5\text{-}9)$$

$$3056 = 3 * V_{LT} * {V_{Opp}}^{0.324} \quad (5\text{-}10)$$

$$2414 = 3 * V_{LT} * {V_{Opp}}^{0.269} \quad (5\text{-}11)$$

$$3056 = 3 * V_{LT} * {V_{Opp}}^{0.301} \quad (5\text{-}12)$$

A chart with all decision boundaries is shown in Figure 5-15. The 10-and 20-second protected green times were again selected to represent the lower and upper limits, respectively.

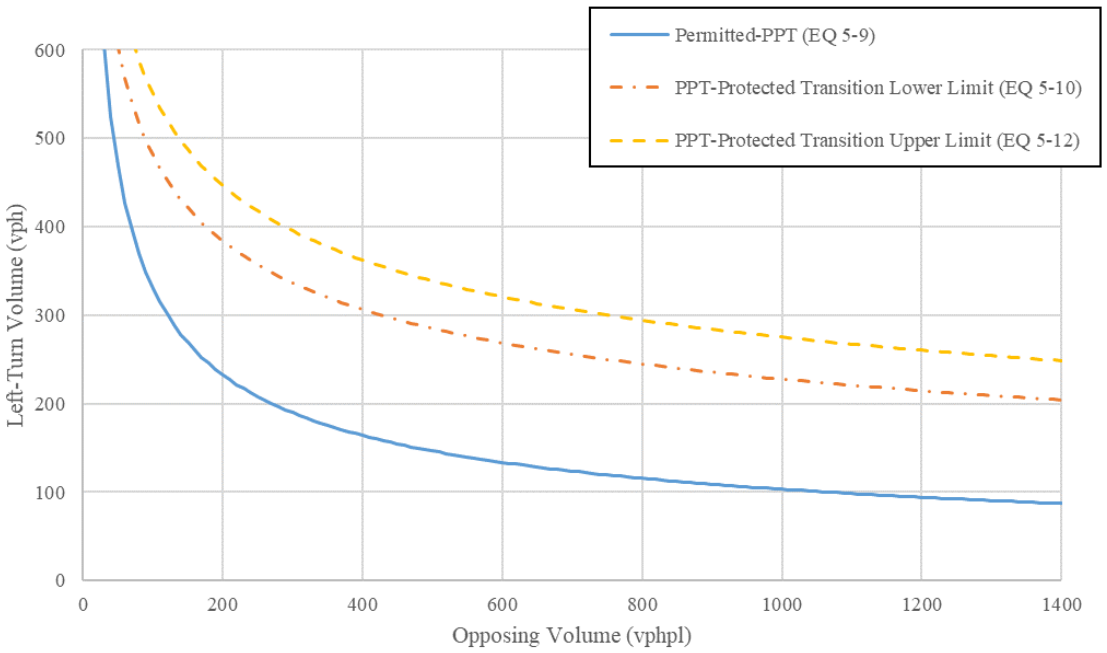

Figure 5-15: Decision boundaries for 3-lane opposing approach configuration.

In interpreting the boundaries generated, it is important to note that the boundaries were compared to the UDOT cross product and dual left-turn standards to determine whether or not the boundaries correlate with UDOT guidelines. In the case of the 1- and 2-lane configurations, the decision boundaries compare well with the current guidelines. For example, the volume cross product boundary for implementing some level of protected phasing, including protected-permitted phasing, is 50,000 for 1-lane opposing approaches and 100,000 for 2- and 3-lane opposing approaches. This is generally met for both the 1- and 2-lane configurations; however, the 3-lane configuration results do not compare as well to current guidelines.

5.4 Proposed Decision Boundaries for Left-Turn Phasing

When comparing the 1-, 2-, and 3-lane configuration decision boundaries, it was noted that the 3-lane configuration boundaries do not match the trends shown by the other two

configurations. The 2-lane boundaries are slightly lower than those of the 1-lane, which is logical, as vehicles crossing two lanes would be less likely to turn left at the same rate of opposing volume as those that only have to cross one. It is expected that the 3-lane boundaries would follow this same trend and be slightly lower than the 2-lane results on a vphpl basis. Because this is not the case and also because of how high the 3-lane boundary results are, it is suspected that the model as currently constructed does not provide enough lane capacity to accurately test the 3-lane configuration. Additionally, UDOT recommended that the models be tested to see if they might vary as the approach speed varies, as noted in Section 3.3.2; however, no significant variation occurred within the models as speed was increased; therefore 35 mph was used for all models.

Based on the results of the analysis, it is recommended that the 2-lane decision boundaries be used to represent both the 2- and 3-lane opposing approach configurations. This recommendation was discussed with and agreed upon by the TAC members. Another adjustment made to all sets of the base decision boundaries was to change the units of the opposing approach volume axis back from vphpl to total vph. Additionally, it was recommended that an upper boundary be added to represent the current UDOT guideline that protected dual left-turns be implemented when left-turn volume at an approach is above 420 vph (UDOT 2014).

With these adjustments, the recommended decision boundaries for the 1-lane opposing approach configuration, as well as the combined boundaries for the 2- and 3-lane opposing approach configurations are shown in Figure 5-16 and Figure 5-17, respectively.

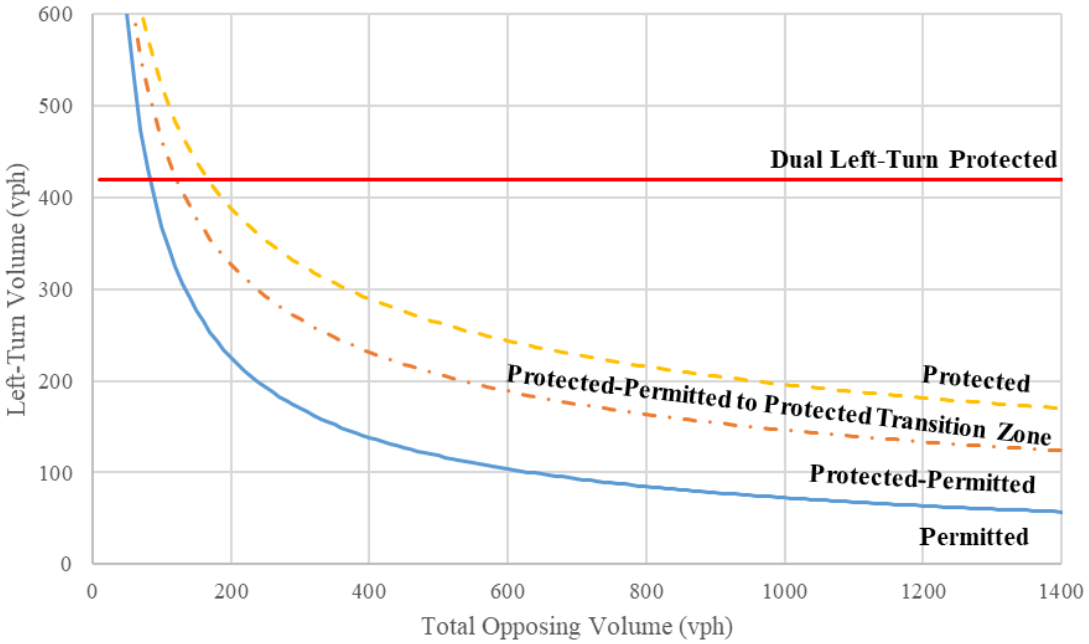

Figure 5-16: Final decision boundaries for 1-lane opposing approach configuration.

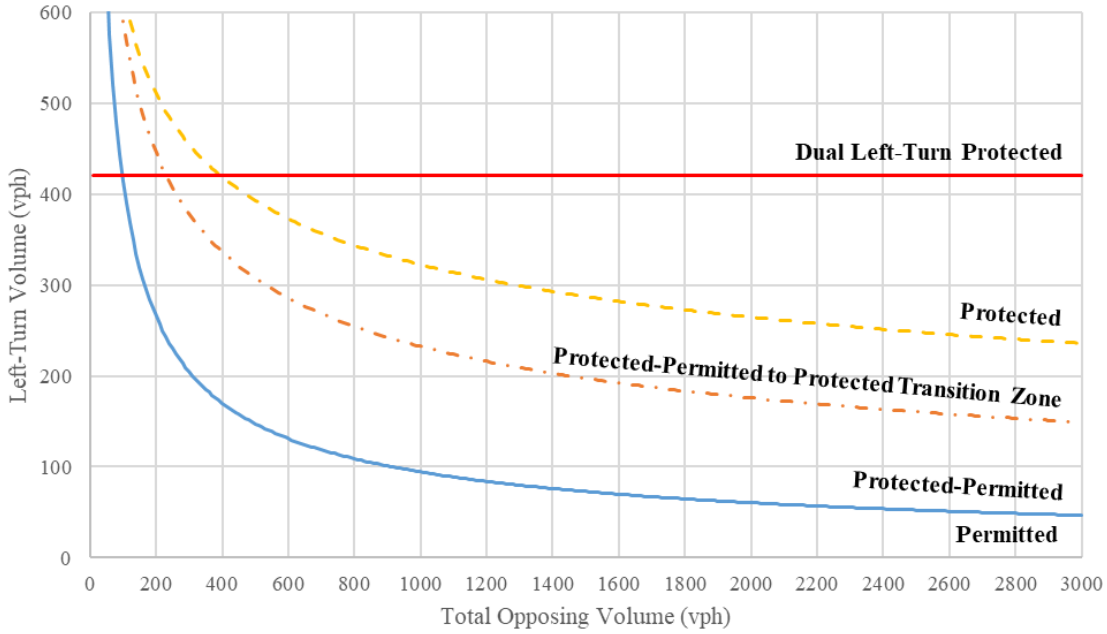

Figure 5-17: Final decision boundaries for 2- and 3-lane opposing approach configurations.

5.5 Comparison of Decision Boundaries with Actual Intersections Analyzed in the Study

The final decision boundaries from Section 5.4 were compared to the signalized intersections in the three intersection datasets presented in Chapter 4. These include those intersections that changed from permitted to protected-permitted and from protected to protected-permitted, as well as the baseline intersections with protected-permitted left-turn phasing that experienced no change. These intersections should fall within the protected-permitted range of the corresponding decision boundaries. Figure 5-18, Figure 5-19, and Figure 5-20 show the existing intersections that fall within the proposed guidelines for protected-permitted phasing for the 1-, 2-, and 3-lane opposing approach configurations, respectively. Figure 5-21 and Figure 5-22 show the existing intersections that fall outside of the proposed guidelines for protected-permitted phasing for the 2- and 3-lane opposing approach configurations, respectively. No intersections with the 1-lane opposing approach configuration were found to fall outside of the proposed guidelines. Table 5-1 lists the intersections used for these comparisons, divided into groups of 1-, 2-, and 3-lane opposing approach configurations.

In all comparisons of decision boundaries, the existing intersection data follow the decision boundaries relatively closely. However, in the comparison of the 2- and 3-lane decision boundaries with the 2-lane opposing approach configuration intersections, intersections 20 and 24 are close to, but still outside of, the protected-permitted range and intersections 5, 7, 9, 16, 21, 25, and 32 are completely outside of the protected-permitted range. Additionally, in the comparison of the 2- and 3-lane decision boundaries with the 3-lane opposing approach configuration intersections, intersections 11 and 30 are close to, but still outside of, the protected-permitted range and intersection 28 is completely outside of the protected-permitted range.

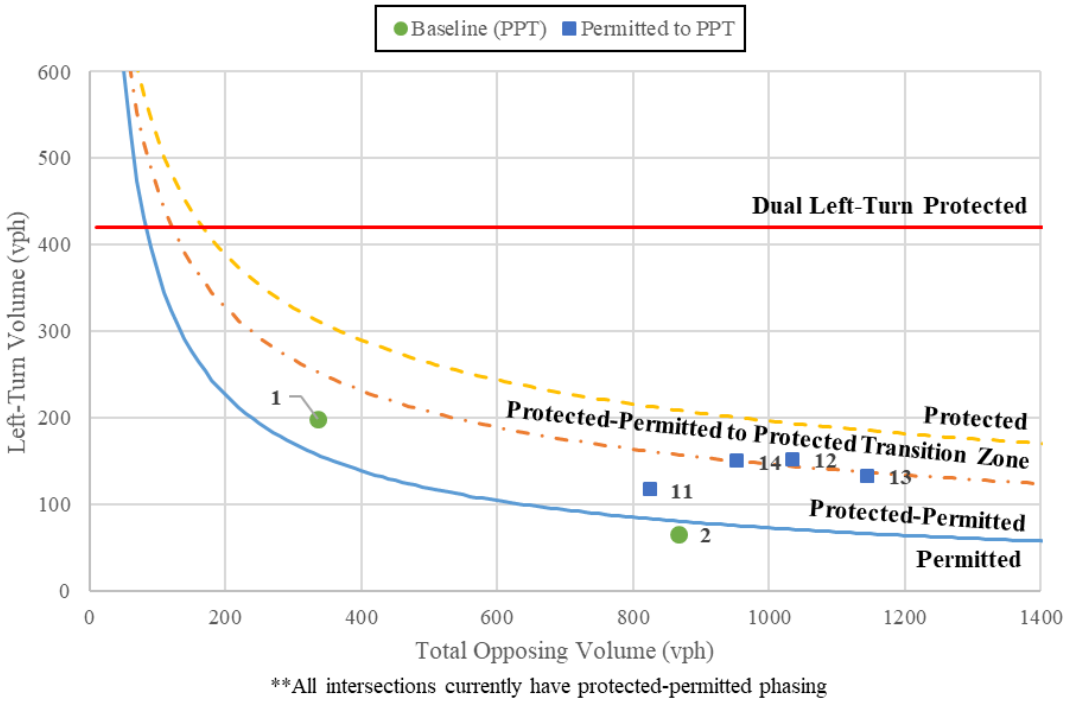

Figure 5-18: Existing 1-lane intersections within the proposed decision boundaries for 1-lane opposing approach configuration.

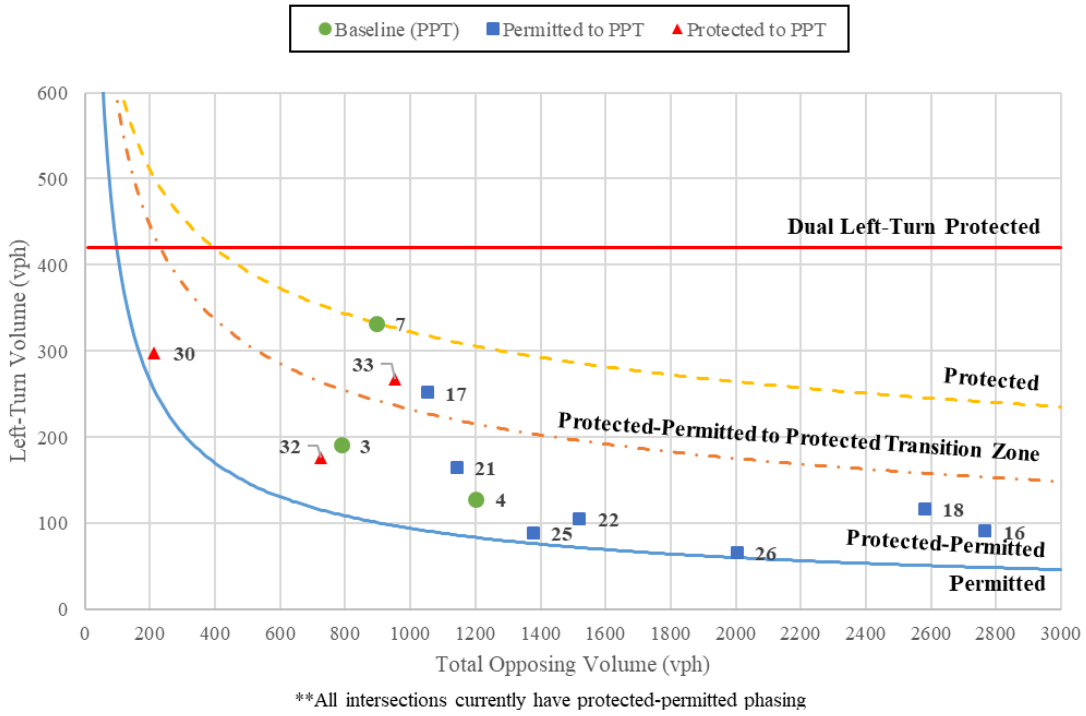

Figure 5-19: Existing 2-lane intersections within the proposed decision boundaries for 2- and 3-lane opposing approach configurations.

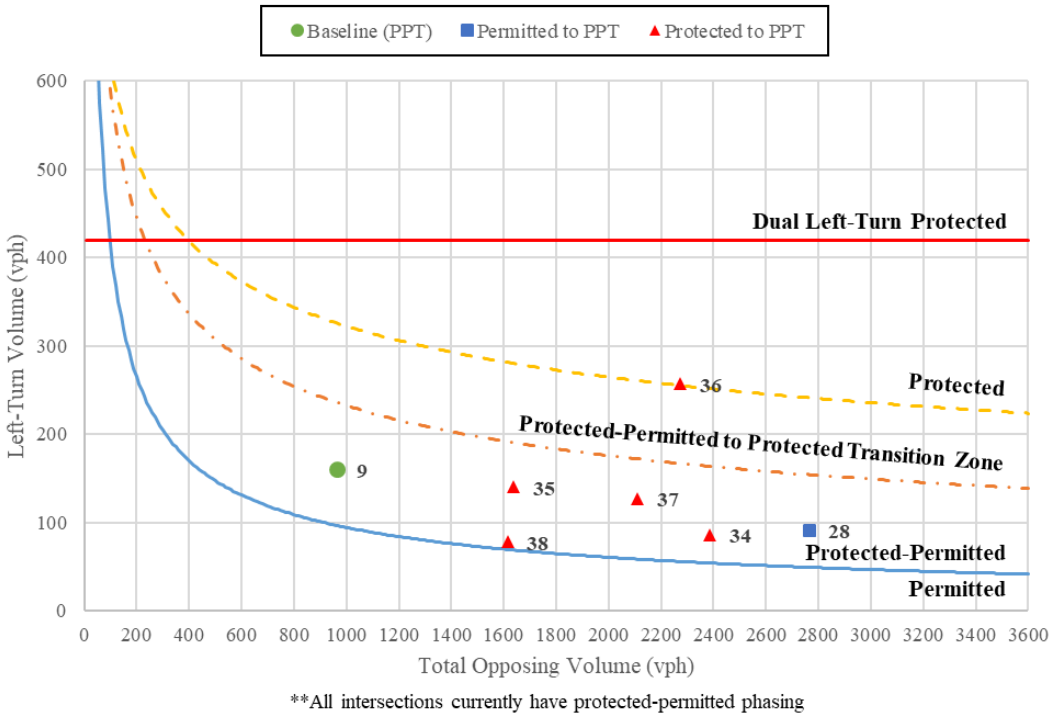

Figure 5-20: Existing 3-lane intersections within the proposed decision boundaries for 2- and 3-lane opposing approach configurations.

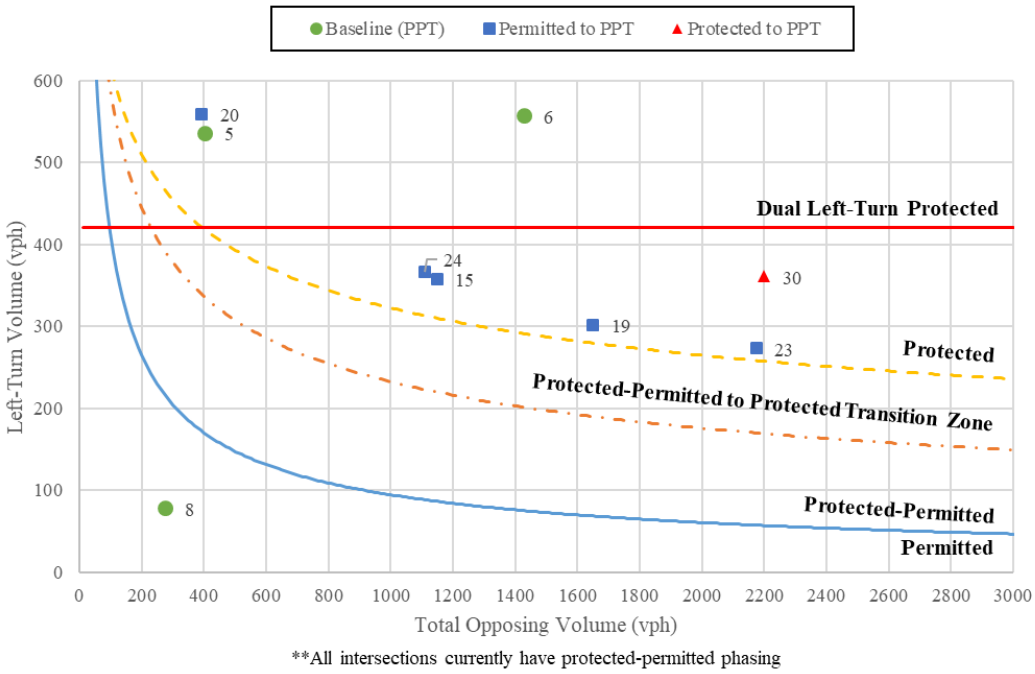

Figure 5-21: Existing 2-lane intersections outside of the proposed decision boundaries for 2- and 3-lane opposing approach configurations.

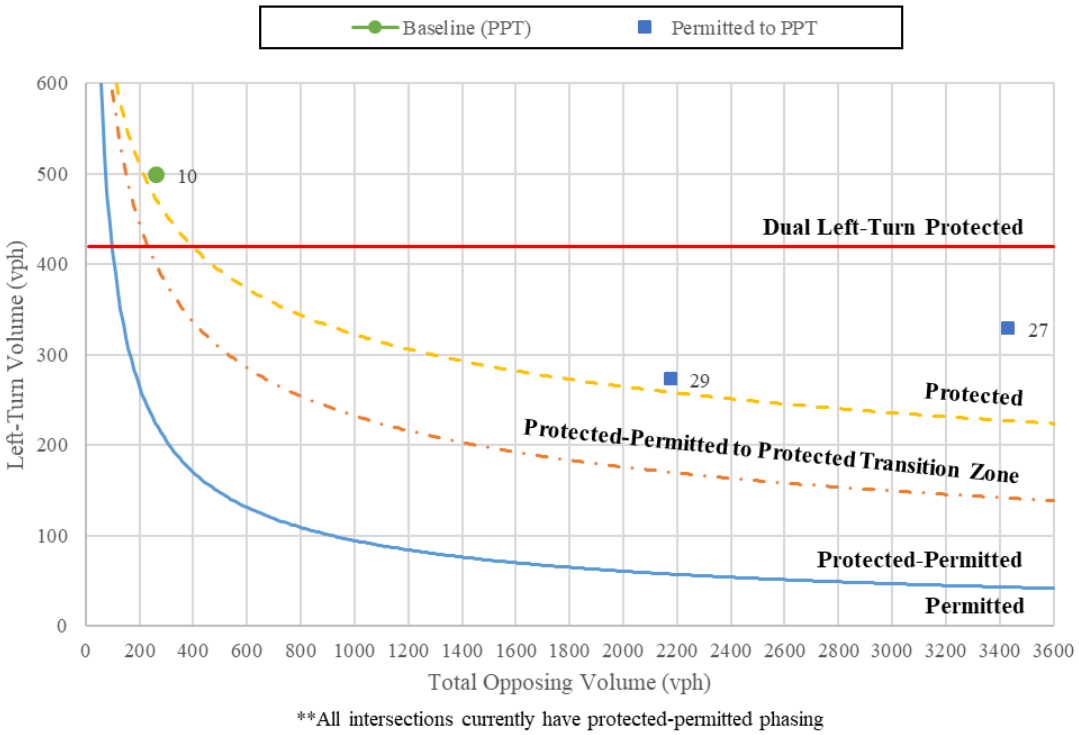

Figure 5-22: Existing 3-lane intersections outside of the proposed decision boundaries for 2- and 3-lane opposing approach configurations.

Table 5-1: Signalized Intersections Used for Decision Boundary Comparison

Baseline Intersections				
#	**Location**	**Configuration**	**LT Volume**	**Tot Opp Volume**
1	2300 E & SR-266 (4500 S), Holladay	1-Lane	199	336
2	SR-68 (Redwood Rd) & 12800 S, Riverton	1-Lane	65	866
3	SR-71 (700 E) & 10600 S, Sandy	2-Lane	191	787
4	2700 W & SR-48 (7800 S), West Jordan	2-Lane	128	1202
5	4800 W & SR-171 (3500 S), West Valley City	2-Lane	536	401
6	SR-68 (Redwood Rd) & 9800 S, South Jordan	2-Lane	557	1427
7	S Temple & SR-186 (N State), Salt Lake City	2-Lane	332	894
8	SR-71 (12600 S) & 2700 W, Riverton	2-Lane	78	275
9	SR-68 (Redwood Rd) & 1700 S, Salt Lake City	3-Lane	160	963
10	SR-268 (600 N) & US-89 (300 W), Salt Lake City	3-Lane	499	262

**These intersections lie outside of the simulated boundary range for protected-permitted phasing.

Table 5-1 continued

Phase Change from Permissive to Protected-Permissive				
#	**Location**	**Configuration**	**LT Volume**	**Tot Opp Volume**
11	SR-235 (Washington Blvd) & North St, Ogden	1-Lane	117	825
12	SR-30 (200 N) & SR-252 (1000 W), Logan	1-Lane	152	1035
13	SR-203 (Harrison Blvd) & SR-79 (30th St), Ogden	1-Lane	133	1145
14	US-91 & 1700 S, Logan	1-Lane	150	953
15	SR-68 (Redwood Rd) & 14400 S, Bluffdale	2-Lane	358	1148
16	SR-156 (Main St) & 800 N, Spanish Fork	2-Lane	91	2766
17	SR-266 (4700 S) & 2200 W, Taylorsville	2-Lane	252	1053
18	SR-151 (South Jordan Pkwy) & 3200 W, South Jordan	2-Lane	117	2581
19	SR-68 (Redwood Rd) & 600 N (Foxboro Dr), North Salt Lake	2-Lane	302	1650
20	SR-193 & 1000 W, Clearfield**	2-Lane	559	392
21	SR-193 & H St, Clearfield	2-Lane	165	1143
22	SR-71 (12600 S) & 1830 W, Riverton	2-Lane	106	1519
23	SR-145 (Pioneer Crossing) & 500 W, Lehi	2-Lane	273	2174
24	SR-36 & Erda Way, Erda	2-Lane	366	1110
25	SR-36 & 2400 N, Erda	2-Lane	89	1377
26	SR-173 (5400 S) & 1900 W, Taylorsville	2-Lane	66	2005
27	US-89 (State St) & 1700 S, Salt Lake City**	3-Lane	329	3429
28	SR-156 (Main St) & 800 N, Spanish Fork	3-Lane	91	2766
29	SR-145 (Pioneer Crossing) & 500 W, Lehi	3-Lane	273	2174
Phase Change from Protected to Protected-Permissive				
#	**Location**	**Configuration**	**LT Volume**	**Tot Opp Volume**
30	SR-266 (4500 S) & 260 W, Murray	2-Lane	298	213
31	SR-173 (5400 S) & 1300 W, Taylorsville	2-Lane	361	2198
32	SR-152 (Van Winkle) & 5600 S, Murray	2-Lane	177	726
33	SR-71 (900 E) & 6600 S, Murray	2-Lane	267	952
34	SR-71 (700 E) & 1300 S, Salt Lake City	3-Lane	86	2386
35	SR-71 (700 E) & 1700 S, Salt Lake City	3-Lane	140	1637
36	US-89 (State St) & 1300 S, Salt Lake City	3-Lane	257	2272
37	US-89 (State St) & Vine St, Murray	3-Lane	127	2111
38	US-89 (State St) & 4800 S, Murray	3-Lane	78	1614

**These intersections lie outside of the simulated boundary range for protected-permitted phasing.

All of the intersections that were completely outside of the protected-permitted range are marked with "**" in Table 5-1. Because all existing intersections chosen for this study currently have protected-permitted left-turn phasing, those that are outside of the protected-permitted range on the decision boundaries show a discrepancy between current left-turn phasing practice in Utah and the proposed decision boundaries. These discrepancies corroborate the findings of Raessler and Yang (2017), which likewise found that the decision boundaries captured the left-turn phasing of the majority of existing intersections within the decision boundary ranges, but that current left-turn phasing practice did not match the boundaries in all cases.

One possible reason that there is not a 100 percent correlation between the current practice and the derived decision boundaries is that the simulated intersection was a generic four-leg intersection and the signal timing was designed to provide a large preference to the major roadway. Although this design represents a majority of intersections within Utah, there are many intersections that adapt their geometry to meet environmental factors or have unique signal timing configurations to meet unique vehicle demand. For example, the intersection of US-89 (State St) and 1700 South in Salt Lake City is located next to a college campus that experiences heavy traffic during peak hours but very light traffic during the rest of the day. A more flexible signal phasing such as protected-permitted phasing may be more appropriate to help mitigate the heavy traffic during the college peak hour.

In the end, the decision boundaries derived by this study are not meant to be applied blindly for all intersections. Instead they were developed as helpful guidelines for decision making that should be supplemented by engineering judgment. Even when taking into account all intersections lying outside of the decision boundaries corresponding to their current left-turn signal phasing, the comparisons between the decision boundaries and the existing intersections

show that the boundaries developed in the study are highly correlated with the current left-turn phasing decision practices of UDOT. It is recommended that these boundaries be applied to current left-turn decision boundaries in the state, and that they be used as part of the dynamic phase changing program that UDOT is currently implementing (as mentioned in Section 1.1).

5.6 Chapter Summary

The purpose of this chapter was to analyze permitted, protected-permitted, and protected phasing using VISSIM and SSAM and to use these to define a set of decision boundaries for 1-, 2-, and 3-lane configurations. The method used for doing this is outlined in Section 3.3.

The final decision boundaries for the 3-lane configuration recommended volume combination boundaries (vphpl) that were higher than the 1- and 2-lane configurations. Logically, the 3-lane configuration would be the most high-risk configuration, as vehicles have to cross more opposing lanes to turn left. As such, it is logical that the vphpl volume combination boundaries for the 3-lane configuration would be lower than any other configuration. However, this is not the case. Because the derived 3-lane decision boundaries did not match logical expectations, the decision boundaries derived for the 2-lane opposing approach configuration were used at the present time to represent the 3-lane boundaries as well.

Final decision boundaries were compiled and were shown in Section 5.4. As part of compiling the final decision boundaries, a boundary for dual left-turn lanes was also added to each final boundary set based on UDOT guidelines. The uses for these boundaries will be further discussed in the following chapter.

6 CONCLUSIONS AND RECOMMENDATIONS

6.1 Conclusions

The purpose of this research was to evaluate the safety and mobility of three left-turn treatments: permitted, protected, and protected-permitted left-turn phasing. Before and after crashes at intersections that had experienced a permanent change from one phase treatment to another were compared. VISSIM traffic modeling software was used to extract conflict data for analysis using SSAM to identify decision boundaries between each left-turn treatment. This chapter details the conclusions from the existing signalized intersection crash data, the decision boundaries derived from simulation, recommendations, future research topics, and concluding remarks.

6.2 Conclusions from Existing Signalized Intersection Crash Data

Availability of crash data was limited for conducting definitive statistical analysis on the safety implication of the effect of changing left-turn phasing on intersection safety. Crashes at intersections that experienced no left-turn phase change as well as those that experienced change from permitted to protected-permitted phasing or from protected to protected-permitted phasing were analyzed. Two years of crash data before and after the phase change were evaluated for those intersections that experienced a left-turn phase change from permitted to protected-permitted. Three years of crash data before and after the phase change were evaluated for all other intersections, with January 1, 2015 selected as the central date for the no-change or

baseline intersections. Trends were analyzed and compared for each set of intersections. Some of the trends observed from this analysis are as follows:

- The crashes tend to increase over time, regardless of the phase change.
- The intersections shifted from protected to protected-permitted left-turn phasing showed a general increase in left-turn crashes, which could indicate that there is a decrease in safety by shifting from protected to protected-permitted phasing.
- All intersections analyzed showed a general increase in crashes during peak hours after the change in phasing.

Further studies are recommended to draw statistically significant conclusions from the existing crash data. For many intersections that had recently experienced changes in left-turn phasing, only two years of crash data before and after were available rather than three years. Ideally, three years of crash data before and after would be required for reliable statistical analysis, which was not possible with the available dataset.

6.3 Decision Boundaries Derived from Simulation

To define decision boundaries between left-turn treatments for 1-, 2-, and 3-lane opposing approach configurations, a total of 12 models were created using VISSIM, with signal timing defined using Synchro. Crossing conflict data were then exported to trajectory files and identified using SSAM. Contour maps showing the change in the number of crossing conflicts as left-turn and opposing volume increases were created using MATLAB, and the maximum acceptable crossing conflict contours were identified. Decision boundaries were then derived for 1-, 2-, and 3-lane opposing approach configurations using JMP Pro.

In evaluating the decision boundaries, the 3-lane configuration decision boundary did not appear to match expectations. Based on the decision boundaries reported by Stramatiadis et al. (2016), the 3-lane boundary is expected to have the lowest left-turn vs. per lane opposing volume threshold of the different lane configurations. However, the analysis results did not follow this trend. Based on this, and on the comparison of existing intersections and their phasing to the 3-lane boundaries, it was recommended that UDOT use the decision boundaries for the 2-lane configuration for the 2- and 3-lane opposing approach configurations until further research can be completed and a more definitive boundary developed. It is recommended that the decision boundaries as shown in Figure 6-1 and Figure 6-2 be used as a supplement to current guidelines for left-turn decision boundaries in the state.

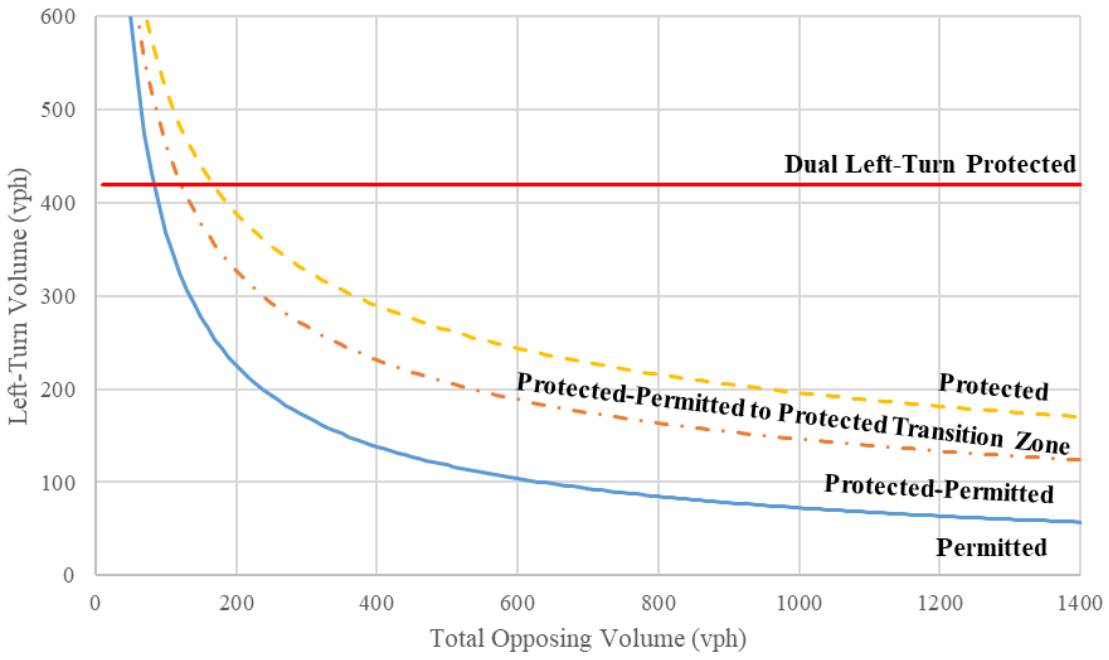

Figure 6-1: Left-turn phasing decision boundary for the 1-lane opposing approach configuration.

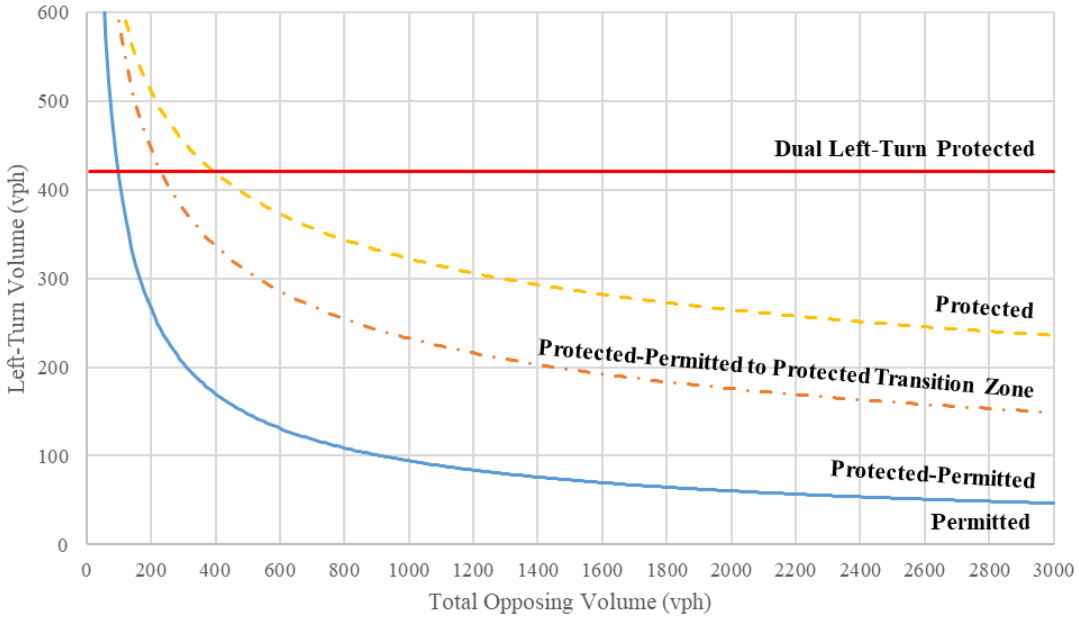

Figure 6-2: Left-turn phasing decision boundary for the 2- and 3-lane opposing approach configuration.

6.4 Recommendations

In evaluating the possible applications of the existing intersection crash data observations, as well as the decision boundaries developed using simulation by VISSIM and conflict analysis by SSAM and the methodology used to derive them, two major recommendations are provided. The first is to apply the decision boundaries developed in this report as a supplement to currently-used UDOT left-turn signal guidelines. The second is to consider the developed decision boundaries in dynamic time-of-day adjustments to signal timing and phasing.

6.5 Future Research Topics

As part of this research, existing intersection data were found to be too limited to draw conclusions on safety and mobility differences between left-turn phasing treatments. Additionally, the simulated decision boundary developed for the 3-lane opposing approach configuration was found to not match trends seen in previous studies and in the 1- and 2-lane opposing approach configurations. To address some of the limitations of this study, it is recommended that the following topics be considered for further research:

1. Perform further research on trends of crash occurrences due to the change in left-turn signal phasing, using crash data available through UDOT's crash database.
2. Perform further research to understand the trends in crash occurrence and conduct conflict analyses using simulation for signalized intersections with three or more lanes in the opposing direction to develop reliable decision boundaries for such configurations.
3. Perform further research to determine the safety effects on simulated intersections of varying approach speeds and opposing approach lane configurations.

6.6 Concluding Remarks

The mobility and safety differences between left-turn signal phasing treatments is of high importance to UDOT, other jurisdictions within the state, and other state DOTs. Supporting flexibility in operations for signalized intersections while still ensuring safety has spurred varied approaches and guidelines for left-turn signal phasing. The left-turn decision boundaries defined in this study have been developed to provide a simpler and more flexible guideline for engineers and planners alike. Additionally, the format of these boundaries and their corresponding

equations will allow for more dynamic application at different times of day. The implementation of these boundaries is anticipated to result in improved safety and mobility at intersections throughout the state.

REFERENCES

Agent, K. R. (1979). "An Evaluation of Permitted Left-Turn Phasing." Report KYP-75.70, Kentucky Department of Transportation, Division of Research, Lexington, KY.

American Association of State and Highway Transportation Officials (AASHTO). (2010). "Highway Safety Manual." Washington, DC.

American Association of State and Highway Transportation Officials (AASHTO). (2011). "A Policy of Geometric Design of Highways and Streets." 6th Edition, Washington, DC.

Asante, S. A., Ardekani, S. A., and Williams, J. C. (1996). "A Simulation Study of the Operational Performance of Left-Turn Phasing and Indication Sequences." *Transportation Science*, 30(2), 112–119.

Chalise, S., Radwan, E., and Abou-Senna, H. (2017). "Analysis of Variable Left Turn Mode by Time of Day for Flashing Yellow Arrow Signals Using the Left Turn Delay Prediction Models." Web site. TRB Annual Meeting Online 2017 and Archived Meeting Content, Transportation Research Board, <http://amonline.trb.org/63532-trb-1.3393340/t024-1.3404251/732-1.3404477/17-06225-1.3400907/17-06225-1.3404486?qr=1> (February 21, 2019).

Chen, L., Chen, C., and Ewing, R. (2015). "Left-turn Phase: Permitted, Protected, or Both? A Quasi-Experimental Design in New York City." *Accident Analysis & Prevention*, Vol. 76, pp. 102-109.

Davis, G. A., Moshtagh, V., and Hourdos, J. (2015). "Safety-Related Guidelines for Time-of-Day Changes in Left-Turn Phasing." *Transportation Research Record: Journal of the Transportation Research Board*, No. 2557, pp. 100-107.

Federal Highway Administration (FHWA). (2008). "Surrogate Safety Assessment Model (SSAM)" Web site. Office of Research, Development, and Technology. <https://www.fhwa.dot.gov/software/research/safety/ssam/ > (February 21, 2019).

Federal Highway Administration (FHWA). (2009). "Manual on Uniform Traffic Control Devices for Streets and Highways." 2009 Edition. <https://mutcd.fhwa.dot.gov/pdfs/2009/pdf_index.htm> (February 21, 2019).

Federal Highway Administration (FHWA). (2013). "Signalized Intersections Informational Guide." Office of Safety. <https://safety.fhwa.dot.gov/intersection/conventional/signalized/fhwasa13027/> (February 21, 2019).

Federal Highway Administration (FHWA). (2018). "Crash Costs for Highway Safety Analysis." Office of Safety. <https://safety.fhwa.dot.gov/hsip/docs/fhwasa17071.pdf> (February 21, 2019).

Fricker, J. D. and Whitford, R. K. (2016) "Fundamentals of Transportation Engineering." 5th Edition, The Scholar Collection.

Hales Engineering. (2016). "Left-turn Phasing Criteria Update," [Memorandum].

MathWorks. (2017). "MATLAB." MathWorks, Version R2017a.

Medina, J. C., Shea, M. S., and Azra, N. (2019). "Safety Effects of Protected and Protected/Permissive Left-Turn Phases," Report UT-19.04, Utah Department of Transportation Traffic and Safety, Research Divisions, Salt Lake City, UT.

National Highway Traffic Safety Association (NHTSA). (2017). "MMUCC Guideline: Model Minimum Uniform Crash Criteria, 5th Edition." <https://crashstats.nhtsa.dot.gov/Api/Public/Publication/812433> (March 19, 2019).

PTV Group (PTV). (2015). "VISSIM." PTV Group, Version 8.0.

Radwan, E., Abou-Senna, H., Navarro, A., and Chalise, S. (2013). "Dynamic Flashing Yellow Arrow (FYA) A Study on Variable Left Turn Mode Operational and Safety Impacts." FDOT Contract BDK78 977-15, Center for Advanced Transportation Systems Simulation (CATSS), University of Central Florida, Orlando, FL.

Radwan, E., Abou-Senna, H., Eldeeb, H., and Navarro, A. (2016). "Dynamic Flashing Yellow Arrow (FYA) A Study on Variable Left-Turn Mode Operational and Safety Impacts Phase II – Model Expansion and Testing." FDOT Contract BDV24-977-10, Center for Advanced Transportation Systems Simulation (CATSS), University of Central Florida, Orlando, FL.

Raessler, A., and Yang, J. (2017). "Derivation of Decision Boundaries for Left Turn Treatments at Signalized Intersections." *Transportation Research Record: Journal of the Transportation Research Board*, No. 2620, pp. 1-9.

Saito, M., Frustaci, J. B., and Schultz, G. G. (2016). "Life-Cycle Benefit-Cost Analysis of Safety Related Improvements on Roadways," Report UT-16.15, Utah Department of Transportation Traffic and Safety, Research Divisions, Salt Lake City, UT.

Saito, M., Kim, K. M., and Schultz, G. G. (2017). "Using the Surrogate Safety Assessment Model for Evaluating Safety Impacts of Access Management Alternatives," Report UT-17.11, Utah Department of Transportation Traffic and Safety, Research Divisions, Salt Lake City, UT.

Saleem, T. (2012). "Evaluation of the Predictive Capabilities of Simulated Peak Hour Conflict Based Crash Prediction Models," University of Toronto, Toronto, Canada.

SAS Institute (SAS). (2018). "JMP Pro." SAS Institute, Version 14.0.

Schultz, G. G., Alpers, J., Saito, M. (2017). "Left-Turn Signal Warrant Procedures: A Synthesis of Practice," Report UT-17.14, Utah Department of Transportation Research Division, Salt Lake City, UT.

Searle, J. (2017). Hales Engineering, Lehi, UT. Personal Communication.

Shea, M. S., Medina, J. C., and Porter, R. J. (2016). "Safety Effects of Protected and Protected/ Permitted Left-Turn Phases: Literature Review and Current State of Practice," University of Utah Traffic Lab, Salt Lake City, UT.

Stamatiadis, N., Kirk, A., Hedges, A., and Sallee, T. (2016). "Integrated Simulation and Safety – UK Final Report." US Department of Transportation, Washington, DC.

Trafficware (2018). "Synchro". Version 10, Trafficware, Sugar Land, TX.

Transportation Research Board (TRB). (2010). "Highway Capacity Manual." 5th Ed. Washington DC.

Utah Department of Transportation (UDOT). (2014). Left-Turn Phases at Signalized Intersections, <https://www.udot.utah.gov/main/uconowner.gf?n=22168023889671869> (Feb. 21, 2019).

Utah Department of Transportation (UDOT). (2018). AADT Traffic Map, <https://www.udot.utah.gov/main/f?p=100:pg:0::::V,T:,528> (February 21, 2019).

Utah Department of Transportation (UDOT). (2019a). Automated Traffic Signal Performance Measures, <https://udottraffic.utah.gov/atspm/> (February 21, 2019).

Utah Department of Transportation (UDOT). (2019b). UDOT Crash Database, <https://udot.numetric.com/> (February 21, 2019).

Wall, D. (2016). "UDOT Crash Costs." Utah Department of Transportation, Salt Lake City, UT. Personal Communication.

LIST OF ACRONYMS

AADT	Annual Average Daily Traffic
AASHTO	American Association of State Highway and Transportation Officials
ATSPM	Automated Traffic Signal Performance Measures
BYU	Brigham Young University
DOT	Department of Transportation
DSS	Decision Support System
FHWA	Federal Highway Administration
FYA	Flashing Yellow Arrow
HCM	Highway Capacity Manual
HSM	Highway Safety Manual
MEV	Million Entering Vehicles
MUTCD	Manual on Uniform Traffic Control Devices
PDO	Property Damage Only
PPT	Protected-Permitted
TAC	Technical Advisory Committee
TMC	Traffic Management Center
TMD	Traffic Management Division
SSAM	Surrogate Safety Assessment Model
UDOT	Utah Department of Transportation